

DTIC FILE COPY

(2)

DOT/FAA/CT-87/38

FAA Technical Center
Atlantic City International Airport
N.J. 08405

Lightning Simulation Test Technique Evaluation

AD-A200 916

William W. Cooley
Deborah L. Shortess

Science & Engineering Associates, Inc.
701 Dexter Avenue N., Suite 400
Seattle, Washington 98109

October 1988

Final Report

This document is available to the U.S. public
through the National Technical Information
Service, Springfield, Virginia 22161.



U.S. Department of Transportation
Federal Aviation Administration

DTIC
SELECTED
DEC 05 1988

88 12 5 007

NOTICE

This document is disseminated under the sponsorship
of the U. S. Department of Transportation in the interest
of information exchange. The United States Government
assumes no liability for the contents or use thereof.

The United States Government does not endorse products
or manufacturers. Trade or manufacturers' names appear
herein solely because they are considered essential to the
objective of this report.

1. Report No. DOT/FAA/CT-87/38	2. Government Accession No.	3. Recipient's Catalog No.	
4. Title and Subtitle Lightning Simulation Test Technique Evaluation		5. Report Date October 1988	
7. Author(s) William W. Cooley, Deborah L. Shortess		6. Performing Organization Code	
9. Performing Organization Name and Address Science and Engineering Associates, Inc 701 Dexter Avenue North, Suite 400 Seattle, WA 98109		8. Performing Organization Report No.	
12. Sponsoring Agency Name and Address Department of Transportation Federal Aviation Administration Technical Center Atlantic City International Airport, NJ 08405		10. Work Unit No. (TRAIS)	
15. Supplementary Notes Technical Contract Monitor: David M. Lawrence		11. Contract or Grant No. DTFA03-84-C-00064	
16. Abstract This report documents the results of four separate lightning simulation tests on a specially designed test bed aircraft. The simulation techniques utilized are low-level swept continuous wave, low-level fast rise pulse, moderate-level pulse, and shock-excitation. The test bed is made up of advanced composite materials with built-in lightning protection and electrical equipment installations. This configuration is electrically and geometrically representative of a general aviation heavy single engine aircraft. Comparative data was developed to determine the effectiveness of the four test methods and used to quantify differences between them. Analysis necessary to extrapolate the results of the tests to the severe lightning environment is discussed. Predicted values from computer models are compared with test results. Key words: Composite materials; EMI; Lightning; Electronic Equipment; Simulation; Lightning Protection.		13. Type of Report and Period Covered Final Technical Report September '84-September '87	
		14. Sponsoring Agency Code	
17. Key Words Composite Materials; EMI; Lightning; Electronic Equipment; Simulation; Lightning Protection.	18. Distribution Statement This document is available through the National Technical Information Service, Springfield, Virginia 22161		
19. Security Class.(of this report) Unclassified	20. Security Class.(of this page) Unclassified	21. No. of pgs. 135	22. Price

PREFACE

This report was prepared by Science and Engineering Associates, Inc. (SEA) under contract DTFA03-84-C-00064 with the Federal Aviation Administration (FAA) Technical Center. Mr. David Lawrence was the contracting officers technical representative.

Dr. Preston Geren provided technical support during the continuous wave simulation test. Dr. Barbara Melander assisted in the modeling analysis.

The test bed was fabricated by August Bellanca of Galena, Maryland.

The lightning simulation tests were performed at the Air Force Flight Dynamics Laboratory/ Atmospheric Electricity Hazards Test Facility under the direction of Larry Walko. Technology Scientific Services, Inc. (TSSI), a contractor to the Air Force, provided technicians for the simulation setup and data collection.

Accession For	
NTIS GRA&I	<input checked="" type="checkbox"/>
DTIC TAB	<input type="checkbox"/>
Unannounced	<input type="checkbox"/>
Justification	
By _____	
Distribution/	
Availability Codes	
Dist	Avail and/or Special
A-1	

6

TABLE OF CONTENTS

	Page
EXECUTIVE SUMMARY	xiii
CHAPTER 1 INTRODUCTION	1
Background	1
Program Requirements	6
Test Organization	6
Test Objectives	6
Scope	7
CHAPTER 2 LIGHTNING SIMULATION TECHNIQUES	8
Review of Lightning Simulation Methods	8
Considerations in Selecting Simulation Techniques	9
Lightning Pulse Generator Techniques	12
Test Methods Selected for Evaluation	13
CHAPTER 3 TEST BED DESCRIPTION	22
Physical Description	22
Electrical Description	25
CHAPTER 4 TEST DATA REQUIREMENTS	26
Simulator Characterization	27
Source Characterization	27
Subsystem Characterization	27
CHAPTER 5 TEST PROCEDURES	32
Instrumentation	32
Test Descriptions	33
Impedance Measurements	35
Data Quality Verification	36
Digital Data Formats	36
Data Logs	37
CHAPTER 6 EXPERIMENTAL DATA	38
CHAPTER 7 DATA ANALYSIS AND MODELING	46
Data Analysis	46
Computer Modeling	47
CONCLUSIONS	52
REFERENCES	115
BIBLIOGRAPHY	117

LIST OF ILLUSTRATIONS

Figure	Page
1 Lightning Flash Current Waveform	53
2 Simulator Return Circuit	54
3 Low-Level Swept Continuous Wave Test Setup	55
4 Measured vs. Fourier Transformed Data	56
5 Low-Level Fast Rise Pulse Test Setup	57
6 Moderate-Level Pulse Test Setup	58
7 Shock-Excitation Test Setup	59
8 Test Bed Configuration	60
9 Test Bed Overall Dimensions	61
10 Test Bed External Detail	62
11 Test Bed Internal Detail	63
12 Forward Bulkhead Detail	64
13 Fuselage Fastener Locations	65
14 Instrument Panel Assembly	66
15 Wing Detail	67
16 Wing Fastener Locations	68
17 EM Source Characterization Sensors	69
18 EM Source Characterization Sensor Locations (Plan View)	70
19 Fuel System Electrical - Installation and Circuit Detail	71
20 Engine Control - Installation and Circuit Detail	72
21 Autopilot Installation	73
22 Autopilot Circuit Detail	74
23 Electric Power to Lights - Installation and Circuit Detail	75
24 Fuel System Mechanical - Installation and Circuit Detail	76
25 Low-Level Swept Continuous Wave Data Acquisition System	77
26 Pulse Data Acquisition System	78

LIST OF ILLUSTRATIONS (Continued)

27	Example Low-Level Pulse Current Waveform	79
28	Moderate-Level Pulse Generator Configuration	80
29	Example 7 kA Moderate-Level Pulse Current Waveform	81
30	Component A Severe Lightning Threat Current Waveform	82
31	Moderate-Level Pulse Current Waveform with 20 Microfarad Generator Capacity	83
32	Example 30 kA Moderate-Level Pulse Current Waveform	84
33	Example Shock-Excitation Current Waveform	85
34	Nose Driven Input Impedance with a Short Circuit at Tail	86
35	Nose Driven Input Impedance with an Open Circuit at Tail	87
36	Wing Driven Input Impedance with a Short Circuit at Tail	88
37	Wing Driven Input Impedance with an Open Circuit at Tail	89
38	Nose Driven Input Impedance with a 50 Ohm Termination at Tail	90
39	Wing Driven Input Impedance with a 50 Ohm Termination at Tail	91
40	Comparison of Pulse Current Spectra with Severe Lightning Spectrum	92
41	Example Transfer Function Measurement	93
42	Example Resistive Response Measurement	94
43	Example dI/dt Response Measurement	95
44	Statistical Distribution of Swept CW Extrapolated Values - Nose Drive	96
45	Statistical Distribution of Low-Level Pulse Extrapolated Values Nose Drive	97
46	Statistical Distribution of Moderate-Level Pulse Extrapolated Values Nose Drive	98
47	Statistical Distribution of Shock-Excitation Extrapolated Values Nose Drive	99
48	Statistical Distribution of Swept CW Extrapolated Values - Wing Drive	100
49	Statistical Distribution of Low-Level Pulse Extrapolated Values Wing Drive	101

LIST OF ILLUSTRATIONS (Continued)

50	Statistical Distribution of Moderate-Level Pulse Extrapolated Values Wing Drive	102
51	Statistical Distribution of Shock-Excitation Extrapolated Values Wing Drive	103
52	Statistical Distribution of Low-Level Pulse Measured Values Nose Drive	104
53	Statistical Distribution of Moderate-Level Pulse Measured Values Nose Drive	105
54	Statistical Distribution of Shock-Excitation Measured Values Nose Drive	106
55	Statistical Distribution of Low-Level Pulse Measured Values Wing Drive	107
56	Statistical Distribution of Moderate-Level Pulse Measured Values Wing Drive	108
57	Statistical Distribution of Shock-Excitation Measured Values Wing Drive	109
58	Elements of EM Modeling and Analysis for Indirect Effects	110
59	REDIST Fuselage Model	111
60	REDIST Wing Model	112
61	Test Bed Resistor Model	113

LIST OF TABLES

Table		Page
1	Range of Effects from Atmospheric Electricity Interactions with Aircraft	2
2	Prior Research and Development Tests on Full-Scale Air Vehicles	10
3	Summary of Simulation Technique Capabilities	14
4	Test Bed Resistance Measurements	23
5	Number of Test Point Current and Voltage Measurements	28
6	Coupling Source Characterization Measurement Point Summary	29
7	Electronic/Electrical Systems Characterization Measurement Point Summary	30
8	SEA CW Data Acquisition System Equipment List	32
9	Pulse Data Acquisition System Equipment List	33
10	Pulse Parameters	33
11	Scaling Factors for Extrapolating Pulse Measurements to Severe Threat Levels	38
12	Extrapolated Peak Values and Times for Each Test Technique - Nose Drive	40
13	Extrapolated Peak Values and Times for Each Test Technique - Wing Drive	43
14	Calculated Statistical Values for Each Simulation Method	46
15	Comparison of Autopilot Measured Values with REDIST Model Calculated Values	50
16	Comparison of Extrapolated Values with Resistor Model Calculated Values	51

LIST OF ACRONYMS AND ABBREVIATIONS

AEHP	Atmospheric Electricity Hazards Program
AFASD	Air Force Aeronautical Systems Division
AFFDL	Air Force Flight Dynamics Laboratory
AFSAMSO	Air Force Space and Missiles Systems Organization
AFWAL	Air Force Wright Aeronautical Laboratory
ALCM	Air Launched Cruise Missile
CRFP	Carbon Filament Reinforced Plastic
CW	Continuous Wave
DAS	Data Acquisition System
DOE	Department of Energy
EM	Electromagnetic
EMI	Electromagnetic Interference
EMC	Electromagnetic Compatibility
EMP	Electromagnetic Pulse
FAA	Federal Aviation Administration
IAGC	International Aerospace and Ground Conference
LRU	Line Replaceable Unit
LTRI	Lightning and Transients Research Institute
NASA	National Aeronautics and Space Administration
NASC	Naval Air Systems Command
NOAA	National Oceanic and Atmospheric Administration
NSWC	Naval Surface Weapons Center
RAE	Royal Aircraft Establishment
RL	Resistor/Inductor
RLC	Resistor/Inductor/Capacitor
RLCM	Resistor/Inductor/Capacitor/Mutual
SAE	Society of Automotive Engineers
SEA	Science and Engineering Associates, Inc.
TSSI	Technology Scientific Services, Inc.
UK	United Kingdom
USAF	United States Air Force

LIST OF SYMBOLS

B	magnetic flux density	Webers per square meter
B Dot	Time rate of change of B	Webers per square meter per second.
C	Capacitance	farads
D	Electric flux density	coulombs per square meter
D Dot	Time rate of change of D	coulombs per square meter per second
E	Electric field strength	volts per meter
H	Magnetic field strength	ampere turns per meter
I	Current	amperes
I Dot	Time rate of change of current	amperes per second
L	Inductance	henrys
R	Resistance	ohms
V	Potential difference	volts

STANDARD UNITS

A	amperes
dB, dBm	decibels
Hz	hertz
kA	kiloamps
kV	kilovolts
ln	natural logarithm
m	meters
MHz	megahertz
mV	millivolts
MV	megavolts
ns	nanoseconds
s	seconds
us	microseconds
uV	microvolts

EXECUTIVE SUMMARY

Because advanced aircraft constructed mostly of composite materials having low electrical conductivity are susceptible to potentially catastrophic direct and indirect effects of lightning, the present program was conducted to investigate experimentally and analytically several lightning simulation test techniques used to demonstrate the adequacy of aircraft lightning protection design and implementation.

A full size test article, geometrically and electrically representative of a high performance single engine general aviation airplane (Bellanca Sky Rocket), was constructed of advanced carbon filament reinforced plastic (CFRP). Fasteners and structural joints were made in the structure to represent those found in advanced aircraft currently under development. Conductive paths for lightning currents were provided, using aluminum screen and foil, conduit, and conductive fasteners as appropriate for protection of equipment and wiring. A low resistance end-to-end path was achieved and maintained throughout the test program.

Sensors to detect electric and magnetic fields and voltage drops were placed at appropriate points in the test article. Measurements of currents, voltages, and electromagnetic fields were made to characterize the interaction between simulated lightning strikes and the structure. Wiring and mock ups for electrical/electronic equipment representative of each of the major systems typically found in a general aviation airplane were installed.

The lightning simulation tests used were low-level swept continuous wave (CW), low-level fast-rise pulse, moderate level pulse, and shock excitation. A co-axial return circuit of wire mesh was used at all times to control electric and magnetic fields about the test article. Current and voltage measurements were made at more than thirty test points for each test technique.

Several test techniques are required to establish adequacy of protection because no single one can simulate all the salient features of any given lightning strike or test waveform. Frequency domain results of the continuous wave (CW) tests are analyzed using Fourier transform methods to obtain a predicted test point response to a severe lightning strike. The low-level pulse reproduces very closely the rate of change of current, I dot, associated with a severe lightning threat. The two pulse generator configurations used for moderate level pulse produced (1) a 7 kA peak amplitude waveform having the same rise and fall times as the SAE-AE4L Component A, and (2) a 30 kA peak amplitude waveform with the same rise time and much faster fall time than Component A. The shock excitation technique is used to simulate the high voltage and electric fields induced on an aircraft just before and during a lightning strike attachment.

Predicted full threat responses were extrapolated by analysis of the test data. The extrapolation technique used was that normally used for each test method, i.e., scaling with respect to I, I dot, or frequency spectrum. The majority of measured responses indicated linear characteristics; a few non-linear effects being noted only at higher levels of injected current. Data analysis showed that of the four simulation techniques evaluated, the 7 kA moderate level pulse provided the most accurate data, because (1) there is little uncertainty in scaling from 7 kA to 200 kA, and (2) the waveform was similar to that of Component A of the SAE-AE4L severe lightning threat reducing the amount of analysis needed to extrapolate results to full threat levels.

CHAPTER 1 - INTRODUCTION

BACKGROUND.

This document describes experimental and analytical investigations made to evaluate lightning simulation techniques commonly used for validation of aircraft protection against the indirect effects of lightning strikes on the electrical and electronic equipment. The four methods selected for evaluation have evolved through government and industry efforts to protect aircraft electrical/electronic equipment against potentially damaging threats from naturally occurring lightning environments.

While the effects of lightning strikes on metal aircraft are considered minimal, there is a greater threat to advanced technology aircraft. This is due to two factors: (1) the increased susceptibility of electronic components to electrical transients and (2) the reduced electrical shielding properties of advanced composite structural materials. Both of these factors reduce the inherent protection of electronic/electrical systems found on previous technology, all-metal aircraft.

Competition in the marketplace for aircraft sales and the increasing cost of fuel is developing pressure on manufacturers to employ advanced technology materials and electronic equipment in the next generation of aircraft. This is evident both in large transport and in general aviation aircraft currently under development. Several general aviation aircraft that employ advanced technology are nearing or are in the certification process. These include the Beech 'Starship', Lear Fan, and AVTEK-400. In addition to the all electric engine control (PW 2037) for the Boeing 757, transport aircraft manufacturers are researching the use of advanced composite structures, digital data busses (beyond ARINC 429), and all-electric systems.

Among the advanced structural materials and processes being employed, is the use of metal to metal bonding with adhesives in place of fasteners and rivets to obtain smooth outer surfaces and reduced drag. Completely non-metallic structures are also being developed using various materials including bonded honeycomb, KEVLAR[®], fiberglass, and graphite/epoxy. These structural fabrication methods also reduce manufacturing costs. Other advantages include reduction in corrosion and fatigue.

There are several potential problems preventing widespread use of the new structural technology. These include the variability of: impact resistance, effect of environmental factors, production controls, lightning protection, static electrification, and electromagnetic compatibility. The range of possible effects from lightning strikes to aircraft in flight, as shown in table 1, comes from two main factors:

- o direct effects -- physical damage from arcing and sparking, and
- o indirect effects -- disruption of the electronic/electrical systems from electrical transients in the wiring and structural elements.

The trend in avionic/electrical equipment toward digital circuits having lower operating voltage and power levels adds to the concerns regarding protection against indirect effects. The poor (lower) conductivity of composite materials and the bonds between structural members makes it difficult to obtain the

TABLE 1
RANGE OF EFFECTS FROM ATMOSPHERIC ELECTRICITY INTERACTIONS WITH AIRCRAFT

EFFECT	CAUSE	CRITICALITY
Flight Control Disruption	Low tolerance to electrical transients caused by <u>indirect</u> lightning or static electrification effects. May simultaneously affect parallel redundant systems.	Minor to Catastrophic
Fuel Tank Fire or Explosion	Fuel vapor ignition cause by static electricity or lightning <u>direct</u> effects on structure. Fuel gauging and flow management electrical/electronics may spark from <u>indirect</u> effects.	Minor to Catastrophic
Loss of Engine Power	Possible <u>direct</u> effects cause thermal or acoustic shock at engine inlet, or <u>indirect</u> effects of electrical transients on engine controls.	Minor to Catastrophic
Radome, Canopy, & Windshield Damage	<u>Direct</u> effects of lightning strikes and arc discharge caused by static.	Minor to Serious
Instrumentation Problems - Communications, Navigation, and Landing System Interference	<u>Indirect</u> transient effects caused by static electricity buildup and nearby or attached lightning strikes.	Minor to Catastrophic
Structural Damage	<u>Direct</u> effects of lightning attachment to aircraft.	Minor to Catastrophic
Physiological Effects on Crew	Flash blindness & distracting electrical shock caused by the <u>direct</u> effect of nearby or attached lightning strikes.	Minor to Catastrophic
Unscheduled Deployment of Landing Gear or Control Surfaces	Premature activation caused by <u>indirect</u> effects of lightning and static electricity buildup on electronics/electrical systems.	Serious to Catastrophic

2.5 milliohm bonding and grounding required by current military specifications. Furthermore, the electromagnetic shielding effectiveness of a composite fuselage without seams or joints is one to two orders of magnitude less than that of an aluminum fuselage. Advanced aircraft digital electronics operate at a few volts compared with a few tens of volts for analog systems.

These factors combine to reduce the margin of safety of the advanced aircraft electronic systems by two to three orders of magnitude. Considerable design efforts may be required to accomplish the protection for these advanced technology aircraft.

The characteristics of electrical transients induced in aircraft wiring and avionics systems are affected by the system response of the entire aircraft to the lightning stimulus. Induced coupling and susceptibility tests may be conducted on electrical hardware and associated wiring at the subsystem level. Determination of what voltage and current levels will be induced into the equipment by a lightning strike must take into consideration the structural interaction with the arc, the subsequent coupling of the magnetic and electrical fields generated by lightning currents on the external surfaces, and finally coupling to the internal wiring and equipment. The presence of an aircraft in the lightning channel may modify the natural lightning current waveform as a result of the resonant responses of the aircraft structure.

Experimental Program. This Federal Aviation Administration (FAA) experimental program was run to investigate the critical problems of lightning protection verification and the simulation techniques used for demonstrating the adequacy of an aircraft lightning protection design. The demonstration of protection design is naturally of greater concern for the new materials and electronics technology than for prior aircraft. The extrapolation of prior protection designs on metal aircraft to those on advanced technology aircraft is not valid because the protection technology is completely different. Very little, if anything, was required to accomplish the indirect effects protection for older metal aircraft. Furthermore, the design margins of safety were never established for the older designs because of prior experience with the inherent insensitivity of metal aircraft to lightning strikes. Advanced technology aircraft are judged to have three to four orders of magnitude less safety margin based upon the reduced shielding effectiveness of the fuselage and the sensitivity of the digital electronics (reference 1). It is natural to question the protection designs with such a great change in design margins.

Because of the increased potential for damage to electronic systems in advanced technology aircraft, simulated lightning tests must be performed to verify the adequacy of the design measures utilized to prevent serious loss or damage resulting from a lightning strike. It is recognized that the necessary protection verification test cannot be performed as a go/no-go test at full lightning threat levels for several reasons as follows:

- o The required electrical storage capacity in the lightning simulator would be excessive for a 200,000 amp discharge through an aircraft.
- o The required fast rise-time ($2.0E+11$ amps/second) for a 200,000 amp discharge could not be attained.

- o The discharge currents and charge densities around the aircraft would be different in flight.
- o There is no predictable method to update test results for airplane modifications.
- o The perceived lightning threat may be changed in the future as more data becomes available through the efforts of NASA, FAA, and others investigating the effects of lightning on aircraft in flight.

Lightning and static electrification protection design and demonstration of the design for aircraft and ground based systems is a current topic for considerable technical research and development. The electrical impedance of a full-scale aircraft precludes the use of severe lightning current pulses such as those used for component indirect-effects tests. Consequently, lower level current pulses have been used to evaluate the transients produced by a lightning strike. Lightning simulation testing is a very challenging technical area because it is very difficult, if not impractical to conduct a full-scale simulated lightning test on large aircraft for several reasons (references 2 and 3). The energy storage and electrical circuits to deliver a full-threat 200 kA peak current requires simulator voltages greater than can be achieved in air, in excess of 2 million volts for a 25-foot long aircraft. Facilities to generate these conditions presently cost over a million dollars. Even with costly tests, there are no methods to update the results for airplane modifications, nor methods to incorporate changes in the lightning threat. For the last several years there have been regular conferences dedicated to these topics (references 2 and 4-16).

Development of lightning simulation techniques for demonstration of protection against indirect effects of lightning has been a key topic of recent research and development efforts. Because of the role of verification testing in the overall electrical and electronic systems protection, the lightning simulation test and analysis techniques have received considerable research and development attention.

Status of Research Efforts. In 1979, the U.S. Air Force conducted an assessment of the potential electrical/electromagnetic impacts created by widespread application of advanced composite materials to aerospace systems (reference 12). Technical specialists from the Air Force Aeronautical Systems Division (AFASD), Air Force Wright Aeronautical Laboratory (AFWAL), and Air Force Space and Missiles Systems Organization (AFSAMSO) formed a working group that collected and analyzed responses from the specific governmental agencies and contractors involved in advanced composite research. Questionnaires were developed and sent out on the two specific composite materials predominantly used for aircraft -- graphite/epoxy and KEVLAR^T. The graphite materials considered were GY-70 and T-300. The first has the higher conductivity and is used for aircraft based on its mechanical properties. KEVLAR^T, essentially an insulator, has many aircraft, missile, and spacecraft applications and is widely used on present aircraft. KEVLAR^T requires special treatments against static electricity and for use as an antenna ground plane.

The results of the survey (reference 12) produced the following ranked list of concerns, which were a direct result of the differences in conductivity of the materials, shielding, and the joint impedances:

- o Lightning spark free fuel system designs
- o Lightning indirect or induced effects
- o Bonding of joints and seams
 - Corrosion control
 - Electrical durability
 - Structural integrity
 - Producibility
- o Power system grounding
- o HF and LF antenna performance
- o Combined space environment effects
- o Specified data on parametric values
- o Technology transition

The Air Force study group also stated that technology development is essential in five major areas:

1. In order to provide universally accepted data concerning electrical parameters of advanced composites and shielding characterizations of structural designs, standardization of manufacturing and fabrication processes and measurement techniques is necessary.
2. Effective, durable, maintainable, and producible, electrically conductive joint technology is necessary to allow accurate design characterization and eliminate many concerns.
3. A lightning proof fuel system is required. In addition to the usual problems of arcing and sparking, the problem of hot spot ignition is a major concern.
4. In order to prevent power distribution loss and lightning induced transient problems in composite structures, alternatives to prior all-metal designs, which provide a ground return path and shielding protection for internal electronics, must be defined and demonstrated.
5. Because little data are currently available, the effects of the space environment on the material and electromagnetic (EM) related design features require definition.

Subsequently, a Tri-service, National Aeronautics and Space Administration (NASA), and FAA working group for Interagency Coordination was established to address these needs, providing program coordination, design guides and handbook development or changes, and development of standard test methods for critical areas such as shielding. The Air Force managed sub-program for Atmospheric Electricity Hazards Protection (AEHP) of the Advanced Development Program is a major effort resulting from this National Interagency Coordination Group. This program is charged with developing design criteria and handbooks for the development of advanced technology aircraft.

PROGRAM REQUIREMENTS.

Because of the practical considerations regarding simulator limitations and emerging design guides for Air Force research (described above), several different simulation test techniques will be used for lightning and static electricity design demonstrations on full vehicles. The simulation and analysis methods are somewhat similar to those for electromagnetic pulse (EMP) protection design demonstrations but are specialized to the unique character of lightning attachment, vehicle charging, high arc current flow, and vehicle discharging.

There are several variants on the high current pulse simulation techniques that are used for full vehicle lightning tests. The four principal lightning simulation test techniques are:

- o low-level swept continuous wave (CW)
- o low-level fast rise pulse
- o full threat fast rise pulse
- o shock-excitation

Included in the accuracy of technique are the analytical models and computations used to checkout and validate the test data. For some methods, analytical techniques provide extrapolation of the test data to other environments and guidance for modifications of the aircraft design.

The major requirement for the FAA and for this experimental effort is to develop a criterion for the test data accuracy and the safety margins. The criterion must also apply for each of the lightning simulation test methods currently in use, and should include an assessment of the limitations and advantages of each of the lightning simulation techniques including the associated modeling and analysis. Because of the critical importance of the protective designs to safety of flight, the assessment of simulation techniques should be supported by test data on an electrically representative aircraft or mockup.

TEST ORGANIZATION.

This experimental program is conducted through the efforts of several government and industry participants. The FAA Flight Safety Research Branch, FAA Technical Center, Atlantic City International Airport, New Jersey is the sponsor. Science and Engineering Associates is responsible for the technical requirements, analysis, and program integration. The test bed was fabricated by August Bellanca, Galena, Maryland. The lightning pulse simulations were provided by the Air Force Flight Dynamics Laboratory (AFFDL) and their contractor, Technology Scientific Services, Inc. (TSSI), both of Dayton, Ohio.

TEST OBJECTIVES.

The FAA must assure that aircraft lightning protection designs are adequately validated by test and analysis. The objective of these tests is to provide a criterion for application of the simulation test methods. This is not a simple task because the lightning simulation techniques currently in use differ in test levels and waveforms. Thus, each test method requires different levels of analytical detail in the extrapolation of measured data, taken at relatively lower current levels than severe lightning current levels, to the expected responses at severe lightning current levels.

The specific objectives of this test program are to:

- o Develop comparative data on the effectiveness of four commonly used lightning simulation test methods.
- o Utilize this data to quantify differences between the test methods.
- o Define the analysis efforts needed to extrapolate results of the tests to severe lightning environments.

SCOPE.

This document covers the entire program of studies and analysis to fulfill the test objectives.

The four lightning simulation techniques utilized for these evaluations are described in chapter 2.

The specially constructed advanced composite test bed aircraft structure utilized as the test bed is described in chapter 3.

Specific test data requirements to meet the test objectives are described in chapter 4.

Test procedures, instrumentation, data recording formats and methods, data quality verifications, and data handling procedures are described in chapter 5.

Chapter 6 contains examples of the experimental data and results of the extrapolation of the data to the 200 kA severe threat level.

The modeling, data analysis, and data reduction efforts are described in chapter 7.

CHAPTER 2 - LIGHTNING SIMULATION TECHNIQUES

REVIEW OF LIGHTNING SIMULATION METHODS.

This chapter presents a review of the lightning simulation technology used for evaluating the effects of lightning and static electrification on air vehicles. It begins with the evolution of the simulation technology, continues with a discussion of the principal simulation methods, and concludes with the specific parameters for the four techniques used in this program.

Lightning Simulation Technology. Several lightning simulation test techniques are currently being utilized for verification and validation of aircraft lightning protection. These different methods are the outgrowth of research using ground based simulations of lightning interactions with aircraft in flight. Under these test methods several aspects of natural lightning are simulated by pulse generators having various waveshapes and energy content as well as swept continuous wave generators. The methods are often utilized, singly and in combinations, throughout an aircraft development cycle. These test methods, together with analysis procedures, characterize the indirect effects of lightning on aircraft electrical/electronic equipment.

The main reason for the different test methods is the difficulty of accurately generating natural lightning in the laboratory for large sized objects. It is very difficult if not impossible to accurately simulate severe lightning environments on an aircraft. This is because of the high levels of energy, current, and electric and magnetic fields associated with naturally occurring lightning. Simulation of these high energy levels requires very large and expensive facilities for an object the size of an airplane. Tests on aircraft and electrical/electronic equipment more commonly attempt to simulate portions of the lightning environment as shown in figure 1. (Figures follow Conclusions at the end of this report.)

High level simulations of lightning appropriate for protection against direct effects, such as investigating structural damage, are easier to implement because only small portions of the aircraft need to be exposed during a test. These simulations for direct effects of lightning on air vehicles have been codified and are generally accepted as published in "Lightning Test Waveforms and Techniques for Aerospace Vehicles and Hardware", a report of the Society of Automotive Engineers (SAE) committee AE4L, 20 June 1978. Simulations for indirect effects, such as for the potential damage to flight control electronics from induced electrical transients, could require the entire aircraft and several attachment locations to fully evaluate. Thus, simulations for the indirect effects of lightning on air vehicles and hardware have evolved along with the research efforts leading to a better understanding of these effects. It was recognized early on that electronic equipment would be affected by induced transients from lightning and other electromagnetic energy. However, the aircraft developments were allowed to go forward while answers were sought for protection against these effects. Research efforts were initiated in the mid 1970's to develop the means of testing, assessment, and protection of the advanced electronics equipment. Since indirect effects testing necessarily involves the full vehicle and simulation of severe lightning levels thereon is impractical, approximate test methods were sought.

Several investigators arrived at a variety of simulation techniques and test equipment because of different starting points and available resources. The data in table 2 summarizes the prior research and development tests on full scale air vehicles. Research and development efforts are still under way. The major efforts are in the AEHP program sponsored by the Air Force Flight Dynamics Laboratory and supported by Tri-Services, FAA, NASA, and the Defense Nuclear Agency. This program is currently in the full-scale demonstration phase for the validation of the test techniques and protection schemes against indirect effects.

CONSIDERATIONS IN SELECTING SIMULATION TECHNIQUES.

Many techniques and facilities are currently available for simulation of atmospheric electricity effects on air vehicles. The selection of an appropriate method is challenging; it depends upon the ultimate use of the data and state of development of an air vehicle.

Existing techniques for simulating static electrification, such as precipitation static, provide adequate data for aircraft design and protection. Nearby lightning strikes may be simulated using simulators developed for electromagnetic pulse (EMP) tests. The real challenge is to adequately simulate effects of lightning directly attached to an aircraft. A simulation technique that imposes all features of the lightning environment in a proper time sequence is desirable for full air vehicle level tests. However, this is not time and cost effective for subsystem tests or to provide design data. It is especially important that the simulation technique provide data on the system, subsystem, or component equipment, line replaceable unit (LRU), responses that can be extrapolated to the values that occur when the air vehicle is exposed to the real lightning environment.

Lightning simulation techniques must account for the significant features of natural lightning, including the number of strokes and the time between them, the rise time, decay time, and peak current amplitude. The desired output from the lightning simulation technique determines which of these features are implemented and the degree of analysis to demonstrate lightning protection. For example,

1. Full vehicle, severe lightning protection demonstration tests with a minimum of analysis require simulation of the extreme values for the lightning parameters.
2. Protection design demonstration tests can be performed with lower levels of pulse or with frequency domain measurements, but require the support of analysis.
3. Avionics and equipment susceptibility can be determined using bench tests on equipment outside the aircraft under test, but require analysis or additional testing to relate to specific vulnerabilities of any aircraft.

The full vehicle test methods, 1 and 2, will be evaluated under this program. The third method is adequately covered by the SAE-AE4L report, reference 3. The most widely applicable methods are the pulse testing at various levels and rates of rise and the swept continuous wave (CW) testing. The CW method differs from the pulse methods in the type of generator used and in the amount of analysis needed for interpretation of the data; these factors are discussed subsequently.

TABLE 2 PRIOR RESEARCH AND DEVELOPMENT TESTS ON FULL-SCALE AIR VEHICLES
(1 of 2 pages)

TEST	DESCRIPTION	RESULTS
USAF FDL F-16 Mockup; G/E Composite 1983	Direct Attached - Coaxial - CW Tests - Moderate Threat 20 kA; 50 kA/us	- V, I, B Dot, D Dot Data - Detailed Model - CW Response Within 4 dB Of Measurement At 28 kA
USAF FDL ALCM 1983	Direct Attached - Coaxial - Full Threat 200 kA; 200 kA/us - Moderate-Level 50 kA	- V, I Data - EM Model - Extrapolated Values 7.7 dB Greater Than Measurement At 200 kA
NASC F/A-18 1982	Direct Attached - Coaxial - High-Level 100 kA; 100 kA/us - Low-level CW 760 A	- Functions - V, I Data - EM Model - No Upset/Damage - Predicted CW Results 7.2 dB Greater Than Measurement At 173 kA
NASC F-14 1982	Direct Attached - Coaxial - High-Level 180 kA; 180 kA/us	- Functions - V, I Data - EM Model - Predictions
NASA F-106 Calibration 1982	Direct Attached - Shock-Excited - Radiated	- V, I, B Dot, D Dot Data - Spectral Analysis - Simple Model
RAE UK JAGUAR 1982	Direct Attached - Damped Sine Wave - Several Levels 100 kA; 20 kA/us	- V, I, E, H Data - Spectral Analysis - External Currents/Fields
NSWC F-16 Mini-Test 1982	Direct Attached - Low-level 30 kA; 30 kA/us	- Currents - Spectral Analysis
USAF FDL C-130 1981	Direct Attached - Radiated - Low-level	- B Dot, D Dot Data - Simple Models
USAF FDL F-111 1978	Direct Attached - Low-level; 2.5 kA	- Voltages - Simple Model
USAF FDL YG-16 Composite; Forward Fuselage 1978	Direct Attached - Moderate To High-Level 30-100 kA; 100 kA/us	- Voltages And Fields - External EM Models

TABLE 2 PRIOR RESEARCH AND DEVELOPMENT TESTS ON FULL-SCALE AIR VEHICLES
(2 of 2 pages)

TEST	DESCRIPTION	RESULTS
USAF FDL A-7 1977	Direct Attached - Low-level 2 kA; 1.25 kA/us	- Voltages - Simple Model
GENERAL DYNAMICS F-16 1975 & 1976	YF-16 #1,2 Lightning Tests 2-30 kA; 50 kA/us	- Voltages - Simple Model
NASA F-8 1975	Direct Attached 5 kA; 5 kA/us	- Voltages - Data Analysis
UH-60 HELICOPTER	Direct Attached - Low-level; 5 kA	- Unknown
757 TRANSPORT	Direct Attached - Low-level CW Test 250 A	- Spectral Analysis

LIGHTNING PULSE GENERATOR TECHNIQUES.

Many pulse techniques exist for generating simulations of lightning waveforms to investigate the induced effects of lightning on air vehicles and avionics equipment. These techniques are based on discharging a high voltage source into the test aircraft, using switches and wave shaping elements to produce the appropriate current waveform. Most lightning simulators use variations of a resistor/inductor/capacitor (RLC) circuit to produce some of the relevant lightning characteristics. The circuit may be configured in either the under-damped, critically damped, or overdamped configuration. Four variants of the RLC circuit are in use today: the linear damped sine wave, critically damped, the double exponential, and a nonlinear generator having sine wave rise and an exponential tail.

The underdamped RLC circuit generates the fast rise times and a moderate level action integral desired with a practical circuit, but the waveform is oscillatory rather than unipolar as in natural lightning. Mr. John Robb of Lightning and Transients Research Institute (LTRI) and Dr. Brian Burrows of Culham Laboratory (England) have used damped sine wave pulsers for achieving high currents and fast rise-times (reference 17).

The critically damped circuit gives a unipolar waveform, but the decay-time to rise-time ratio is smaller than that of natural lightning. However, the simplicity of constructing this type of pulser makes it attractive to generate a moderate-level pulse. With a low inductance aircraft and return circuit this type of pulser can provide moderate rise-times and peak currents. The Air Force Flight Dynamics Laboratory has built moderate-level pulse generators using the standard RLC circuit arrangement. Significant improvements to the pulse generator switch and transient measurement system have been incorporated into this system (reference 18).

An overdamped circuit requires a large amount of stored energy to produce the desired waveform. Therefore, this configuration is generally not used to provide both fast rise times and high current levels on a single pulse. Burrows of Culham Laboratory utilized a pulse generator with an overdamped RLC circuit. This arrangement was combined with an approximately coaxial return conductor arrangement to produce moderate-level current pulses of 20 kA with a peak rise rate of 170 kA/microsecond (reference 19). Field distribution calculations were used to determine the placement for the return conductors.

The nonlinear "crow-bar" generator provides an efficient means for generating high peak currents with high energy in the decay. The sine wave efficiently transfers energy from the main capacitor bank into the test aircraft inductance. This energy is then short circuited by a spark gap and discharges with a resistive/inductive (RL) decay, producing the long decay tail on the test airplane current pulse. Sandia National Laboratories has built a high-level lightning simulator for DOE using a crowbar circuit design. This produces an essentially nonlinear circuit, because before the crowbar switch is closed it is an RLC circuit and after the switch is closed it is an RL circuit.

Return Circuit Configuration. The return circuit for the lightning simulator and test aircraft determines the field distribution around the test aircraft. Return circuit wiring under the test aircraft has been used, reference 8, however, this arrangement did not simulate the field distribution for natural lightning.

More uniform field, voltage, and current distributions are produced by configuring the aircraft and return circuit as a coaxial transmission line. An example of the required simulator return circuit is shown in figure 2. The return conductors form an approximate coaxial outer conductor around the aircraft. The electric and magnetic fields around the airplane approximate field distributions for the aircraft in free space. An additional benefit is that this arrangement provides low inductance and resistance which is required by some pulsers to produce a satisfactory waveform. This is particularly true for the RLC pulse generators.

TEST METHODS SELECTED FOR EVALUATION.

Four test methods were used for evaluation under this program as appropriate methods for testing for indirect effects of lightning on full size air vehicles having advanced technology structural materials and electronics equipment. These methods, described in the following sections, are defined as follows:

- o low-level swept continuous wave
- o low-level fast-rise pulse
- o moderate-level pulse
- o shock excited pulse

The capabilities and limitations of each of these methods are summarized in table 3.

Low-Level Swept Continuous Wave (CW). This lightning simulation technique utilizes a continuous wave rather than a pulse to excite the transients. Because the levels of testing are generally at low levels of current relative to the severe threat lightning, there is more uncertainty and consequently more analysis is required to extrapolate to severe current levels.

Basically, this method utilizes a network analyzer to measure transfer functions (amplitude and phase) from a lightning attachment point to test points (voltage or current) within the aircraft (see figure 3). These transfer functions, measured over a wide frequency range, are subsequently processed by multiplying by the severe lightning current spectrum to develop test point spectral responses. These test point responses are then numerically Fourier transformed to generate the pulse response expected from severe lightning. The method is generally applicable to other EM threats as well. Standard swept CW network analyzers provide coupling transfer function data as amplitude and phase versus frequency. Figure 4 provides an example of the data obtained by Fourier transform processing of the CW measurements and the similar pulse measurements taken with moderate levels and the same instrumentation.

A principal advantage of the CW test method is the low level of injected current that can be applied (a few amperes) while attaining a high level of signal-to-noise. This is because of the wide frequency range contained in the lightning induced transients interaction and coupling within the aircraft. Hence, the energy delivered to the test object can be averaged over a relatively long time compared to pulse methods. This provides an improved signal-to-noise ratio particularly when a narrow band receiver is used in the network analyzer.

TABLE 3 SUMMARY OF SIMULATION TECHNIQUE CAPABILITIES

	Low Level			High Level
Required Features for Direct Strike Simulation on Full Vehicles	Swept CW Bench Test	Fast-Rise Pulse Test	Shock Excited Pulse	Fast-Rise Pulse Test
High Voltage - E Field Phase	Linear Only	Limited By Pulse	Limited By Pulse	Ok
High Current - H Field	Yes	Yes	Yes	Ok
Continuing Current	Yes	Yes	Yes	Ok
Fast Rise Times (30 - 100 ns)	Yes	Yes	Yes	Limited By Pulse
Electromagnetic Test Cell				
o In-Flight Conditions	Yes	Yes	?	Yes
o Currents and Fields	Yes	Yes	?	Yes
Lightning Channel Attachment	Yes	Limited By Pulse	Limited By Pulse	Limited By Pulse
Functional Responses				
o Upset	Yes	No	?	Yes
o Damage	Yes	No	?	Yes
Adapt to New Threat Parameters				
o EM Coupling	Yes	Limited By Pulse	Limited By Pulse	Limited By Pulse
o Functional Responses	Yes	Limited to Observed	Limited to Observed	Limited to Observed

Because of transfer function complexity for most coupling responses, data are much easier to understand when obtained with CW measurements than with pulse techniques. This is because of clearly displayed and quantified resonances, superior signal-to-noise, and lower required generator levels than for pulse methods. With the CW method, an attached current of a few amperes can provide as high a signal to noise ratio as a severe lightning pulse. With these low levels of testing the CW measurement method offers several advantages for obtaining parametric sensitivity data as, for example, the quick evaluation of a variety of mock-up protection options.

Swept CW measurement techniques for full vehicle lightning protection design demonstration are as follows:

- a. Conduct time-delay-reflectometer (very low-level pulse) measurements to identify apertures and locations where electromagnetic (EM) coupling occurs.
- b. Conduct CW measurements to measure transfer functions from the external lightning current attachments to the EM coupling sources. Also develop transfer functions from the sources to wiring and from the wiring to equipment.
- c. Combine the CW measured transfer functions with a model of the external lightning threat to obtain an overall computer model for EM response prediction.
- d. Excite the computer models with the applicable severe lightning current spectrum and transform to time domain determining the full-threat level transients at critical circuits.
- e. Using the predicted severe lightning pulses (possibly including timing from apertures and restrikes), perform bench tests (induced cable current or pin voltage injection tests) at critical circuits on the aircraft.
- f. Determine protection safety margins for the equipment. If the protection is inadequate, determine design to reduce transients or reduce equipment susceptibility to the transients.

This method is also applicable to evaluating coupling coefficients for the high-voltage leader-attachment phase and nearby strike, as well as for the high-current phase by means of piece-part linear simulation techniques. For this technique, the generator, airplane, and return circuit are configured to represent the electromagnetic environment for each of the phases, one at a time. The coupling parameters included for the current and fields response of a given subsystem to the various aspects of the threat may be used to define the appropriate threat waveforms for a bench test. These time-ordered threats may then be imposed upon the component or subsystem in the proper sequence.

The bench tests referred to in e. are similar to electromagnetic interference /electromagnetic compatibility (EMI/EMC) tests required for MIL-STD-461/462 compliance. Currents are injected into interconnecting cables by magnetic coupling using a clamp-on current transformer. Alternatively, electric and magnetic fields are injected into cables and enclosures by a parallel plate transmission line excited by a high current pulser. Power system transients are

induced by direct series connection of a coupling capacitor and pulse generator across the power supply.

Low-Level Fast-Rise Pulse. Under this method, current pulses are generated by means of a pulse generator that is tightly coupled to the test aircraft (see figure 5). For this application, the test aircraft return circuit inductance and pulse generator capacitance combine to provide a critically damped circuit. This results in a current pulse having a high rate of rise with a relatively short decay time. The parameters are chosen so that the peak rate of rise matches the rate of rise for severe lightning currents while the peak amplitude is near that for moderate levels of lightning current. The generator decay time is much faster than natural lightning. Nominal values for the low-level fast rise generator used for this test are as follows:

Peak current	- 1 kA
Peak rate of rise	- 1.4 kA/microsecond
Time to peak	- 80 nanoseconds
Time to one half amplitude	- 13 microseconds

This simulation provides stress levels that match the severe rates of rise of natural lightning. This is appropriate when the principal electromagnetic coupling mechanism is mutual inductance or mutual capacitance, as is the case for balanced circuits isolated from structure. For composite structures where the coupling mechanism may be due to resistive drops, the simulated currents are not high enough to match the expected levels of moderate lightning strikes.

Since such a generator produces less than a moderate lightning stress on much of the equipment in an aircraft, the survival of equipment under the test condition only provides confidence in the survival of minor lightning strikes.

Careful analysis and interpretation of the test data is necessary in order to provide confidence in the survival of severe lightning strikes. This analysis must include interpretations of the coupling mechanism (I-dot or I) for each cable run and equipment area on the aircraft. The coupling mechanisms are necessary in order to extrapolate measured voltages and currents to higher severe lightning responses. The I-dot driven responses scale according to the rate of rise parameters while the resistive driven responses scale according to I parameters. For many responses it will be found that they are driven by both I and I-dot coupling mechanisms. Since the generator circuit is tightly coupled to the aircraft under test, it may not be possible to separate the I and I-dot coupling from the data. This is because the internal coupling in the aircraft provides a different scale factor for I and I-dot at different test points, due to internal resistance/inductance/ capacitance/mutual (RLCM) parameters, from the fixed I/I-dot parameters built into the generator. Thus the separation of the test results into purely I or I-dot will not be possible in general without considerable test efforts using different generator parameters.

If the generator waveform parameters match lightning parameters except for peak amplitude, then the response can be scaled by a multiplicative constant. For any other generator or choice of waveform parameters this will not be the case.

Based upon linearity arguments, Walko et al. (reference 18) developed such a test based upon the use of a very-low-level double-exponential current pulse with a peak magnitude as low as 200 A. If rise and fall time constants match the values for lightning, then this current pulse theoretically contains all of the frequency components of a 200,000 A waveform in proper proportion, thereby

allowing transients to be scaled linearly. The pulse is passed through the aircraft structure (from nose to tail, for example) and the resulting transients produced on critical wire runs inside the aircraft are monitored by connecting voltage/current measurement instrumentation across the circuit to be monitored. The peak values of the measured transients are then extrapolated upward to the severe lightning current level. In the case of a 200 A test pulse with a 2 microsecond rise time and a 50 microsecond decay to half value, the peak levels are multiplied by 1000 to determine the anticipated transients for a 200,000 A strike with the same waveform. Since the test wave shape is the same as the threat waveform, the I-dot and the peak current I have the same scaling factor.

Unless the generator rise and fall time constants match lightning parameters, it is probably better to use the basic measured responses as representative of a low to moderate lightning stress and not try to extrapolate the measured responses to higher levels.

The most accurate approach to extrapolation of the voltage and current measurements to higher levels of stress is through an analytical model based upon electrical equivalent circuits. This approach to modeling is similar to the analysis required for the CW method described previously. The major difference is that the measured data for comparison with the models is derived from the pulse measurements.

Low-level pulse measurement techniques for full vehicle lightning protection design demonstration are as follows:

- a. Conduct time-delay-reflectometer (very low-level pulse) measurements to identify apertures and locations where EM coupling occurs.
- b. Conduct CW measurements to measure transfer functions from the external lightning current attachments to the EM coupling sources. Also develop transfer functions from the sources to wiring and from the wiring to equipment.
- c. Combine the CW measured transfer functions with a model of the low-level pulse generator to obtain an overall computer model for EM response prediction of the test responses.
- d. Compare the measured pulses with the model predictions to provide confidence in the computer models. Determine the error bars in the model responses from the measurement comparisons.
- e. Excite the computer models with the applicable severe lightning current spectrum and transform to time domain determining the full-threat level transients at critical circuits.
- f. Using the predicted severe lightning pulses (possibly including timing from apertures and restrikes), perform bench tests (induced cable current or pin voltage injection tests) at critical circuits on the aircraft.
- g. Determine protection safety margins for the equipment. If the protection is inadequate, determine design to reduce transients or reduce equipment susceptibility to the transients.

It should be noted that the first steps a. through c. are the same as for the CW test method. This is because the CW method provides a higher degree of confidence in the modeling of the various coupling mechanisms. The pulse data could also be used to refine the models but there would be lower confidence in the extrapolation using a model that had been refined with the pulse test alone. This is due to the difficulty of separating the various RLCM parameters from the time domain test responses.

Moderate-Level Pulse. Under this method, current pulses are generated by means of a large pulse generator that is tightly coupled to the test aircraft and return circuit. An example is shown in figure 6. There is considerably more energy required in the main pulse generator for this method than the fast-rise low-level method. In the usual application, the test aircraft and return circuit resonate with the pulse generator capacity to provide high rate of rise current pulses having a damped sinusoidal waveform. The generator and return circuit parameters are chosen so that the pulse rise time matches the rise time for severe lightning currents. The peak amplitude is near enough to the severe lightning current levels that the data extrapolations can be made with high confidence. The generator decay time can be adjusted to the same as or much faster than natural lightning. Nominal values for the two configurations of a moderate-level generator used are as follows:

Peak current	- 7 kA	30 kA
Peak rate of rise	- 3.13 kA/microsecond	23 kA/microsecond
Time to peak	- 6.3 microseconds	6.3 microseconds
Time to one half amplitude	- 51 microseconds	17 microseconds

This simulation provides levels at and above the moderate lightning strike current amplitude. This test method is appropriate when the amount of analysis is to be minimized. This test is appropriate for providing high confidence in the survival of the aircraft and equipment under severe lightning strikes.

The principal advantage of the moderate-level pulse simulation technique is that the stress is near that expected from lightning strikes. This test stress increases the confidence in the protection design over that of a low level test technique used alone. For example, portions of the protection system, such as cable shields and grounding schemes, could function at levels associated with low-level testing but be damaged at higher levels.

Since a moderate-level generator will provide a moderate lightning stress on the test aircraft, the survival of equipment under the test condition provides confidence in the survival of the aircraft against all but severe lightning strikes.

The principal advantage of this test method is that the amount of scaling or extrapolation is not very great. Careful interpretation of the test data is necessary in order to provide confidence in an aircraft survival of severe lightning strikes. However, there is greater confidence in scaling factors of seven (from 30 kA to 200 kA) than factors of 200 required for the low-level pulse method. The data analysis must of course include interpretations of the measurements to validate the measurement process. But this analysis effort is much simpler and more readily accepted than the analysis required for lower level test methods.

Severe Full-Threat Pulse. Unfortunately, it is difficult or impossible to generate the severe lightning currents in large aircraft as can be demonstrated by a relatively simple analysis. The primary reason for this limitation is due to the inductance and resistance of the return circuit and the airplane. For an ideal conductor and the return circuit coaxial, the test circuit surge impedance is typically 50 ohms. For 200 kA, this requires 1 MV to drive the test aircraft and 1.3 MV for the charge voltage of the pulser. These values are achievable but require specialized high voltage construction practices. For a large aircraft, the circuit impedance is more inductive. The inductance is approximately given by:

$$L = 120 \ln(h/2d) h/c$$

where h is the aircraft length, d is the aircraft diameter, and c is the speed of light. For a 50-meter aircraft 3 meters in diameter, this results in an inductance of approximately 40 microhenrys. It requires 8 MV to drive 200 kA/microsecond into this inductance. Such a generator is not presently achievable. However, for a small general aviation size aircraft the inductance can be on the order of 3 to 4 microhenrys and only require 600 to 800 kV to reach the 200 kA/microsecond rate of rise. While this is a large order for most general aviation manufacturers, such generators are well within the reach of several lightning test organizations.

Shock-Excited Pulse. The pulse techniques described above focus on the directly attached current waveform simulation and associated EM fields. There is some concern that the high voltage and electric fields induced on an aircraft, just before a strike and during the aircraft charging should also be considered in the simulation. The electric field mode can be simulated by using a spark gap between the aircraft and the pulse generator and between the generator and the ground (see figure 7). These spark gaps are to be placed at a structural extremity away from the pulser attachment. When the pulser is fired, the aircraft will be charged, through the pulser gap, toward the pulser voltage. The charging will be terminated when the aircraft to ground spark gap discharges to ground. This technique produces high voltage and electric field gradients on the aircraft to simulate the natural lightning effects. Nominal values for the shock-excitation pulse test performed for this program are as follows:

Peak Voltage	- 160 kilovolts
Peak Current	- 7 kA
Current Rise Time	- 6.3 microseconds

Evolution of the High-Voltage Shock-Excitation Tests. Questions surrounding some of the early full-vehicle lightning test results led to a closer study of induced coupling phenomena by Clifford and by Skouby and Pearlman, utilizing high-voltage techniques (reference 20). The combined experimental and analytical program disclosed that the lightning coupling phenomena are very complex, involving a number of test setup effects, and at least three different excitation mechanisms.

The results of this test program indicated that the fast oscillatory transients usually observed during low-level current tests of aircraft are system resonances which can be excited by either a) pulsing the structure with a fast voltage-step waveform, b) passing a current pulse through the system, or c) irradiating the structure with a fast-changing external field.

The shock excited test technique was developed to isolate these different driving functions utilizing long high-voltage arcs whose lengths and impedances could be adjusted to decouple the aircraft from the external simulator setup. When the high-voltage generator is fired, an abruptly changing electric field is produced between the output electrode and the vehicle. A few microseconds later, a second arc will be established from the isolated vehicle to ground, rapidly discharging the vehicle. The completed circuit to ground will then allow the high voltage generator to discharge a high current through the vehicle.

The transients produced by each driving function can be separated in time because of the finite time (microseconds) required for the long arcs to be established. By adjusting the arc lengths and circuit impedances, transients produced by the electric field change, the charging of the vehicle, and the discharging of the vehicle capacitance can be separated from each other and from the transients produced by the generator current waveform. These different excitation mechanisms are related by Clifford et al. to the natural lightning conditions of a) nearby lightning (fast electric field change), b) stepped-leader attachment (charging of the vehicle), and c) return stroke (discharging of the vehicle).

The high-voltage shock-excitation test is the result of this development program. The major setup difference from prior techniques is that, in the shock-excitation test, the aircraft functions as the peaking capacitor. If the aircraft is isolated from ground, an additional peaking capacitor is unnecessary presumably. The discharge of the aircraft, when the output gap arcs over, should excite the internal circuits in much the same way as the discharge of an aircraft in a preionized lightning channel would when it is discharged by the return stroke.

Shock-excitation tests have been conducted on the NASA space shuttle orbiter, Enterprise, on the Air Force YF-16 fighter aircraft, the NASA F-106 research aircraft, and the USAF/NOAA C-130 research aircraft. These tests are characterized by several unique features because of the high-voltage aspects of the technique. First, the aircraft must be well isolated above ground. Specially designed high-voltage isolation pads placed under the wheels allow testing up to 400 kV on most aircraft.

A shielded high-voltage impulse generator is used as the excitation source. This shielding is required so that a clean output voltage waveform may be applied to the vehicle. In order to simulate the natural lightning charging and discharging of the aircraft, it is desirable to charge the aircraft to over one million volts with respect to the coaxially arranged return lines. At these voltages, realistic corona should be developed so that, when the aircraft discharges to ground, the transients produced will be representative of natural lightning. Essential elements of the test are fiber-optic data links which allow system transients to be monitored while the system is charged to very high voltages.

An important result of the shock excited test investigation was that capacitive coupling ($C \frac{dV}{dt}$) was found to be the dominant coupling mechanism in some very important cases. In particular, the transients on high-impedance signal circuits used for single wire computer logic circuit interconnections were found to be dominated by capacitive coupling. The situation is reversed for low-impedance circuits where inductive ($L \frac{dI}{dt}$) coupling dominates.

For these tests, the maximum values of the lightning parameters of interest (I , dI/dt , E and dE/dt) are determined by the amount of charge stored on the aircraft before discharge occurs. The YF-16 shock-excitation test, which was limited to around 300 kV charging potential by the dielectric isolation under the wheels, produced a peak discharge current of about 8 kA with a pulse width of about 60 ns. The discharge resulted in a peak dI/dt of $2.0E11$ A/s, a peak electric field of $3.0E6$ V/m, and a maximum dE/dt of $5.0E10$ V/m-s.

The major implication of these results for simulation testing is that sufficiently high voltages and rates of change of voltage must be present in the test to reproduce the natural lightning conditions. Since nonlinear corona and streamering effects are expected to play a role in the induced voltages and currents experienced by an aircraft struck by lightning, testing with low voltages (grounded vehicles) may not yield an accurate simulation. The amplitude and duration of the oscillatory currents produced on the structure by the rapid discharge of the aircraft on ground (free response) are controlled by the dissipation factors in the test setup. These factors include arc impedance and corona streamering effects. When the test article is grounded, neither of these dissipation factors is present. It still remains to determine exactly what the correct values for the dissipation factors are, but additional laboratory studies, coupled with forthcoming flight data, should resolve those uncertainties.

CHAPTER 3 - TEST BED DESCRIPTION

PHYSICAL DESCRIPTION.

A specially designed and fabricated test bed aircraft, consisting of a fuselage, tail, and left wing as used on an experimental aircraft, was used for these investigations. The test bed aircraft configuration is electrically and geometrically representative of a general aviation type, heavy single engine category aircraft. Since the investigations focus on the electrical/ electronic equipment installations, an airworthy structure is not required. The only difference in the skin from a flying aircraft is that the test bed has an external skin only. The flying version is a monocoque having an external skin, nomex core, and internal skin. The internal skin is fiberglass which is not intended to carry any currents, so the omission is not important for simulation of lightning protection.

During the experimental program, the test bed was exposed to simulated lightning currents by the four methods discussed in chapter 2. Lightning protection measures are provided in the test bed to mitigate any potential damage to the structure at levels up to moderate lightning currents. These measures were effective at all measured current levels as determined by resistance measurements of the test bed before and after each simulation test (see table 4). Note that the injection of current has caused the resistance to decrease in most cases.

The current flowing along the structure will be concentrated in the wiring and other metallic elements of the test bed. The current at each metal fastener must be distributed between the graphite fibers and any adjoining metal. The number of fibers available depends on the area of the fastener junction to the base material. Low levels of current may cause arcing between metals in the area of the joint. The arcing could weld the aluminum foil on the bulkhead to the aluminum bracket, making a better electrical connection and causing the measured resistance to decrease. The decrease in resistance may continue, until the current level becomes high enough that some graphite fibers reach their current burnout limit. The remaining fibers must then increase their share of the total current leading to an avalanche failure of the fibers at the joint. The joint resistance will begin to increase as fibers reach burnout. Some measurements at high currents showed evidence of possible sparking, however no permanent damage was seen from the resistance measurements of the test bed structure.

The test bed is made of advanced composite materials with the main emphasis on the use of epoxy carbon fiber laminates. Removable panels and doors are made of protected fiberglass or KEVLAR[®]. The structural joints and fasteners are made according to the attached drawings with the objective of achieving a configuration representative of fabrication methods for advanced aircraft currently under development. The overall test bed configuration and dimensions are shown in figures 8 and 9.

Five major components make up the test bed. These components are the fuselage, left wing, tail, engine block, and test stand.

TABLE 4 TEST BED RESISTANCE MEASUREMENTS

Measurement Point	Resistance (milliohms)					
	CW Test 8/85	Low-level Pulse 6/16/86 Before	Low-level Pulse 6/23/86 After	moderate-level 12/3/86 Before	moderate-level 12/15/86 After	Shock 12/16/86 After
Engine Controller Equipment (BNC disconnected)						
to Structure	6.5	9	5.5	7.4	9.5	18.5
BNC (disconnected)						
to Structure	88.5	69	68	73.3	69.5	76.7
Pigtail (disconnected)						
to Structure	91.5	99	80	96.6	80.5	81.5
Autopilot ***						
Pigtail A	70.5	104	53	59.7	52.5	-
Pigtail B	191.5	237	122	120.6	122.5	119.5
Pigtail D	-	368	151	109.4	112.4	130.3
Shell to Structure	-	8.5	13	17.6	11.2	8.7
Nose to Tail (short on tail)						
	8 *	2000	51700	58900	31	
Front Bulkhead to Rear Bulkhead						
A to B	10 **	16	20	13	17	16.3
A to C	140 **	162	42	13	17	16.3
A to D	180 **	231	152	13	17	16.3
Wingtip to Rear Bulkhead						
Front Spar	20.5	126	24	18	19	41.3
Rear Spar	-	114	12	21	-	-
Fuel Electrical Box		109	12	18	-	18.3
Autopilot Box				22		
				30		

* Measurement made without the return circuit.

** Measurements made on fuselage without electronics or return circuit used for the CW test.

*** Autopilot pigtails disconnected at box #3 for measurements. Box was not mounted in place for 6/16 and 12/15 resistance measurements.

50 ohm resistor added to tail after 6/16 measurements; 50 ohm resistor in place for 12/3 lab demonstration - then removed.

Top wing skin removed for wing to spar measurements.

Sheet metal replaced foil on two aft bulkheads for 12/86 measurements.

Fuselage. The composite material fuselage is a molded structure built using molds and a vacuum bag with room temperature epoxy cure techniques. The fuselage consists of right and left hand shells bonded and bolted to a plywood framework as in figure 10. Windows are unfinished cutouts as shown in figure 10. A door is provided in the aft of the right side of the fuselage for personnel access. This door is a mockup structure, fabricated with the objective of achieving the electrical properties of a flight quality structural door.

Conductive paths are provided for lightning currents through the fuselage shells via the use of 3 mil aluminum foil, aluminum screen, and conductive fasteners. Aluminum screen mesh is applied on the bottom of the fuselage; see figure 11. This interior metal is bonded electrically to the fuselage skins, front and rear bulkheads, and to the interior bulkheads by means of typical 100 degree countersunk aircraft fasteners. The interior fuselage bulkheads have aluminum foil to provide a good electrically conducting path between right and left shells. In addition, there are metal angle brackets at the attaching areas in the bottom of the fuselage to assure a good electrical path between the bulkheads, wing spars and the fuselage skin. These brackets which provide electrical connections are shown on the forward bulkhead detail drawing, figure 12. The fastener locations throughout the fuselage are shown in figure 13. There is a simulated instrument panel, as shown in figure 14, fabricated from wood and aluminum foil. A wooden floor is provided inside the test bed for access into the fuselage.

Wing. The wing consists of an upper skin and a lower skin, molded using a vacuum bag and room temperature epoxy cure techniques. These skins are bolted or bonded, depending on the location, to an internal plywood framework; see figure 11.

The lightning protection incorporated into the wing structure is accomplished by providing adequate thickness, four plies, in the skin materials and electrically conductive paths for lightning currents. A conductive path runs from the wing tip, a .050 aluminum sheet, through the spar faces which are covered with 3 mil aluminum foil and bolted directly to bulkheads -3 and -4; see figure 11.

The electrically conductive paths through the wing skin and spars consist of aluminum angle brackets, shown on figure 15, which flush bolt into the wing skin covers and the spars. These brackets provide alternate parallel paths for lightning currents. The fasteners are typical 100 degree countersunk aircraft structural fasteners. Fastener locations throughout the wing are seen in figure 16. A conductive path for lightning currents at the wing-body joint is afforded by the use of four battery cables from the aluminum covered spars and bulkheads to the fuselage shells. A special wing-body conducting path is provided consisting of an aluminum attachment fixture to spread the lightning currents from the wing spar cables to the fuselage shells.

A wheel door is provided in the lower skin between the inboard ribs -17 and -18 (see figure 11). This door is a mockup structure that is electrically similar to a well shielded door.

Tail. The tail structure, shown in figures 10 and 11 is a mockup structure intended only to provide an attachment for lightning and a conducting path to the empennage structure. This tail consists of a plywood sheet with a partial aluminum face. It has a conductive path provided by an aluminum sheet down to the empennage attachment points on bulkheads -9 and -10 (see figure 11). The tail is attached with aircraft bolts to these bulkheads to provide a metal-to-metal contact at this attachment point.

Engine Block. The engine block, -1 shown in figure 11, is made of 1/2 inch plywood with 0.050 inch aluminum sheet outside faces. The block is mounted against the aluminum firewall with aluminum brackets to make a good electrically conductive path.

Test Stand. A wooden stand supports the test bed to facilitate entry to the fuselage and to isolate the test bed from the return circuit for high voltage test operations. This test stand, built to fit the test bed contours, supports the structure with at least two, but no more than four, feet of clearance between any part of the structure and the building floor.

ELECTRICAL DESCRIPTION.

The test bed contains several built-in systems that electrically represent elements of the following systems.

1. Fuel Electrical
2. Engine Controls
3. Autopilot
4. Electrical Power
5. Fuel Mechanical

Simulated lightning tests induce voltages and currents within the systems listed above. The measured responses are used for characterizing the response to the various simulated lightning environments. The installation locations and circuits of the above systems are detailed in chapter 4.

Several fixed sensors were installed to measure sources of EM coupling into the test bed. These sensors measure the electric coupling to simple wires, magnetic field coupling to simple wire loops, and the voltage drop in sections of the skin and joints. A diagram of the sensors is seen in figure 17. The sensor locations are shown in chapter 4.

CHAPTER 4 - TEST DATA REQUIREMENTS

Four separate lightning simulation tests were conducted on the test article described in chapter 3, utilizing the simulation techniques described in chapter 2. Induced voltages, currents, and electric and magnetic fields were measured in response to the simulated lightning environments. The test data from each of the separate simulations will be compared to establish safety margins on the application of test techniques by extrapolation to high-level severe lightning threats. An analysis of this data also provides a measure of the protection afforded by the test bed.

These tests were structured to develop sufficient data (30 or more measurements in each configuration) of high quality that would provide statistical measures of the uncertainty in the simulation techniques. Mean value and standard deviations were developed for all data of sufficiently high quality. The judgement of quality shall be based upon data typical of the test technique being applied. The test results and data were analyzed to develop specific advantages and disadvantages of the individual methods.

Analysis techniques were utilized in conjunction with the testing. Computer modeling was used to support the tests and to validate the test data, i.e., to confirm that everything was connected properly and that the instrument setup was correct. Simple models were used as needed for establishing ranges for testing as the data was taken. Modeling is described in detail in chapter 7. The final decision on accuracy will be in favor of the test data rather than the analysis. Accuracy of the analysis techniques will then be judged in comparison with the test data by means of statistical averages and standard deviations.

These analysis efforts are necessary because of limitations in present simulation techniques. The lightning/static electrification simulation experimental setup requires several features to adequately simulate the natural electromagnetic environments. These environments ultimately determine the indirect effects on advanced aircraft electronic equipment. Features necessary in the simulation setup include:

1. Developing the proper EM environment geometric configuration around the test bed and the proper time phasing.
2. The high voltage and electric fields associated with approaching leaders and static charging must precede the high current and magnetic fields associated with the lightning return strokes.
3. The pulse rise-time must also reflect the fast rise-times recently measured on natural lightning strikes.
4. Lightning channel impedance and attachment must be accounted for in the simulation.
5. Voltage and current levels used for these simulation tests must be high enough to excite arcs and nonlinear effects, if any.

It is not possible to meet all these requirements with any one of the simulation techniques currently in use. The best present techniques only satisfy a few of the necessary requirements in a typical setup. Hence differences are expected in the test data comparisons.

Data were collected to characterize several aspects of the interaction of simulated lightning environments on the test bed aircraft. These data may be separated into categories, such as, data for characterizing the simulator, data for characterizing the interaction and coupling of the environment with the simulator, and data characterizing the effects on aircraft electronic and electrical systems. These categories are described in the following sections. A summary tabulation of the number of voltage and current measurements made at various locations within the above categories during each level of testing is given in table 5.

SIMULATOR CHARACTERIZATION.

Measurements were made to characterize the simulator performance. These data were taken on every shot of the pulse generators and every sweep of the continuous wave generator. These measurements were used as reference levels and to monitor the proper operation of the pulse generators.

SOURCE CHARACTERIZATION.

Measurements were made to characterize the interaction and coupling of the simulated lightning strikes and the aircraft structure. Measurements were made on individual sources or source regions of voltages or currents and used to gain an understanding of the overall interaction and coupling process from the aircraft structure to the installed systems. This data is used to compare with the analysis models for these sources. A summary of specific source characterization measurements for each simulation method is listed in table 6. The two categories under each test method refer to nose (N) or wing (W) drive.

Measurement locations are shown in figure 18. EM source characterization sensors, described in chapter 3, were permanently installed at these locations in the test bed so that repeat measurements for the different simulations were made at the same location. Voltage drop/electric field sensors were installed at measurement points at the apertures and joints. Magnetic field sensors were located at all other source characterization test points.

SUBSYSTEM CHARACTERIZATION.

Measurements were made on mockup installations of wiring and equipment that are representative of the major aircraft systems. A summary of specific subsystem characterization measurements for each simulation method is listed in table 7. The listing shows measurements for a nose (N) and wing (W) drive for each test method.

These mockups cover a range of interconnect circuitry and wiring that is typical of equipment installation in a general aviation aircraft. Each of the major systems is represented. The wiring interconnects represent digital and analog signals, power, and grounds. Only a few wires and loads are included; it is assumed that the induced levels will be somewhat lower with more wires and loads present. However, future aircraft tend toward fewer wires and interconnects because of the trend toward digital systems and data busses.

These subsystem locations and circuit details are shown in figures 19 through 24. These systems were permanently installed so that repeat measurements using the different simulation techniques were made at the same locations.

TABLE 5 NUMBER OF TEST POINT VOLTAGE AND CURRENT MEASUREMENTS

Nose - Tail Drive

Location	30 kA		Shock		7 kA		1 kA		CW	
	V	I	V	I	V	I	V	I	V	I
Source Characterization										
Front and Rear Spar			2		2		2		2	
Wing Fuel Cavity					5		3			
Engine Compartment			1		2		2			2
Fuselage, Cockpit	1	7	1	12			1	12	1	12
Joints and Doors	3		5				6		1	
Subsystem Characterization										
Engine Control	3	3			4	1	4	1	4	1
Fuel-Electrical	2				2	1	2	1	2	1
Fuel-Mechanical	2	2			4	1	4	1	4	1
Power to Lights	2	2	2		4	2	4	2	4	2
Autopilot	3	3	3		13	3	13	3	9	3
Autopilot (pigtails removed)					3				5	
Total	12	14	15	36	29	34	27	30	22	

Wing - Tail Drive

Location	Shock		7 kA		1 kA		CW	
	V	I	V	I	V	I	V	I
Source Characterization								
Front and Rear Spar			2		2		4	
Wing Fuel Cavity							5	
Engine Compartment			1		1			
Fuselage, Cockpit	1	7	1	7	1	12	1	8
Joints and Doors	5		5		7		7	
Subsystem Characterization								
Engine Control	3		3		4	1	4	1
Fuel-Electrical	2		2		2		2	1
Fuel-Mechanical	2		2		4	1	4	1
Power to Lights	2	2	2	2	4	2	4	2
Autopilot	3	3	3	3	13	3	9	3
Autopilot (pigtails removed)	3		3		3		6	
Total	21	15	21	15	38	28	37	25

TABLE 6 COUPLING SOURCE CHARACTERIZATION MEASUREMENT POINT SUMMARY

Measurement Point	Test Technique									
	low-level swept CW		low-level pulse (1 kA)		mod-level pulse (7 kA)		shock excited		30 kA pulse	
	N	W	N	W	N	W	N	W	N	
I.2 Fuselage Currents and Fields										
IE1	scc		x		x		x	x	x	x
IE2	scc		x		x		x			
IF1	scc	x	x		x	x	x	x	x	x
IF2	scc	x	x		x	x	x	x	x	x
IF3	scc	x	x		x	x	x	x	x	x
IF4	scc	x			x	x	x			
IF5	scc	x			x	x	x	x	x	x
IF6	scc	x			x	x	x			
IF7	scc	x			x	x	x			
IF8	scc	x	x		x	x	x			
IF9	scc	x	x		x	x	x	x	x	x
IF10	scc	x	x		x	x	x			
IF11	scc	x	x		x	x	x	x	x	x
IF12	scc	x	x		x	x	x	x	x	x
VF12	ocv	x	x		x	x	x	x	x	x
I.3 Apertures and Joints										
VJ1	voltage drop		x		x	x	x	x	x	x
VJ2	voltage drop		x		x	x	x	x	x	x
VJ3	voltage drop	x	x		x	x	x	x	x	x
VJ4	voltage drop	x			x					
VJ5	voltage drop	x			x	x				
VJ6	voltage drop	x			x	x	x	x		x
VJ7	voltage drop	x			x	x	x	x		x
I.4 Wing Front and Rear Spars										
IW1	scc		x		x					
IW2	scc		x		x					
IW3	scc	x		x	x		x	x	x	x
IW4	scc	x		x	x		x	x	x	x
I.5 Wing Fuel Cavity										
IW5	scc		x		x	x	x			
IW6	scc		x		x	x	x			
IW7	scc		x		x	x	x			
IW8	scc		x		x		x			
IW9	scc	x			x		x			

x indicates measurement taken; 'scc' is short circuit current measured on the loop sensors; 'ocv' is open circuit voltage measured on the loop sensors

TABLE 7
ELECTRONIC/ELECTRICAL SYSTEMS CHARACTERIZATION MEASUREMENT POINT SUMMARY
(1 of 2 pages)

Measurement Point	Test Technique									
	low-level swept CW		low-level pulse (1 kA)		mod-level pulse (7 kA)		shock excited		30 kA pulse	
	N	W	N	W	N	W	N	W	N	W
II.1 Fuel System Electrical										
1I1 shield current	x	x		x		x				
1V1 cmv	x	x	x	x	x	x	x		x	x
1V2 cmv	x	x	x	x	x	x	x		x	x
II.2 Engine Control										
2I1 shield current	x	x	x	x	x	x				
2V1 cmv	x	x	x	x	x	x				
2V2 cmv	x	x	x	x	x	x	x	x	x	x
2V3 cmv	x	x	x	x	x	x	x	x	x	x
2V4 cmv	x	x	x	x	x	x	x	x	x	x
II.3 Autopilot										
3I1 bundle current	x	x	x	x	x	x	x	x	x	x
3I2 bundle current	x	x	x	x	x	x	x	x	x	x
3I3 bundle current	x	x	x	x	x	x	x	x	x	x
3V1 cmv	x	x	x	x	x	x	x	x	x	x
3V2 cmv	x	x	x	x	x	x	x	x	x	x
3V3 cmv	x	x	x	x	x	x	x	x	x	x
3V4 cmv	x	x	x	x	x	x	x			
3V5 cmv	x	x	x	x	x	x	x			
3V6 cmv	x	x	x	x	x	x	x			
3V7 cmv	x	x	x	x	x	x	x			
3V8 cmv	x	x	x	x	x	x	x			
3V9 cmv	x	x	x	x	x	x	x			
3V10 cmv			x	x	x	x	x			
3V11 cmv			x	x	x	x	x			
3V12 cmv			x	x	x	x	x			
3V13 cmv			x	x	x	x	x			
II.4 Power Lights										
4V1 cmv	x	x	x	x	x	x				
4V2 cmv	x	x	x	x	x	x	x	x	x	x
4V3 cmv	x	x	x	x	x	x	x	x	x	x
4V4 cmv	x	x	x	x	x	x	x	x	x	x
4I1 bundle current	x	x	x	x	x	x	x	x	x	x
4I2 bundle current	x	x	x	x	x	x	x	x	x	x

x indicates measurement taken; 'cmv' is common mode voltage to chassis

TABLE 7
ELECTRONIC/ELECTRICAL SYSTEMS CHARACTERIZATION MEASUREMENT POINT SUMMARY
(2 of 2 pages)

Measurement Point	Test Technique									
	low-level swept CW		low-level pulse (1 kA)		mod-level pulse (7 kA)		shock excited		30 kA	
	N	W	N	W	N	W	N	W	N	
II.5 Fuel Mechanical										
5V1A	cmv	x	x	x	x	x	x	x	x	x
5V1B	cmv	x	x	x	x	x	x	x	x	x
5V2A	cmv	x	x	x	x	x				
5V2B	cmv	x	x	x	x	x				
5I1	shield current	x	x	x	x	x				
II.6 Autopilot (Pigtails Removed)										
6V1	cmv	x	x		x	x	x	x	x	
6V2	cmv	x	x		x	x	x	x	x	
6V3	cmv	x	x		x	x	x	x	x	
6V4	cmv	x	x							
6V5	cmv	x	x							
6V6	cmv	x	x							

x indicates measurement taken; 'cmv' is common mode voltage to chassis

CHAPTER 5 - TEST PROCEDURES

INSTRUMENTATION.

Swept Continuous Wave Test. The continuous wave data acquisition system (CWDAS) developed by Science and Engineering Associates (SEA) consists of the equipment listed in table 8. This system is based on one that SEA developed for the Naval Surface Weapons Center. The system is computer controlled using the IEEE-488 HP-Interface Bus. The instrumentation was located in a wire mesh screen box during testing. Transfer functions, amplitude and phase, of the test point current or voltage referenced to the input current were displayed for each measurement. The command to store the data on disk was given by the operator. A diagram of the CWDAS is shown in figure 25.

TABLE 8 SEA CW DATA ACQUISITION SYSTEM EQUIPMENT LIST

Computer Controller	HP9816
Disk Drive	HP9121D
Network Analyzer	HP3577A
Printer	HP Thinkjet
Data Links	Lab Fiber Optics
Reference Current Probe	Pearson 110A
Test Current Probes	Singer 91550-2
	Tektronix 6022
Voltage Probe	High-impedance Fiber Optics

The same 50 ohm fiber optics unit was used throughout the test to measure the input current. A Pearson 110A current probe was used in the measurements of currents at the wing or nose. Short circuit loop sensor currents were measured using a Tektronix 6022 probe into a 50 ohm optics unit and wire bundle currents were measured using a Singer 91550-2 probe and the 50 ohm optics. Electronic subsystem voltages were measured using a fiber optics unit modified to have a high impedance input. A more complete description of the continuous wave simulation test is found in reference 21.

Pulse Tests. The data acquisition system used for all three pulse simulation tests was provided and operated by TSSI. It consisted of several battery powered fiber optic transmitter-receiver units, a waveform digitizer with 2 kilobytes of memory and 20 ns sampling rate capability, a dual 5.25 inch disk drive, and a plotter enclosed in a wire mesh screen box. The digitizer recorded 2 channels simultaneously so that for each pulse, the input current and measurement point data were stored in memory and displayed. Commands to store the data on disk were given by the operator. A list of equipment used is given in table 9 and figure 26 shows the test setup used for all of the pulse simulation tests.

The waveform digitizer had 256 levels of resolution approximately centered about 0. Full scale input was -1.27 V to +1.18 V with a minimum resolution of 10 mV. Data were digitized at a 20 or 40 ns sampling rate dependent on the decay time of the input pulse. A pretrigger time of 2 or 5 microseconds was set. The total data window was about 82 microseconds for 40 nanosecond sampling and approximately 41 microseconds for 20 nanosecond sampling.

TABLE 9 PULSE DATA ACQUISITION SYSTEM EQUIPMENT LIST

Data Links	Lab Fiber Optics
System Analyzer	Data Precision 6000
Input Amplifier	Data Precision 620
Disk Drive	Data Precision
Plotter	HP 7470
Reference Current Probes	T&M Research CT - .01 & .5 ohm CVR
Test Current Probes	Pearson 1025 EG&G COP-1 EG&G SCP-1
Voltage Probe	Pearson 110A High-Impedance Optics

A 50-ohm resistor was placed between the tail and the back plate of the return circuit for the low-level pulse test. This was done to match the measured input impedance of the combined test bed/return circuit using the CW system.

The same 50-ohm fiber optics unit was used throughout the test to measure the input current. Several current probes were used for measuring input currents and tail currents, dependent on the current amplitude. We chose to use the Pearson 1025 probe for moderate-level current measurements whenever possible because of the improved signal-to-noise ratio with the isolated probe. The short circuit loop sensor currents were measured using an EG&G COP-1 probe into a 50-ohm optics unit and currents on wire bundles between electronics were measured using an EG&G SCP-1 probe and the 50-ohm optics. Specifications for the various current probes used during the pulse tests are given in the test reports, references 22, 23 and 24. Electronic subsystem voltages were measured using a high impedance fiber optics unit.

TEST DESCRIPTIONS.

The lightning simulation tests were conducted using the test bed aircraft described in chapter 4 as the test article for these investigations. The four selected simulation test techniques were performed on the same instrumented test article with pre-test and post-test analysis. All tests were conducted at the Air Force Lightning Laboratory at Wright-Patterson Air Force Base, Dayton, Ohio. The test data were taken by TSSI personnel. A tabulation of the input pulse parameters for the various simulation methods is contained in table 10.

TABLE 10 PULSE PARAMETERS

Test	Peak Current (kA)	10-90% Rise-time (μs)	Time to Peak (μs)	Time to Half Value (μs)	Action Integral (A ² s)	Peak dI/dt (A/s)
low-level	1		.08	13	9.4	1.4 E10
moderate-level	7	2.8	6.3	51	1.92E3	3.13E9
	30	2.8	6.3	17	1.27E4	7.3 E9
Component A	200	2.8	6.4	69	2.0 E6	1.0 E11
shock-excited	7	2.8	6.3	51	1.92E3	3.13E9

Low-Level Swept Continuous Wave. The first lightning simulation test utilized a HP3577A network analyzer to excite the transients within the test bed aircraft. The network analyzer has a sensitivity of -130 dBm with a dynamic range of greater than 100 dB. The output drive level used was +15 dBm. Measurements were made over the frequency range of 100 Hz to 100 MHz with a resolution bandwidth of 1 Hz. Transfer functions were measured of the aircraft test points relative to the current at the lightning attachment point. They were then processed, considering the severe lightning current spectrum, to develop test point spectral responses. A major advantage of the CW test method is the low level of injected current that can be applied, while attaining a high signal-to-noise ratio.

SEA personnel prepared detailed test plans and were present to assist during data acquisition and to interpret the test results. Some initial testing was done to assure quality of the CW data.

Low-Level Fast-Rise Pulse. Low-level pulse tests were conducted on the test bed aircraft using the AFFDL Lightning Laboratory pulse generator. This generator consists of single gap capacitors, tightly coupled to the test article and return circuit. The generator has been used for the F-16/F-14 and F-18 aircraft lightning tests. The pulse generator was powered by a 50 kV power supply and delivered a pulse of 1 kA amplitude, 80₂ ns rise, 13 microseconds decay to half value, with an action integral of 9.4 A²s, and 1.4E10 A/s peak dI/dt. An example input waveform is seen in figure 27.

To produce the rise time, decay time, and peak amplitude defined for the low-level pulse waveform, the total circuit inductance and resistance must be held to low levels. Using a return circuit with upper and lower conductors shorted to the test cylinder will produce a low-resistance and low-inductance transmission line. Test circuit impedance, including inductance of the test article and return circuit, should be less than 80 milliohms. The test bed measured between 10 and 30 milliohms at DC. These test circuit parameters allow the Marx generator voltage and capacitance to be held at reasonable levels in terms of component cost and interconnection requirements.

The return circuit arrangement determines the field distribution around the airplane, and also affects the crowbar pulser performance. The conductors can be wire mesh, parallel cables, or thin metal sheets. The return circuit for the pulse tests consisted of parallel conductors - in this case wire mesh, above and below the test article. This return circuit and test bed arrangement presents the low inductance and resistance required for the pulser operation and produces a uniform field distribution around the test bed.

A high impedance 10x attenuator was made for this series of tests to use in conjunction with the high impedance fiber optics. This attenuator was necessary to keep some of the measurements within the ± 1 V maximum input level of the fiber optic transmitters.

Moderate-Level Pulse. The moderate-level pulse tests were conducted using the same test bed aircraft and return circuit as for the prior low-level pulse and swept CW tests. These tests were also conducted at the AFFDL Lightning Laboratory using their pulse generator, a schematic of which is given in figure 28. The generator was powered by a 160 kV DC power supply and delivered a pulse of 7 kA amplitude, 2.8 microseconds 10 - 90% rise, 6.3 microseconds time to peak, 51 microseconds decay to half value, with an action integral of 1920 A²s, and 3.13E9 peak dI/dt. An example input current waveform is shown in figure 29. The wave

shape parameters with the exception of amplitude are similar to those of Component A of the SAE-AE4L committee defined lightning threat, seen in figure 30.

The generator was not capable of producing a pulse of 30 kA current amplitude with the same rise and fall times of Component A. Figure 31 shows that a 20 microfarad capacity is required to do this. A limited number of measurements were made with peak input currents near 30 kA. The generator parameters are shown in figure 28. This pulse had the same rise time as the 7 kA generated pulse, but a much faster decay time of 17 microseconds and an action integral of 1.27E4 A²s. An example waveform is shown in figure 32.

Several high impedance attenuators were made for this series of tests to use in conjunction with the high impedance fiber optics. Attenuation factors of up to 10,000 were necessary to keep the measurements within the ± 1 V maximum input level of the fiber optic transmitters.

Shock-Excited Test. Tests were conducted on the test bed aircraft to determine the responses for the shock excited technique. The same test bed configuration (i.e. wiring and instrumentation) was used as for prior tests. The pulse generator was configured as for the 7 kA moderate-level test. The test bed was charged to a maximum of 150 kV with a 4 inch spark gap placed at the tail. The input pulse had a peak of about 7 kA, a 10-90% risetime of 2.8 microseconds, and time to half value of 51 microseconds. The peak electric field between the test bed and return circuit was 355 kV/m and the peak dE/dt was 7.1E11 V/m-s. An example waveform is seen in figure 33.

IMPEDANCE MEASUREMENTS.

Input impedance of the coaxial test bed/return circuit was measured using the CWDAS at the nose and the wing looking into a short circuit, open circuit, and 50 ohms. Figures 34 and 35 show the short and open circuit input impedance at the nose. The wing short and open circuit input impedances are seen in figures 36 and 37. The structure resonance at 5 MHz is a prominent feature in each of these measurements. Both measurements into 50 ohms, figures 38 and 39 indicate that the system is well-matched, within one dB of 50 ohms. The DC resistance and inductance were determined using the short circuit measurements.

$$R_{dc}(\text{nose}) = 1 \text{ ohm}$$

$$R_{dc}(\text{wing}) = 0.8 \text{ ohms}$$

At 1 MHz,

$$\begin{aligned} L_{\text{nose}} &= 26 \text{ dB} / 2\pi \mu\text{H} \\ &= 3.18 \mu\text{H} \end{aligned}$$

$$\begin{aligned} L_{\text{wing}} &= 20 \text{ dB} / 2\pi \mu\text{H} \\ &= 1.59 \mu\text{H} \end{aligned}$$

The system capacitance was found using the open circuit results at 1 MHz.

$$\begin{aligned} C_{\text{nose}} &= 1 / (2\pi * 45 \text{ dB}) \mu\text{F} \\ &= 0.9 \text{ nF} \end{aligned}$$

$$\begin{aligned} C_{\text{wing}} &= 1 / (2\pi * 42 \text{ dB}) \mu\text{F} \\ &= 1.26 \text{ nF} \end{aligned}$$

Input impedance was calculated from the calculated capacitance and inductance.

$$Z = \sqrt{L/C}$$

$$\begin{aligned} Z_{\text{nose}} &= \sqrt{3.18E-6 / .9E-9} \\ &= 59 \text{ ohms} \end{aligned}$$

$$\begin{aligned} Z_{\text{wing}} &= \sqrt{1.59E-6 / 1.26E-9} \\ &= 36 \text{ ohms} \end{aligned}$$

DATA QUALITY VERIFICATION.

System Calibrations. System calibrations were performed daily to verify the correct operation of the CW measurement equipment and to obtain system inherent responses for proper data calibration. The measurements were taken twice daily or at any time the system configuration changed. The data obtained from system calibrations were subtracted from measurement data to remove inherent system responses. These data are referred to as calibration data and are stored along with measurement data on magnetic storage media.

Pulse tests began each day with a calibration of the fiber optic units. A calibration was also done whenever an optics units was replaced. For calibration, a ± 1 V sine wave was input to each fiber optic unit. The output signal was read by the Data Precision digitizer and the receiver was adjusted until the digitizer indicated the signal was ± 1 V.

Noise Measurements. Noise measurements were taken at each measurement location during the CW test with a coaxial cable terminated in 50 ohms or a current probe with nothing through its center as input to the fiber optics. These measurements were compared to the corresponding test point measurement to determine the ratio of signal-to-noise. The measurement was checked across the entire 100 Hz to 100 MHz range. A signal level 10 dB above the noise level is considered reliable data. The noise measurements are referred to as noise data and are saved on magnetic storage media.

Noise measurements were taken at several points within the test bed during the pulse tests. The measurements were made with either a coaxial cable terminated in 50 ohms or a current probe with nothing through the center as the input to the fiber optics. Both optics units, at the reference point and the test point, were shielded with aluminum foil for the moderate-level tests. This shielding prevented pulser noise from degrading the measurements.

Validity Checks. Validity checks were performed by the senior scientist during each test. These checks consisted of comparing the measured responses against theoretical models for their behavior to make sure the measured response curves were "reasonable". Any failure to produce "reasonable" data was considered a failure in the instrument setup and/or test bed connection and steps were taken to correct the problem.

DIGITAL DATA FORMATS.

All measurements taken during the CW test were taken on an HP-3577A network analyzer using IEEE 64 bit binary format. The data were passed to the HP-9816 computer for organization, calibration, display, and storage. Measurement data consists of all data necessary to duplicate the measurement, instrument state data, the calibration data used on the measurement, and the actual data measured (amplitude and phase).

Measurements taken during the pulse tests were taken using a Data Precision Analyzer 6000. The resolution of the digitizer was 8 bits. The data were stored on disk in a two's complement floating point format. A header containing the number of points, the time base, the attenuation factor, the x and y offsets, and title of the measurement was stored with each measurement. The measurement parameters of the Data Precision were stored on disk for recall each day during testing.

DATA LOGS.

Data logs were kept to associate test point number with measurement description, calibration data, instrument state, and data file name. These logs were filed daily in the test notebook along with a plot of each measurement and the test setup. Descriptions of any changes made in the test bed setup or any problems encountered were logged daily.

CHAPTER 6 - EXPERIMENTAL DATA

All data were extrapolated to severe lightning threat levels for comparison. The waveform used as the severe threat is Component A as defined by the SAE-AE4L committee (see figure 30). The parameters of this waveform are 200 kA peak amplitude, 2.85 microsecond 10-90% rise time, 6.4 microsecond zero-to-peak time, 69 microsecond decay time to half value, and dI/dt of $1.0E11$ A/s at 0.5 microseconds. Figure 40 shows a comparison of the frequency spectrum of Component A and nominal spectra for the 1 kA low-level pulse, the 7 kA moderate-level pulse, the 30 kA moderate-level pulse, and the shock-excited pulse. As can be seen in this figure, the difference in amplitudes between the lightning spectrum and each pulse spectrum is a constant over the entire frequency range only for the 7 kA moderate-level spectrum (variations less than 2 dB). This indicates that extrapolation to the severe threat level will be most accurate using the 7 kA pulse data. No judgement as to the type of response, IR or dI/dt , needs to be made. The scaling factor used for the extrapolation will be a constant for any measurement. Results from all other simulation tests will require a different scaling factor for resistive and dI/dt responses. Nominal scaling factors obtained from the differences in amplitudes and rates-of-rise between Component A and each of the pulse simulations are given in table 11 below.

TABLE 11
SCALING FACTORS FOR EXTRAPOLATING PULSE MEASUREMENTS TO SEVERE THREAT LEVELS

Simulation Technique	Scaling Factor	
	IR	dI/dt
1 kA pulse	200	8
7 kA pulse	29.4	29.4
30 kA pulse	6.7	13.7
shock-excited	29.4	29.4

Tables 12 and 13 contain extrapolated peak amplitudes and times for each test point and simulation method for nose and wing drives respectively. In a few instances when data did not get stored on the disk, no times are listed and peak values are estimated from maximum values recorded during testing. In order to obtain the extrapolated data, each time domain waveform was classed as either an IR or dI/dt response. In cases when both responses were present, the largest was picked and used to determine the scaling factor. In order to obtain time domain responses from frequency domain transfer functions measured with the CW system, the frequency spectrum of Component A was added to the measured data and Fourier transformed to obtain the pulse response due to a severe lightning strike. Examples of the extrapolation for both pulse and CW are discussed below.

Figure 41 shows the CW measured transfer function at test point N3V1, a shielded cable from the autopilot system, and the analysis sequence required to obtain a pulse response extrapolated to the severe lightning threat. The measured data, instrumentation response and probe factors have already been removed, are shown in (a). From 10 MHz to 100 MHz, the noise level is greater than the signal. This was determined from an independent noise measurement at that test point. The noise was removed from the data to obtain the smoothed curve in (b). This transfer function is multiplied by the Component A frequency spectrum to yield (c), which is Fourier transformed to the time domain to obtain the pulse shown in (d). The peak magnitude and time of (d) are those listed in table 12.

The data shown in figure 42 is an example resistive response measured at the same test point, 3V1 using a nose-tail drive, for each of the pulse simulations. The time scales for the low-level and 30 kA pulses are half that of the other two. Note the amplitude is nearly the same for the 7 kA and the shock-excited pulse responses. The individual test point responses do not scale linearly at the different drive levels. A resonance is superposed on the leading edge of the shock-excited response. In order to obtain the extrapolated values given in table 12, the peak measured value was determined and used in equation 6-1.

$$\text{Extrapolated peak} = \text{Measured peak} * \text{SF} * (\text{Nominal peak input} / \text{Actual peak input}) \quad (6-1)$$

where SF is the scaling factor for an IR response determined from table 11 for the appropriate simulation technique. The measured peak value includes in-line attenuation used during the test point measurement. The nominal peak values are 1 kA, 7 kA, and 30 kA for each of the simulations. There were some differences in the output of the generator so that the actual peak current input was recorded for each shot. These values are given in the test reports, references 22, 23, and 24.

For example, the 1 kA measured peak response at N3V1 was 150 mV and the actual peak input current was 1130 A. The extrapolated peak, 26.6 V, given in table 12 was determined by:

$$\begin{aligned} \text{Extrapolated peak} &= .151 \text{ V} * 200 * (1000 \text{ A} / 1130 \text{ A}) \\ &= 26.6 \text{ V} \end{aligned}$$

The extrapolated values for the remaining pulse simulation measurements at N3V1 are given below.

$$\begin{aligned} \text{Extrapolated peak (7 kA)} &= 8.47 \text{ V} * 29.4 * (7000 \text{ A} / 6840 \text{ A}) \\ &= 255 \text{ V} \end{aligned}$$

$$\begin{aligned} \text{Extrapolated peak (30 kA)} &= 17.8 \text{ V} * 6.7 * (30 \text{ kA} / 25 \text{ kA}) \\ &= 143 \text{ V} \end{aligned}$$

$$\begin{aligned} \text{Extrapolated peak (shock)} &= 8.2 \text{ V} * 29.4 * (7000 \text{ A} / 6970 \text{ A}) \\ &= 244 \text{ V} \end{aligned}$$

An example of a dI/dt response at test point VF12 for the nose-tail drive is presented in figure 43. This test point was not measured using the 30 kA drive. Again note the resonance which appears on the shock-excitation response and the different time scale on the low-level pulse response. It is possible to get a lower bound only on the low-level and shock-excited responses. These responses were extrapolated to severe threat levels using equation 6-2.

$$\text{Extrapolated peak} = \text{Measured peak} * \text{SF} \quad (6-2)$$

where the SF is the scaling factor determined from table 11 under the dI/dt response category. For the 7 kA simulation, this scaling factor is the same as for an IR response. The measured peak includes attenuation factors.

For the 1 kA measured response at test point NVF12, the measured peak was 11.8 V, the digitizer saturated at this point. The extrapolated peak can be given only as a lower bound.

$$\text{Extrapolated peak} > 11.8 \text{ V} * 8 = 94.4 \text{ V}$$

TABLE 12
EXTRAPOLATED PEAK VALUES AND TIMES FOR EACH TEST TECHNIQUE - NOSE DRIVE
(1 of 3 pages)

Test Point	low-level CW		low-level pulse (1 kA)		moderate-level pulse (7 kA)		shock excitation	
	Peak (A)	Time (μs)	Peak (A)	Time (μs)	Peak (A)	Time (μs)	Peak (A)	Time (μs)
I.2 Fuselage Currents and Fields								
NIE1	3440	2.0	2127	.1	1313	1.1	1193	1.0
NIE2	140	4.0	33.7	.1	35.5	1.8		
NIF1	498	6.0	149	1.1	237	3.5	223	3.1
NIF2	714	8.0	172	2.9	171	4.2	204	4.7
NIF3	622	44.0	80.7	1.6	33.7	10.7	77	10.0
NIF4	62.3	6.2	42.2	.1	9.1	1.1		
NIF5	487	15.6	99	.1	332.8	3.6	352	3.3
NIF6	noise		.9	.1	6.7	3.3		
NIF7	906	42.0	67.4	.1	149.4	3.8		
NIF8	540	25	58.6	2.2	60	4.5		
NIF9	548	4.0	112	6.2	148	9.1	87	7.6
NIF10	380	44.0	54.7	1.6	94.7	5.3		
NIF11	1970	6.2	1796	.1	982	1.6	714	1.4
NIF12	1710	2.4	1451	.1	1030	1.8	728	1.3
NVF12	520	0.25	> 94.4	.1	436	.2	> 768	
I.3 Apertures and Joints								
NVJ1			306	.1	170	.2	149	1.0
NVJ2			113	.1	154	.1	96	.2
NVJ3	1700	3.3	953	.7	1059	3.1	1079	3.1
NVJ4								
NVJ5			11.3	.1				
NVJ6			11.7	.1	5.4	5.8		
NVJ7			noise		9	26.7		
I.4 Wing Front and Rear Spars								
NIW1								
NIW2								
NIW3			22	.4	22.6	1.1	35	3.0
NIW4			406	.1	205	1.3	218	1.6
I.5 Wing Fuel Cavity								
NIW5			41.9	1.1	44.6	5.3		
NIW6			noise		5.6	1.7		
NIW7			31.1	5.3	28.2	8.2		
NIW8					353	3.8		
NIW9					54.4	13.3		

* indicates measurement also taken at 30 kA in moderate-level pulse setup

TABLE 12
EXTRAPOLATED PEAK VALUES AND TIMES FOR EACH TEST TECHNIQUE - NOSE DRIVE
(2 of 3 pages)

Test Point	Test Technique							
	low-level CW		low-level pulse (1 kA)		moderate-level pulse (7 kA)		shock excitation	
	Peak (A)	Time (μs)	Peak (A)	Time (μs)	Peak (A)	Time (μs)	Peak (A)	Time (μs)
II.1 Fuel System - Electrical								
N1I1	34	.08	> 10.2	.1	9.2	.1		
*N1V1	300	2.5	52.3	1.3	124	2.0		
*N1V2	100	1.2	33	1.3	43.7	1.1		
II.2 Engine Control								
N2I1	806	3.2	698	.1	503	3.5		
N2V1	10	1.8	noise		6.7	22.1		
*N2V2	50	3.8	noise		noise		4.4	.1
*N2V3	54	2.0	123	.1	187	3.3	74.8	.1
*N2V4	53	1.6	90	.1	185	3.6	75.7	.1
II.3 Autopilot								
N3I1	1790	16	680	7.8	1581	7.9	1570	7.4
N3I2	5820	16	677		763	4.9	702	4.8
N3I3	7010	44	1214	10.9	1839	7.1	1812	7.3
*N3V1	220	40.0	26.6	1.8	255	23.1	244	22.8
*N3V2	1065	1.6	52	1.6	315	.9	207	1.8
*N3V3	535	30.0	154	.1	617	29.1	610	30.2
N3V4	125	62.5	8	.1	95.4	39.6		
N3V5	225	43.0	23.3	10.2	318	50.0		
N3V6	210	9.8	11.9	1.8	46	9.5		
N3V7	54	60.0	8	9.8	17.8	1.4		
N3V8	54	44	44.6		88	32.2		
N3V9	105	40.0	48.4	.7	105	31.6		
N3V10			2.7	.1	9.5	.1		
N3V11			188	.1	335			
N3V12			8	1.8	19.3	6.9		
N3V13			27.4	11.3	309	50.0		
II.4 Electrical Power - Lights								
N4V1	235	0.08	26.2	3.3	44.6	.4		
*N4V2	7500	0.04	1031	2.2	4146	2.2	> 4608	
*N4V3	1575	16	1938	.2	1776	12.7	1435	18.9
N4V4	41	0.2	49.1	.1	570	.1		
N4I1	46.7	.15	50.8	.1	73	.1	> 154	
N4I2	17.7	.1	> 9.4	.1	9.7	.1	56.8	.1

* indicates measurement also taken at 30 kA in moderate-level pulse setup

TABLE 12
EXTRAPOLATED PEAK VALUES AND TIMES FOR EACH TEST TECHNIQUE - NOSE DRIVE
(3 of 3 pages)

Test Point	Test Technique							
	low-level CW		low-level pulse (1 kA)		moderate-level pulse (7 kA)		shock excitation	
	Peak (A)	Time (μs)	Peak (A)	Time (μs)	Peak (A)	Time (μs)	Peak (A)	Time (μs)
II.5 Fuel - Mechanical								
*N5V1A	206	.4	132	.1	172	1.6	149	2.2
*N5V1B	98	.4	84.3	.1	63.7	.9	no signal	
N5V2A	60	.16	87.6	.1	31.5	.9		
N5V2B	30	.6	7.3	.1	9.6	1.6		
N5I1	6.6	.16	noise		28.4	.1		
II.6 Autopilot - Pigtails Removed								
N6V1	565	2.4			466	3.6		
N6V2	2350	1.2			1118	.9		
N6V3	1280	16.0			5485	.1		
N6V4	250	1.6						
N6V5	620	16						
N6V6	1580	1.2						
Test Point	Input Peak Current (kA)			moderate-level pulse (30 kA)				
				Peak (A)	Time (μs)			
II.1 Fuel System - Electrical								
N1V1	25.0			121	2.7			
N1V2	25.0			41.6	1.4			
II.2 Engine Control								
N2V2	26.0			1.5	.2			
N2V3	25.0			84.4	3.6			
N2V4	25.5			80	3.8			
II.3 Autopilot								
N3V1	25.0			143	5.4			
N3V2	25.0			322	2.0			
N3V3	25.5			592	6.0			
II.4 Electrical Power - Lights								
N4V2 \	9.5			6279	1.7			
N4V2 at varied currents	15.7			5656	1.9			
N4V2 /	21.0			7533	1.1			
II.5 Fuel - Mechanical								
N5V1A	27.7			102	2.0			

TABLE 13
EXTRAPOLATED PEAK VALUES AND TIMES FOR EACH TEST TECHNIQUE - WING DRIVE
(1 of 3 pages)

Test Point	Test Technique							
	low-level CW		low-level pulse (1 kA)		moderate-level pulse (7 kA)		shock excitation	
	Peak (A)	Time (μs)	Peak (A)	Time (μs)	Peak (A)	Time (μs)	Peak (A)	Time (μs)
I.2 Fuselage Currents and Fields								
WIE1					82.2	1.4	50.7	10.7
WIE2								
WIF1	660	38	120	.7	183	3.1	156	3.6
WIF2	200	3.8	> 249	.1	117	5.6	112	4.9
WIF3	478	24	31.6	2.2	87.4	5.8	54.5	5.6
WIF4			52.7					
WIF5			319	1.1	424	3.6	390	3.4
WIF6			84.1	.1				
WIF7			25.8					
WIF8	noise		25.3	.2				
WIF9	474	2.8	115	6.0	163	10.0	144	9.3
WIF10	428	44	108	2.2				
WIF11	1580	2.4	1824	.1	1041	1.3	913	1.3
WIF12	1750	2.0	1775	.1	869	1.2	862	1.2
WVF12	660	.2	> 94	.1	528		> 1705	
I.3 Apertures and Joints								
WVJ1	7300	4.8	302	.1	426	.1	266	.5
WVJ2	510	.2	300	.1	220	.4	302	.2
WVJ3	920	3.2	1103	.2	1016	2.2	1019	3.1
WVJ4	970	1.6	1215	.2				
WVJ5	1000	1.9	1165	.2				
WVJ6	320	3.4	114	.1	225	6.0	48.3	3.6
WVJ7	380	4.0	184	.1	217	8.0	141	2.7
I.4 Wing Front and Rear Spars								
WIW1	3430	7.2	292	.7				
WIW2	3720	7.3	1485	2.2				
WIW3	754	1.2	2069	.1	932	1.3	1311	.9
WIW4	445	1.2	1590	.2	792	.9	833	1.0
I.5 Wing Fuel Cavity								
WIW5			769	2.7				
WIW6			126	5.3				
WIW7			739	2.4				
WIW8	2660	3.2	2281	1.8				
WIW9	4920	5.6	1936	2.2				

TABLE 13
EXTRAPOLATED PEAK VALUES AND TIMES FOR EACH TEST TECHNIQUE - WING DRIVE
(2 of 3 pages)

Test Point	Test Technique							
	low-level CW		low-level pulse (1 kA)		moderate-level pulse (7 kA)		shock excitation	
	Peak (A)	Time (μs)	Peak (A)	Time (μs)	Peak (A)	Time (μs)	Peak (A)	Time (μs)
II.1 Fuel System - Electrical								
W1I1	20.2	.16	noise					
W1V1	2545	3.6	934	.1	516	1.8	505	2.8
W1V2	800	1.2	578	.1	155	.9	218	.4
II.2 Engine Control								
W2I1	141	3.6	90.2	.1				
W2V1	noise		noise					
W2V2	10	4.2	noise		noise		5	.1
W2V3	400	1	192	.1	8.9	.8		
W2V4	150	1.2	177	.1	102	.5		
II.3 Autopilot								
W3I1	17100	18.0	605	4.4	275	5.3	182	4.0
W3I2	60600	16	5372	2.7	4356	2.8	4487	3.1
W3I3	15300	44.0	1905	6.4	3358	4.9	3651	4.2
W3V1	1150	2.4	152	.1	57	2.0	38.4	2.2
W3V2	9100	2.0	5222	.1	1813	1.6	1578	1.8
W3V3	1850	2.4	971	.1	821	31.6	1853	2.2
W3V4	350	32	18	5.8				
W3V5	550	24	114	10.7				
W3V6	2550	22	252	4.7				
W3V7	250	32	19.5	5.8				
W3V8	350	3.2	109	.2				
W3V9	400	3.2	112	.2				
W3V10			28.3	.2				
W3V11			83	.1				
W3V12			186	4.9				
W3V13			119	8.9				
II.4 Electrical Power - Lights								
W4V1	255	.06	62.6	.1				
W4V2	32000	1.4	35500	.1	11300	1.2	23000	.7
W4V3	2950	2.2	5765	.1	3214	1.8	4220	2.2
W4V4	8	3.6	noise					
W4I1	212	.08	> 50.8	.1	10.9	4.8	610	.4
W4I2	17	.56	> 9.4	.1	1.8	8.2	58	.04

TABLE 13
EXTRAPOLATED PEAK VALUES AND TIMES FOR EACH TEST TECHNIQUE - WING DRIVE
(3 of 3 pages)

Test Point	Test Technique							
	low-level CW		low-level pulse (1 kA)		moderate-level pulse (7 kA)		shock excitation	
	Peak (A)	Time (μs)	Peak (A)	Time (μs)	Peak (A)	Time (μs)	Peak (A)	Time (μs)
II.5 Fuel - Mechanical								
W5V1A	1175	1.4	1670	.2	351	1.2	350	.1
W5V1B	465	1.6	70.3	.1	162	.9	159	.9
W5V2A	430	2	51.6	.2				
W5V2B	90	4.6	noise					
W5I1	56	.01	28.1	.2				
II.6 Autopilot - Pigtails Removed								
W6V1	1500	8.0	226	.4	82.5	2.2	79.3	2.7
W6V2	20000	1.9	30200	.1	6791	1.3	5815	1.3
W6V3	2500	4.8	950	.7	1435	13.0	2526	4.0
W6V4	700	2.4						
W6V5	1350	2						
W6V6	10650	.01						

CHAPTER 7 - DATA ANALYSIS AND MODELING

DATA ANALYSIS.

The measurement points placed throughout the test bed yielded values from very large to very small. Pigtail currents on long wire runs were large, induced currents on short runs of internal shielded wiring were small, and measured values at other test points ranged in between. The extrapolated currents and voltages given in tables 12 and 13 for the nose and wing drives of each simulation technique were ranked in order. If we assume that each set of measurements covers 98% of the possible range of values, i.e., between the 1 and 99 percentiles, then the cumulative percentage of measurements exceeding each value can be determined. The log normal values were calculated using the inverse probability function given in equation 7-1.

$$x = \sqrt{(-\pi/2) * \ln(1 - 4 * (P(x)/100 - .5)^2)} \quad \text{for } P(x) \geq 50$$

$$= -\sqrt{(-\pi/2) * \ln(1 - 4 * (P(x)/100 - .5)^2)} \quad \text{for } P(x) < 50 \quad (7-1)$$

where $P(x)$ is the cumulative percentage. These values were plotted on a log normal probability grid of the percentage of measurements exceeding a level versus the logarithm of the magnitude of the extrapolated values.

The log normal plots are shown in figures 44 through 51. A linear regression was performed to determine the best fit line to the values on each plot. Thirty or more measurements were included for each configuration. The mean and 50% values were calculated and are tabulated in table 14. Standard deviation was also calculated. The plus one sigma value at the fifty percent level is indicated on figures 44 through 51 using an 'x'. Data from the 30 kA pulse simulation were not treated in this way, because the sample volume was less than 30.

TABLE 14 CALCULATED STATISTICAL VALUES FOR EACH SIMULATION METHOD

	low-level CW		low-level pulse (1 kA)		moderate-level pulse (7 kA)		shock excitation	
	N	W	N	W	N	W	N	W
Extrapolated Data								
Mean	300	620	72	280	130	330	270	410
50% Value	270	570	66	260	120	290	230	370

The fit to the 7 kA moderate-level pulse results was used as the baseline for comparison of the four simulation techniques. These moderate-level pulse extrapolated data were determined to be the most accurate for several reasons.

1. There is less uncertainty in scaling from 7 kA to 200 kA than from very low current levels.

2. Non-linear effects, noted at several test points, were not evident at lower levels of injected current.

3. The waveshape was similar to that of Component A of the severe lightning threat which decreased the amount of analysis necessary to obtain extrapolated responses due to the severe lightning threat. A determination of IR or DI/dt type coupling responses was not necessary, since the scaling factor was the same for either type of response.

Mean values for all the test results, both measured and extrapolated, were a factor of two to four larger for the wing drive compared to the nose drive, so, for the test bed aircraft, a wing-tail strike represents a worse case than a nose-tail strike.

Mean values for the moderate-level extrapolations are larger by a factor of two over the low-level pulse mean values. The CW and shock-excitation mean values are both larger than the moderate-level mean values by factors of two.

A comparison of figures 44 through 47, extrapolated results in the nose drive configuration, shows that the slopes of the best fit lines are nearly equal. The low-level fit is about 4 dB less overall than the moderate-level fit. The shock-excitation is skewed higher at low levels, indicating the larger uncertainty in the determination of peak values in small measurements. The CW fit is higher overall by 8 dB than the moderate-level fit. Thus, the extrapolated values from the CW simulation technique are more conservative.

Similar results are apparent when comparing figures 48 through 51, extrapolated results from the wing drive configuration. In this case, the low-level and moderate-level pulse fits are nearly equal. The skew in the shock-excitation fit at low levels is not as great as in the nose drive. The CW fit shows the same value at the moderate-level fit at low levels, but is up to 12 dB larger at high levels. For the wing attachment configuration, the CW simulation technique is also more conservative at the larger, more critical levels.

A comparison of the measured currents and voltages for the pulse tests plotted in the same format, figures 52 through 57, shows the factor of seven difference between the low-level and moderate-level responses which corresponds to the ratio of injected current magnitudes. The shock-excitation and moderate-level pulse results are nearly the same, within factors of two, as expected. Some skew is evident at low levels where the signal-to-noise ratio is small. These observations are similar for both the nose and wing drives.

COMPUTER MODELING.

Computer models were developed to aid the test effort; figure 58 illustrates the modeling process. The coupling parameters included will define physical parameters of the test article for the current on the aircraft. These models include internal and external coupling terms.

The external coupling region contains resistive and inductive terms. The early time, inductive term appears as magnetic fields around the test bed. The late time, resistive term appears as a voltage along the structure. The internal fields due to leakage through apertures contribute to fast rise voltages. Effects due to diffusion through the skin will have a much slower rise time.

Sources of internal currents in the wiring include B-dot coupling, E-dot coupling, and IR coupling. The magnitude of these sources is dependent on local structure, currents, and fields. When lightning currents flow in the structure, electric and magnetic (EM) fields build up and change rapidly in accordance with the lightning current pulses. Some of these EM fields will leak into the internal portions of the aircraft through openings in the structure such as windows, radomes, access panels, and doors. Electrical imperfections such as joints, gaps, and holes also allow the entry of some EM fields. In addition to the EM fields coupling, there may be resistive voltage drops in the structure as lightning currents flow. Currents may also flow inside the structure as a result of structural interconnections which can affect the internal EM environments.

Voltages are coupled into aircraft wiring in several ways. If part of a circuit connecting electronic equipment connects to structure, there will be a voltage difference between the wires and the structure. Voltages are also coupled between wires by electric and magnetic induction, even if the wires are not connected to structure. The effects of induction depend upon the time rates of change of the lightning currents and EM fields. Since the total structural voltage drops depend upon both the inductive and resistive terms, voltages in the wiring depend upon the lightning current time rate of change as well as the peak current values.

For an aircraft made of aluminum, the coupled voltages are rarely important except when the lightning current flows through joints and hinges. However, the resistance of an advanced structural material such as graphite epoxy is many times that of aluminum. Voltages of a few tenths of a volt have no effect in an aluminum structure. Voltages that are larger by a factor of several hundred to a thousand times than those for aluminum because of the much lower conductivity of the composite materials can become very serious.

Results of EM coupling modeling were used to predict the results of each test prior to the experiments and updated from test results. This established limitations on the modeling methods and of the uncertainties inherent in the application of these analysis tools. The models continue to be upgraded based upon the results of the testing and the understanding of test setups and the limitations of the simulation process.

These results lead to criteria for application of the four methods to demonstration of lightning protection design. The criteria contain specific recommendations on methods and ranges for test conditions and appropriate error bars for uncertainty in the results of the application to aircraft. Prior test reports have been used as applicable for supporting the findings of this program so as not to work in isolation.

Modeling Methods For Composite Structures. The modeling of energy penetration from the exterior to the interior has several common elements for any aircraft particularly in the apertures and exterior wiring and cables. The principal difference between metal and composite aircraft lies in the increased contribution of the resistive voltage drop (IR) in the fuselage and wing skins and in the increased current flow paths in the structure. This is because the graphite epoxy structure has typically 1000-3000 times higher resistance than the similar aluminum metal structure. For frequencies above a few megahertz, or early time on the order of a few microseconds, there is no difference in the lightning response between aluminum and graphite structures. This is because at high frequencies, electromagnetic "skin-effect" forces the currents to the outside of the materials

and to the outside of the structure. Protection against the early pulse is essentially the same for both structural materials; keep wiring near metal of structure to reduce the magnetic field B-dot coupling factors.

The main difference in energy penetration between graphite and aluminum structures is at low frequencies below the megahertz range, or late time on the order of a few tens of microseconds. Considerable current flows into the interior as a result of the range of thicknesses and materials used in aircraft structure. Since the current flow is resistive for graphite epoxy materials, the protection measure of keeping the wiring close to structure will not have any protective effect. Furthermore, the IR voltage drop will be much larger for graphite epoxy than for aluminum.

The Bellanca test bed has been designed with consideration for protection of the internal equipment against these internal currents and fields. The entire structure has been provided with a current path for the low frequency, late time lightning currents. The current path in the fuselage is provided by means of an aluminum screen mesh bonded to the inside of the skin. The wing front and rear spars have been lined with three mil aluminum foil and a thin wall conduit runs along the leading edge to provide a current path in the wing. This design is also intended to improve the grounding and bonding of the electronic equipment and wiring.

REDIST Models. Two-dimensional models of the wing and the fuselage were run using a computer code, REDIST, developed by SEA. REDIST was devised to compute the current distribution and electromagnetic fields external and internal to a two-dimensional structure composed of electrically connected thin strips of arbitrary conductivity and thickness. The assumptions fundamental to the code are:

1. The structure may be locally approximated as two-dimensional.
2. Current flow is directed along the axis of the structure.
3. The cross-section of the structure is electrically small across the frequency range of interest.

The solution technique, based on the method-of-moments, proceeds as follows. First, the conducting surface is finely divided into axially-directed strips. The surface current density is assumed constant across the width of each strip; this is true for resistive and inductive current division, the frequency regimes for which this code is valid. If, after the current distribution is obtained, the currents in adjacent strips exhibit abrupt changes, then finer divisions are tried. The process is continued until the variation of current between adjoining strips is sufficiently small. After the surface has been subdivided, the vector potential is expressed as the superposition of the strip potentials. The strip potential is the surface current density of the strip, multiplied by the potential for unit current density. The latter is a function of position, as well as strip width and orientation.

Having expressed the vector potential in terms of the unknown current densities, the next step is to solve for the current distribution by imposing the boundary condition that the sum of the electric field and vector potential equals one. Finally, the desired shield currents, electric fields, and magnetic fields are calculated.

Verification of REDIST and a more complete discussion of the code is found in reference 25.

Two models, fuselage and wing, are shown in figures 59 and 60. The fuselage was modeled at body station 179, aft of the wing. The model includes the graphite skin and the aluminum mesh integrated into the bottom of the test bed. The shield representing the autopilot cable is shown. The configuration at station 88 was used for the wing model. It contains the front and rear spars, the graphite top and bottom skins, the conduit at the leading edge, and the autopilot shield parallel to the rear spar. In both cases, a symmetric model was run which assumes two shields present.

The output from REDIST is a transfer function of shield current relative to total current given in real and imaginary parts, magnitude, and phase. This transfer function is multiplied by the lightning threat spectrum and then Fourier transformed into a current pulse in the time domain. The values given in table 15 were obtained in this way. The calculated transfer function was multiplied by the low-level pulse spectrum, the moderate-level pulse spectrum, and the severe threat lightning spectrum for comparison to the measured results from the various simulation tests. Good agreement is found between measurements and the REDIST calculated values. The values measured in the wing drive configuration vary by a factor of six or less from the model results. The measured values of the nose drive configuration differ by factors of four or less from the model results.

TABLE 15
COMPARISON OF AUTOPILOT MEASURED VALUES WITH REDIST MODEL CALCULATED VALUES

Test Point	Simulation Method	Measured Values (Amps)		REDIST Values Amps
		Nose Drive	Wing Drive	
3I2 wing	low-level		30	25.4
	moderate-level		150	291
	CW (200 kA)	60600		9000
3I3 fuselage	low-level	7	9	14
	moderate-level	60	110	248
	CW (200 kA)	7010	15300	8500

Resistor Model. A detailed resistor model of the test bed was put together using measured resistances from table 4 along with known thicknesses and conductivities of the four-ply graphite epoxy skin, the aluminum foil, the aluminum screen, the aluminum conduit, and aluminum sheet metal. Conductivities used were 1.5E4 mhos/m for the graphite and 3.5E7 mhos/m for aluminum. Each fastener was assumed to have 10 milliohms resistance. Models for the fasteners were developed in reference 26. The model was input to PC SPICE 2.6, a circuit analysis package, which performed a transient analysis of the model. A schematic of the model is shown in figure 61. The input to the model was user-defined as a double exponential pulse with the parameters of Component A, the severe lightning threat. Several runs were made to obtain results with a lightning attachment at the nose and wing and to use resistances of cable shields which changed during the course of the tests. The peak currents calculated at various test points are listed in table 16. The column labelled CW resistances used the resistances measured during the CW test. The column labelled pulse resistances used an average of the measured cable resistance values, listed in table 4, of the three pulse simulation tests.

TABLE 16
COMPARISON OF EXTRAPOLATED VALUES WITH RESISTOR MODEL CALCULATED VALUES

Test Point	Predicted Values (Amps)		Extrapolated Values (Amps)	
	CW Resistances	Pulse Resistances	CW	Moderate-Level Pulse
Nose Drive				
VJ1	363	377		170
VJ2	567	563		154
VJ6	59.5	34		5.4
VJ7	10	4.3		9
3I1	1818	1927	1700	1581
3I2	1963	2581	5820	763
3I3	2344	3654	7010	1839
VF12	203	201	520	436
Wing Drive				
VJ1	3203	2231	7300	426
VJ2	867	911	510	220
VJ6	1950	857	320	225
VJ7	1885	811	380	217
3I1	1696	1968	17100	275
3I2	15080	13230	60600	4356
3I3	2214	3431	15300	3358
VF12	211	212	660	528

Comparisons of the model results using the pulse resistances were made with the 7 kA moderate-level extrapolated values. The 7 kA pulse waveform is similar to the Component A waveform except for a constant difference in amplitude. This constant gives less uncertainty in the extrapolations than in the other pulse simulation scaled results. Currents measured on the autopilot cable bundles and the voltage drop measured across some joints and the fuselage were the test points used for comparison.

The model predictions agree quite well with extrapolated values from nose drive configuration measurements. Predictions agree within factors of three for the CW test and within factors of four for the moderate-level pulse simulation. The CW and pulse extrapolated values are generally greater and less than, respectively, the predicted results.

For the wing drive configuration, the agreement between the pulse predicted and extrapolated values is within factors of four for all but VJ1 and 3I1. The agreement for the CW scaled results is not as good with as much as a factor of ten difference at 3I1. The pulse extrapolated values are generally less than the predicted values for this configuration. The autopilot cable bundle currents were some of the test points at which non-linear effects were probably occurring during the moderate-level testing. This could be a factor in the discrepancies seen, especially in the wing drive, between the extrapolated pulse and CW results.

CONCLUSIONS

Conclusions leading to hard and fast criteria for application of the four methods of verification or evaluation of lightning protection design cannot be readily drawn from this series of tests on a single test article. It is possible, however, to identify several important considerations that must be borne in mind when selecting lightning simulation methods for a specific application:

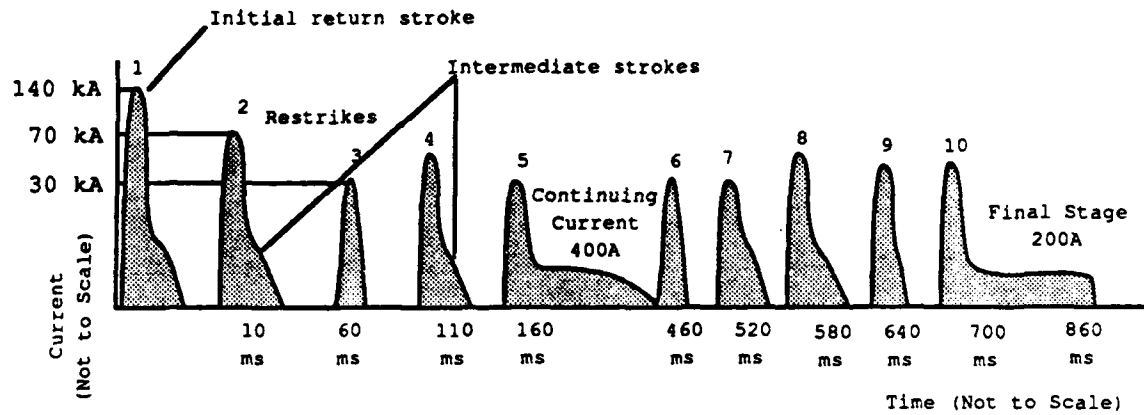
- 1) It was advantageous to use the 7 kA moderate-level pulse because:
 - a) The pulse waveform closely approximated component A of the SAE-AE4L test waveform.
 - b) Use of the 7 kA pulse resulted in a constant extrapolation factor being required for all measurements, whether resistive (IR) or inductive (dI/dt).
 - c) The smaller extrapolation factor led to less uncertainty in the final results.
 - d) Nonlinear effects and poorly conducting joints are discovered by high current tests.
- 2) All other pulse simulations require different scaling factors depending on whether resistive (IR) or inductive (dI/dt) responses are being considered. Although the CW method requires Fourier transforms of the data, the scale factor is automatically calculated frequency by frequency for the threat versus test environment.
- 3) The test responses can be described statistically. A minimum of thirty (30) measurement points is required for a statistically significant data sample.
- 4) The logarithm of the magnitude of the extrapolated values plots nearly linearly on a log normal probability grid for all test methods. The best linear fit was obtained with the moderate level pulse extrapolated data.
- 5) The magnitude of the measured and extrapolated currents and voltages is dependent on where the test pulse enters and exits - wing-tail strike values were two to four times larger than those obtained for nose-tail strikes. This difference in response is dependent on the test article.
- 6) Agreement among the different simulation methods was close by the standards applicable in this type of work - for example, mean values for the moderate-level extrapolated results were larger by a factor of two than those obtained from the low-level pulse; CW and shock excitation are more conservative, both having mean values larger than the moderate-level mean values by a factor of two.

For Each Stroke:

Time to peak current = 1.5 μ s
Time to half value = 40 μ s

For the complete flash:

$$\int i^2 dt = 1.9E6 A^2 s$$

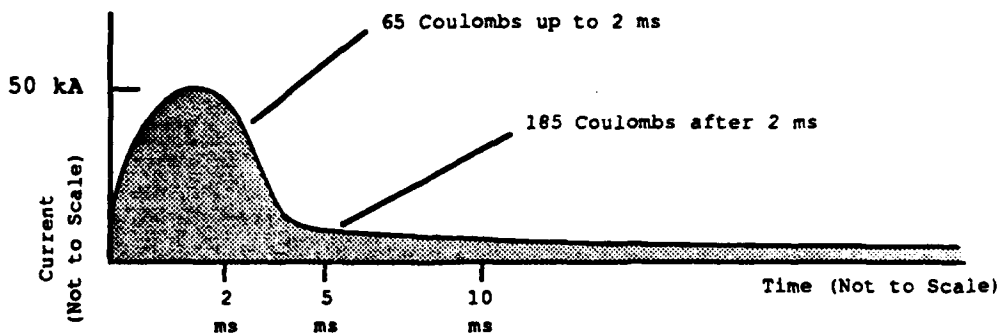


(A) Severe negative lightning flash current waveform.

(Courtesy of Cianos/Pierce)

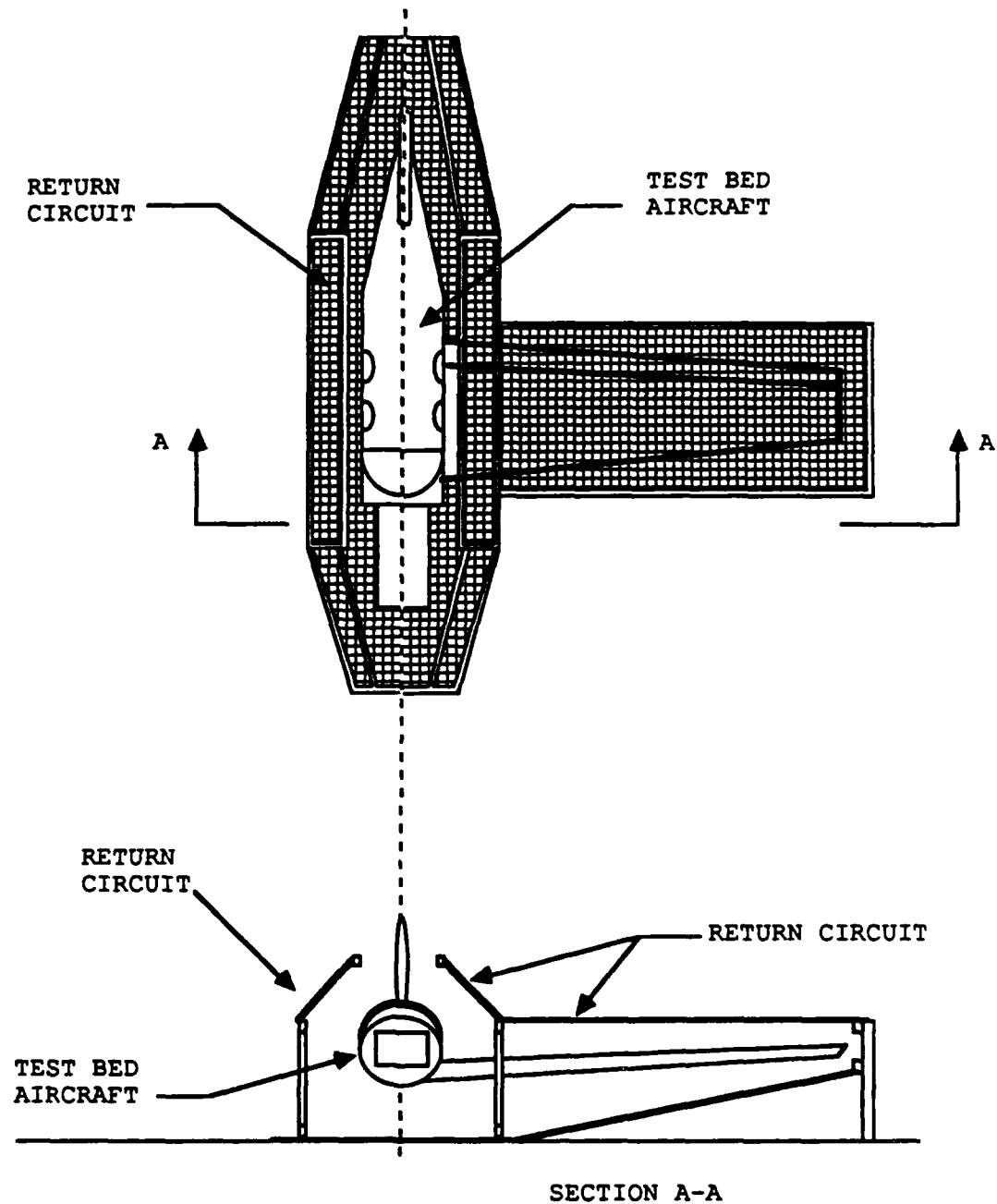
For the complete flash:

$$\int i^2 dt = 2.5E6 A^2 s$$



(B) Moderate Positive Lightning Flash Current Waveform

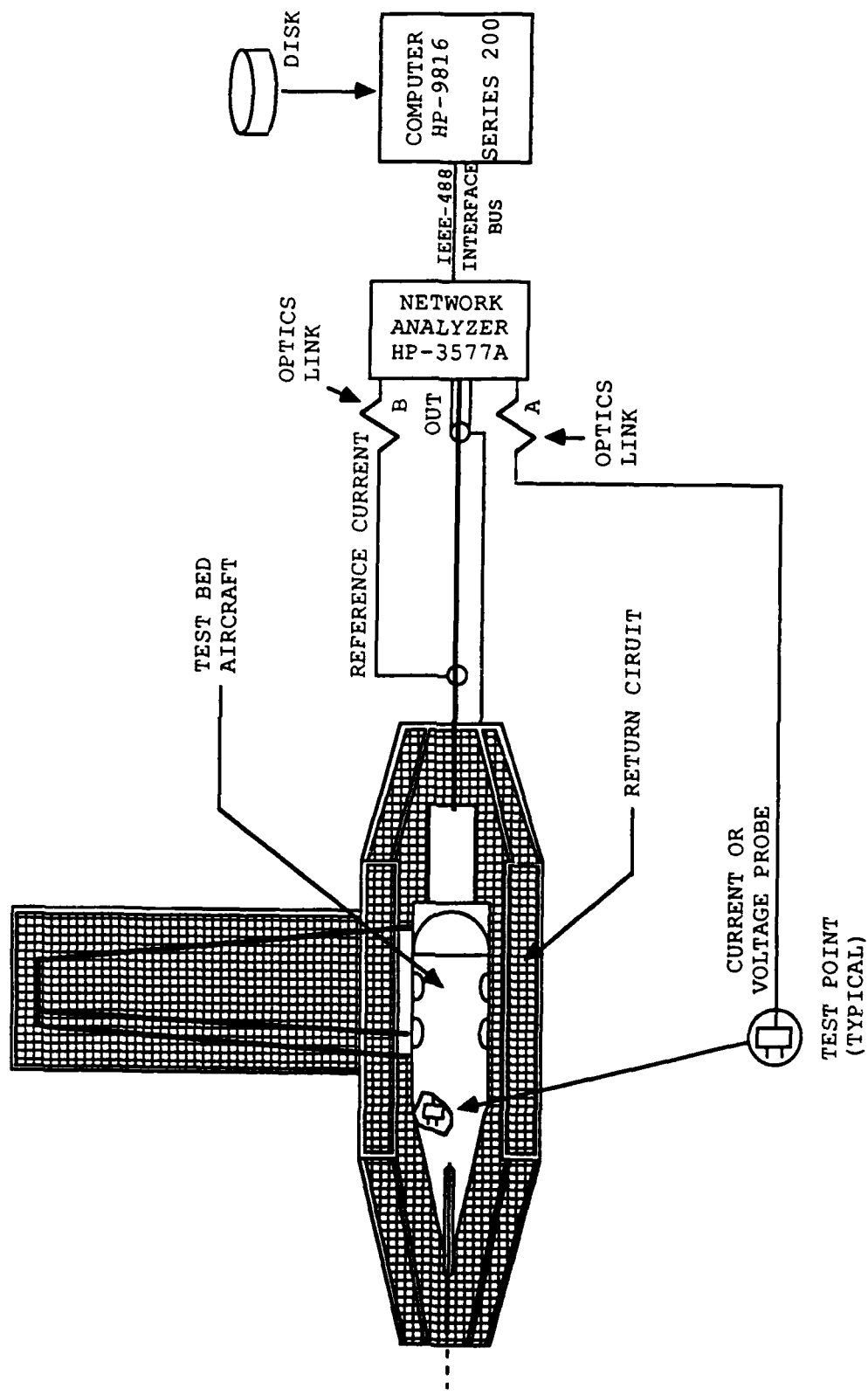
FIGURE 1 LIGHTNING FLASH CURRENT WAVEFORM



Note: The return conductors form an approximate coaxial outer conductor around the test bed aircraft.

FIGURE 2 SIMULATOR RETURN CIRCUIT

FIGURE 3 LOW-LEVEL SWEEP CONTINUOUS WAVE TEST SETUP



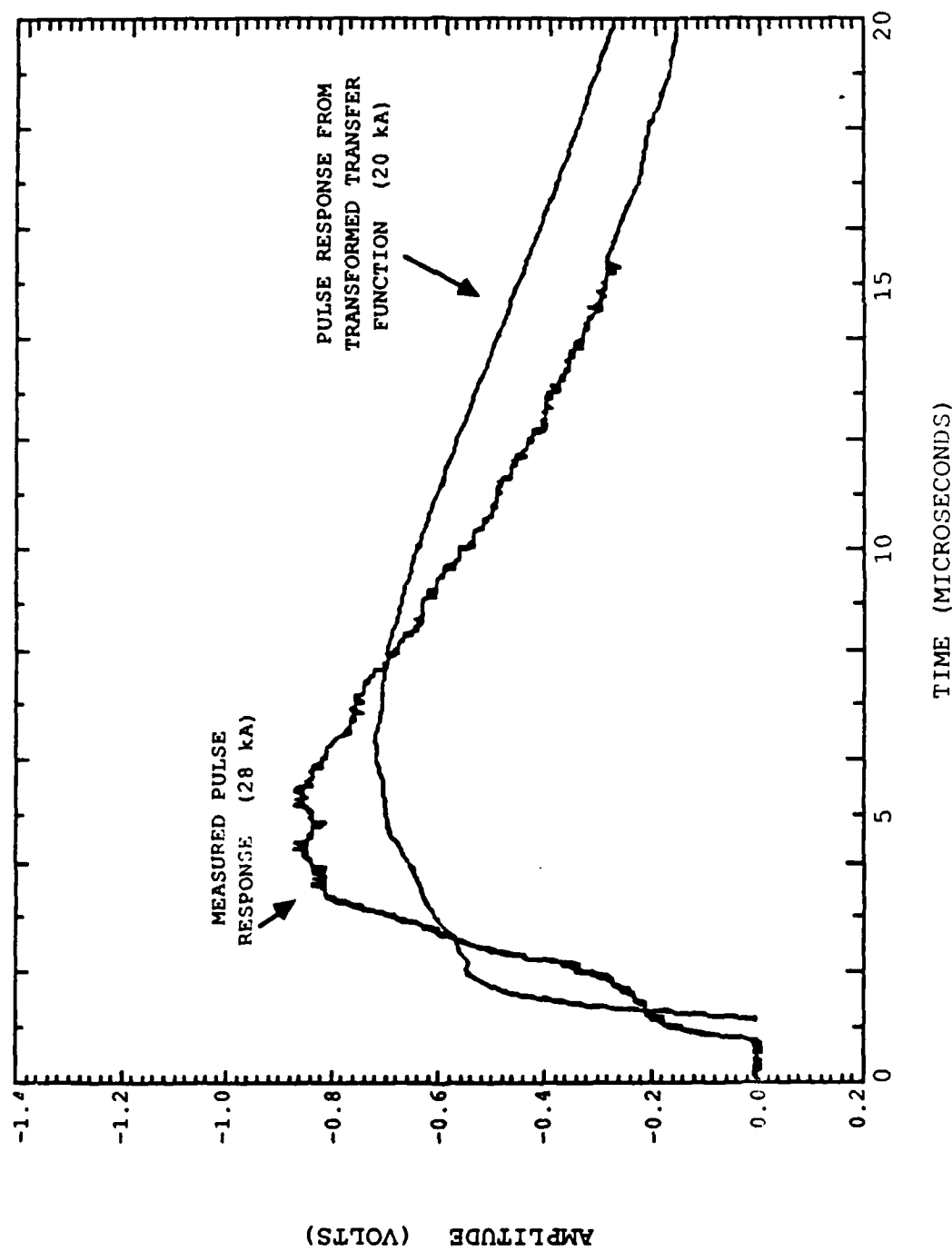


FIGURE 4 MEASURED VS. FOURIER TRANSFORMED DATA

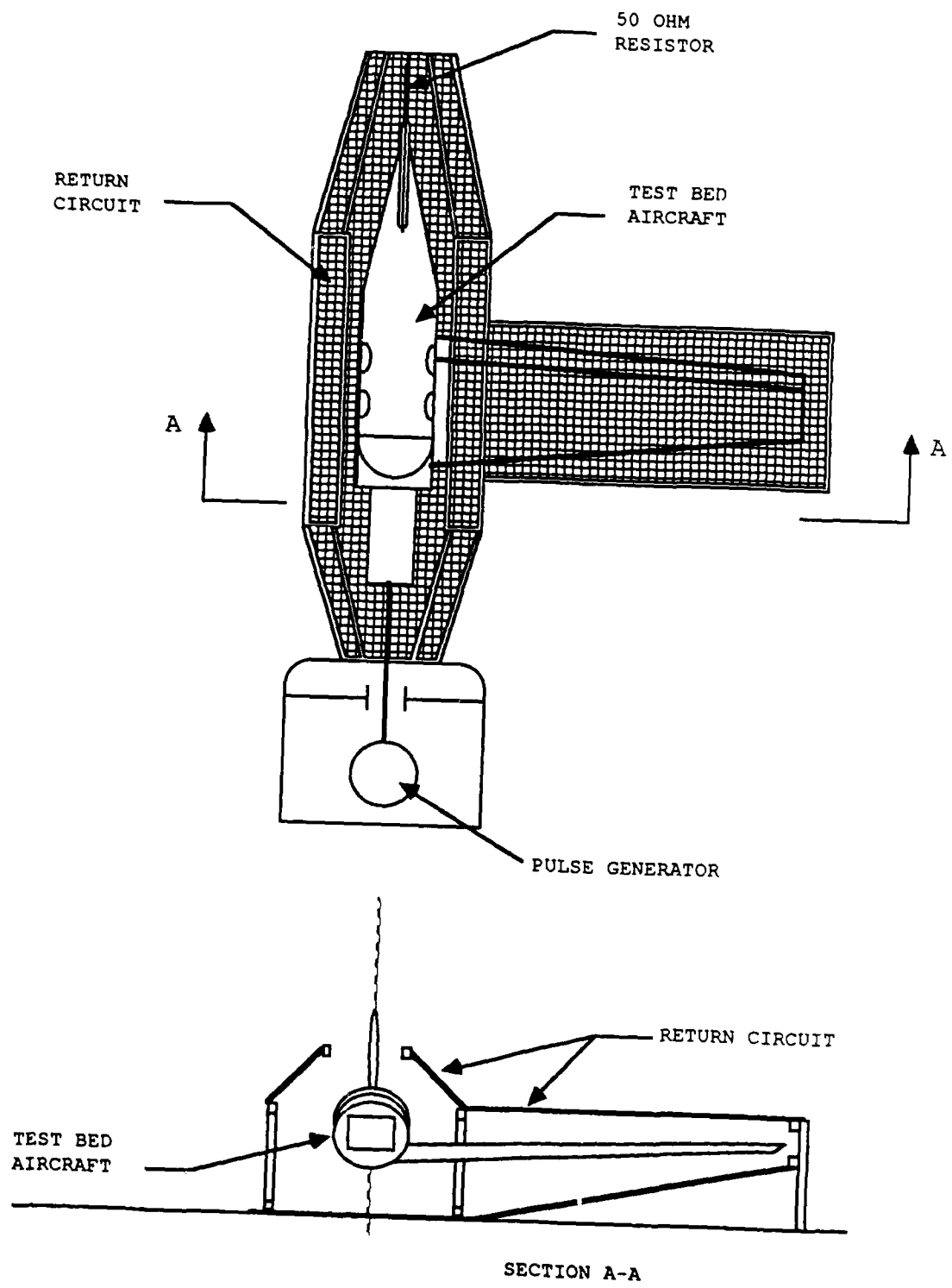


FIGURE 5 LOW-LEVEL FAST-RISE PULSE TEST SETUP

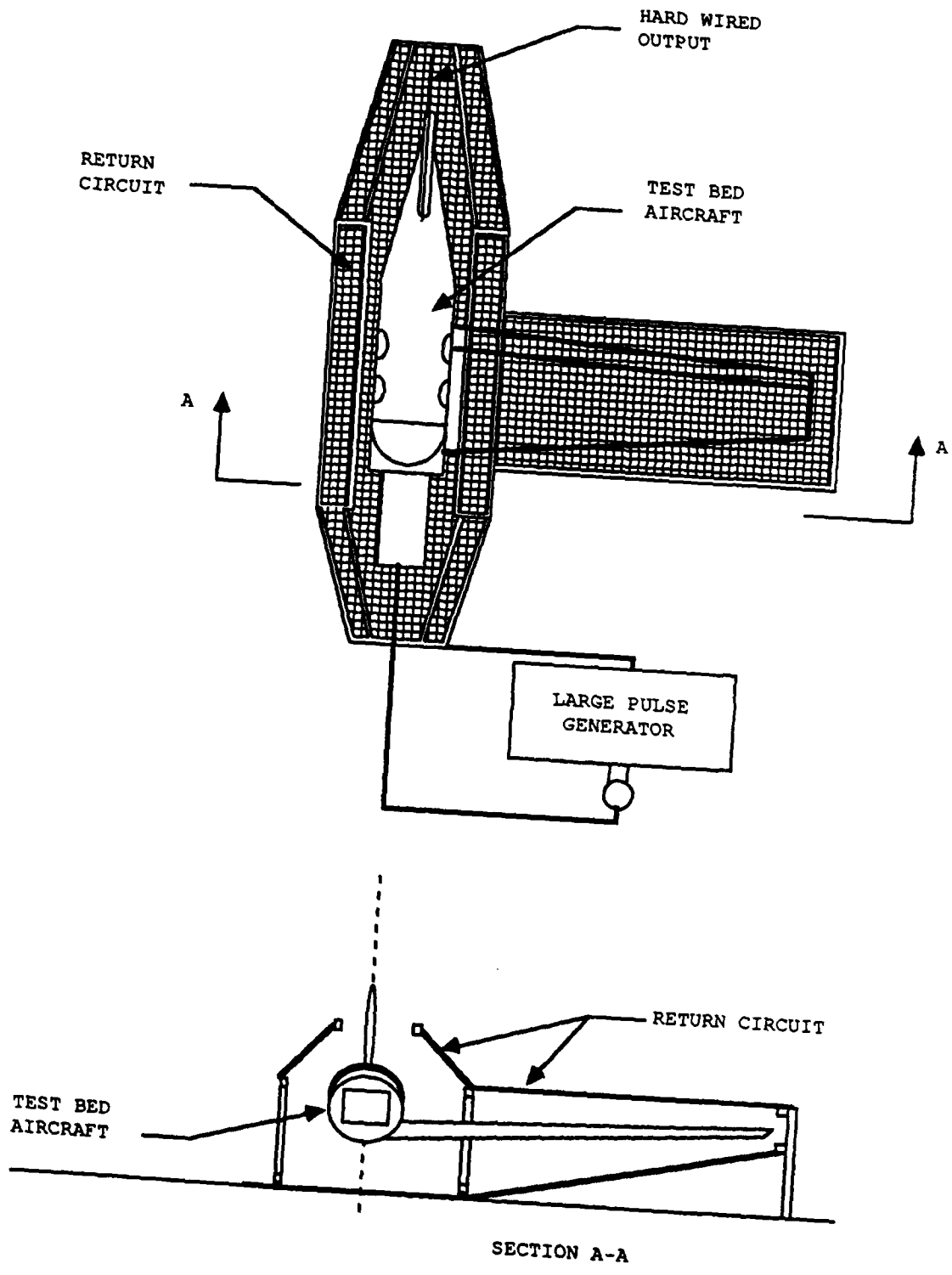


FIGURE 6 MODERATE LEVEL PULSE TEST SETUP

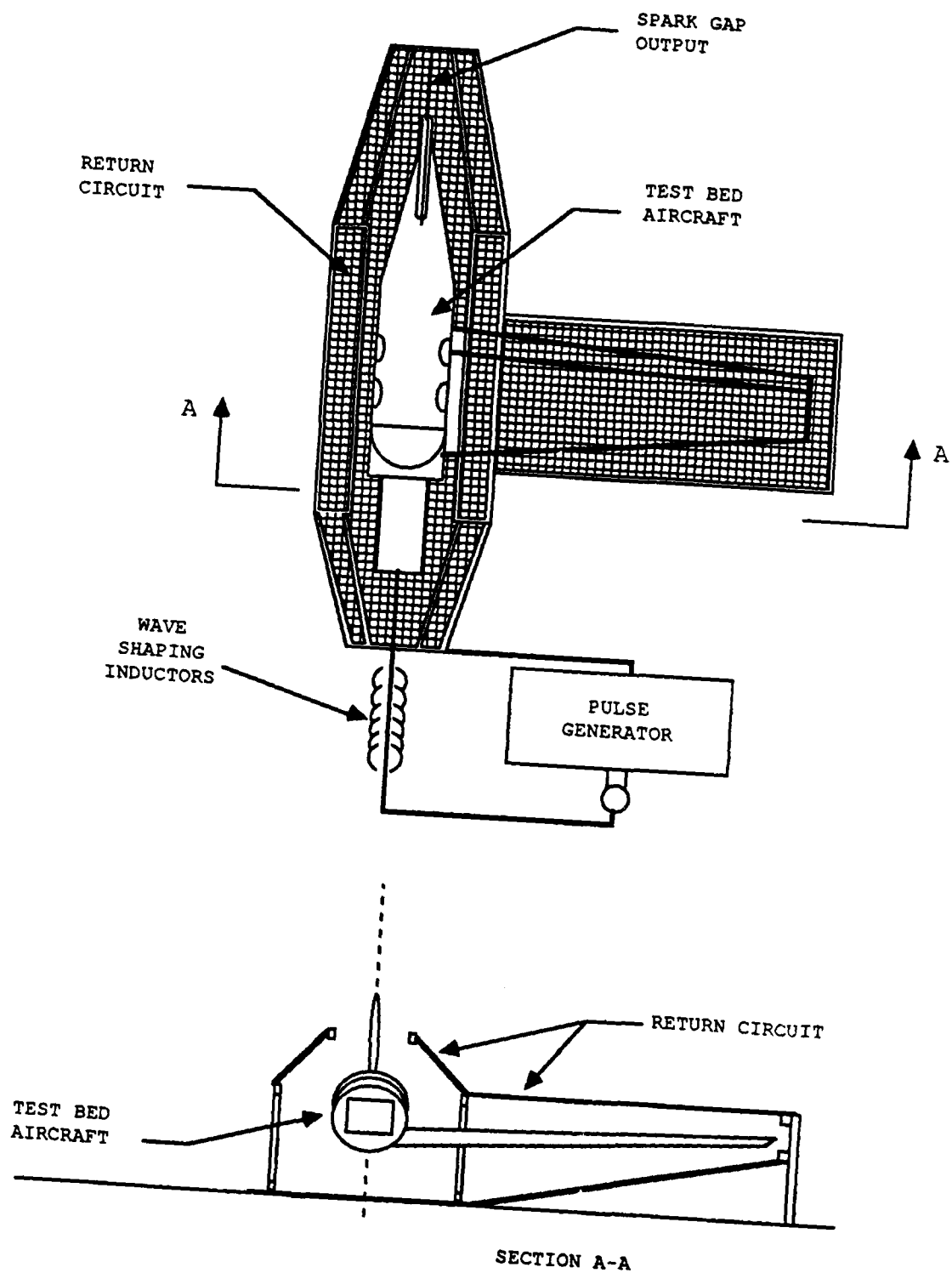


FIGURE 7 SHOCK-EXCITED TEST SETUP

FIGURE 8 TEST BED CONFIGURATION

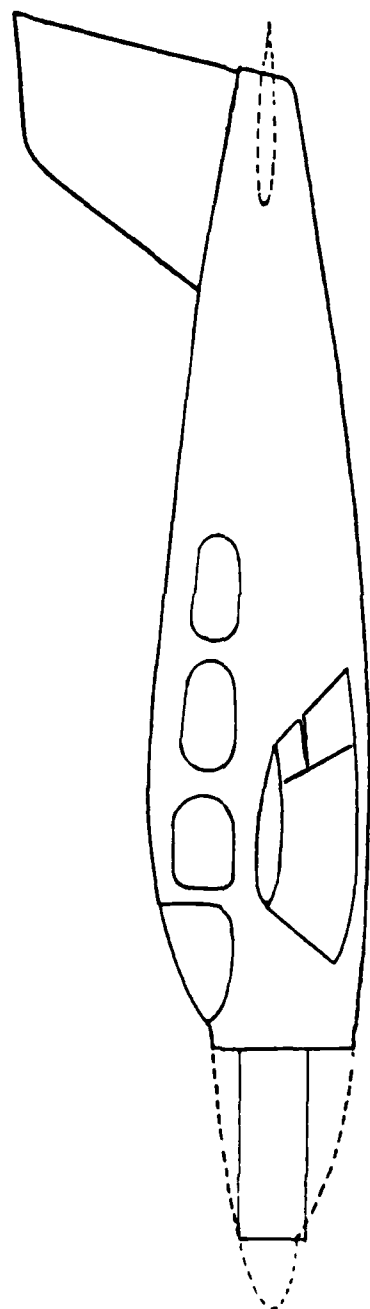


FIGURE 9 TEST BED OVERALL DIMENSIONS

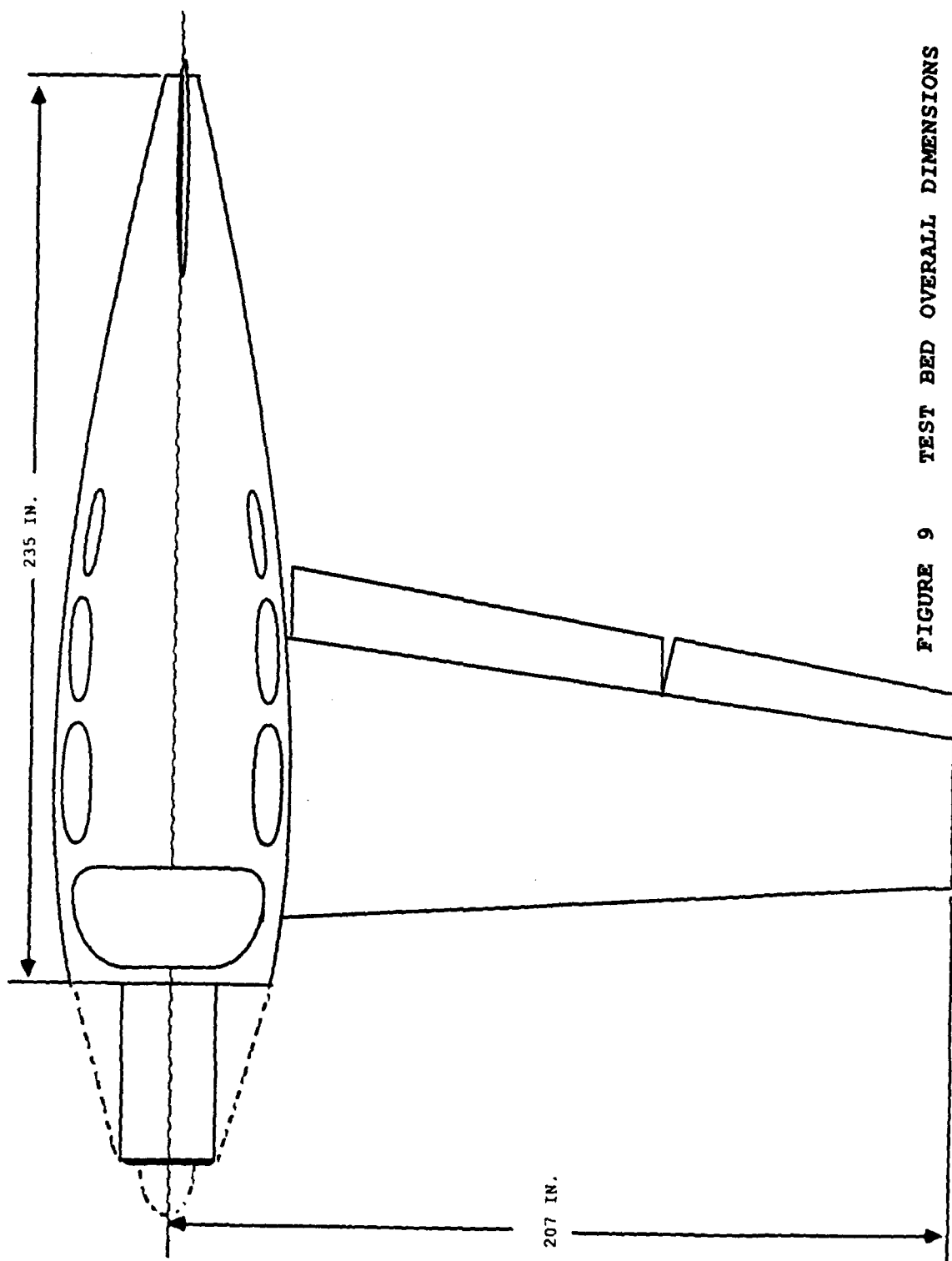
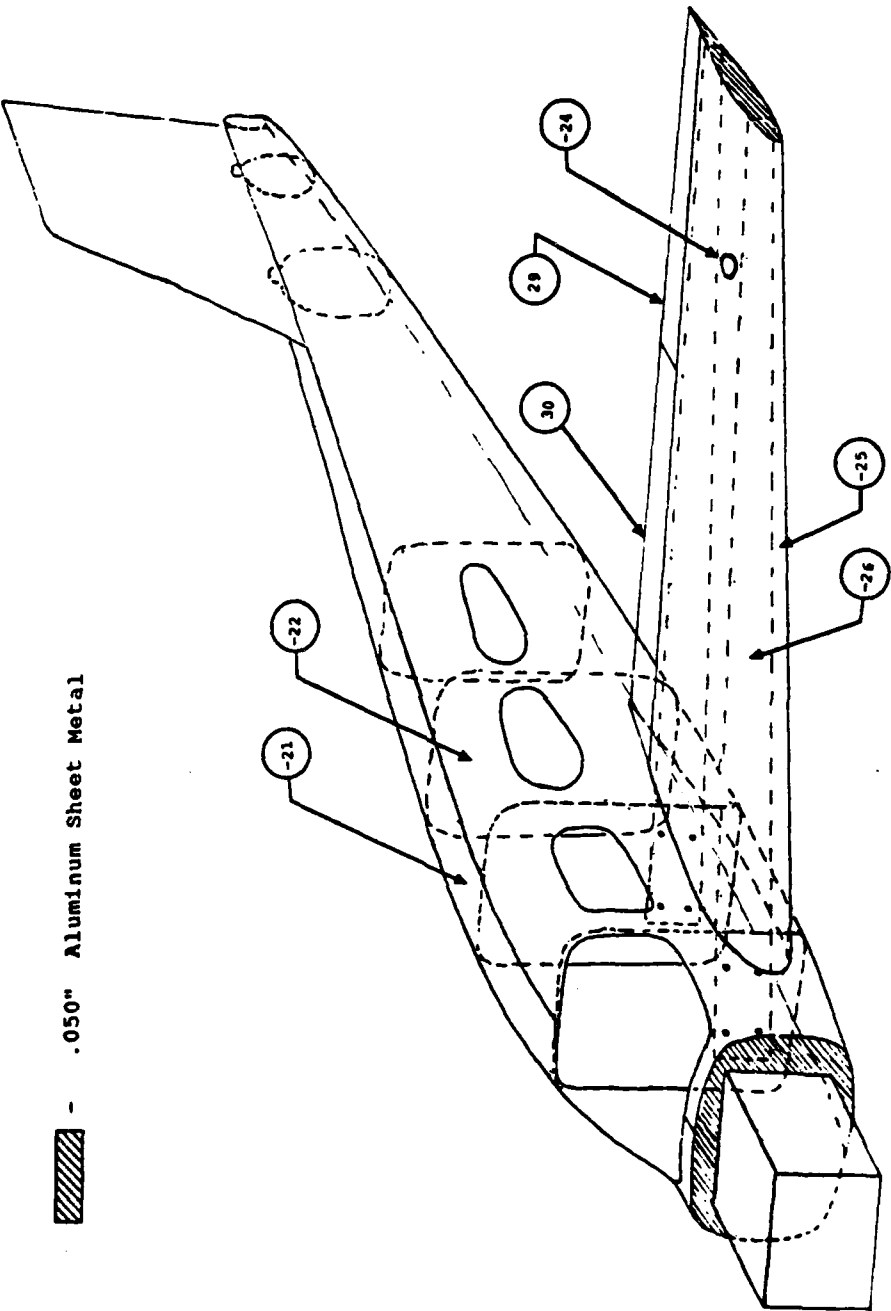


FIGURE 10 TEST BED EXTERNAL DETAIL



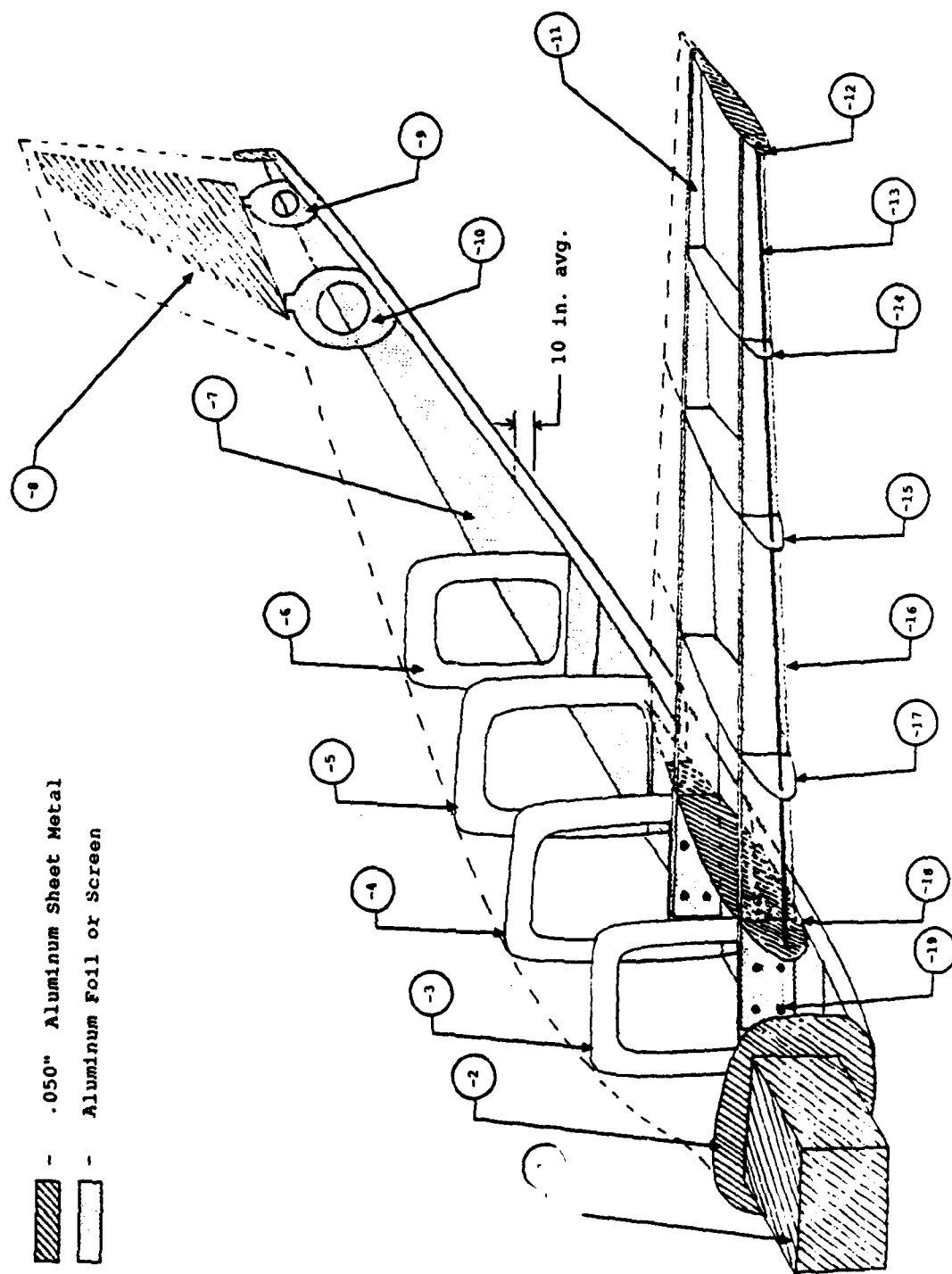


FIGURE 11 TEST BED INTERNAL DETAIL

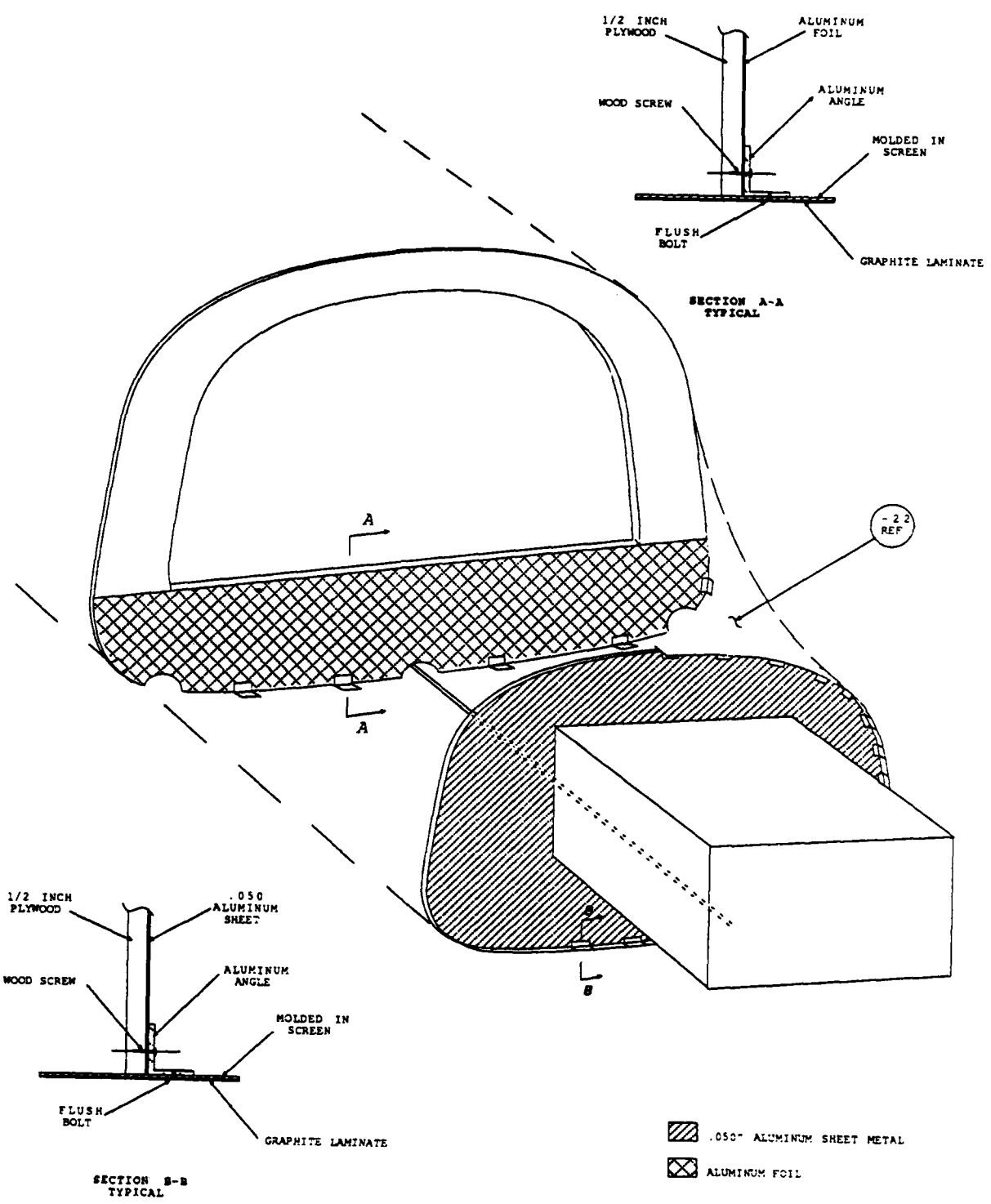


FIGURE 12 FORWARD BULKHEAD DETAIL

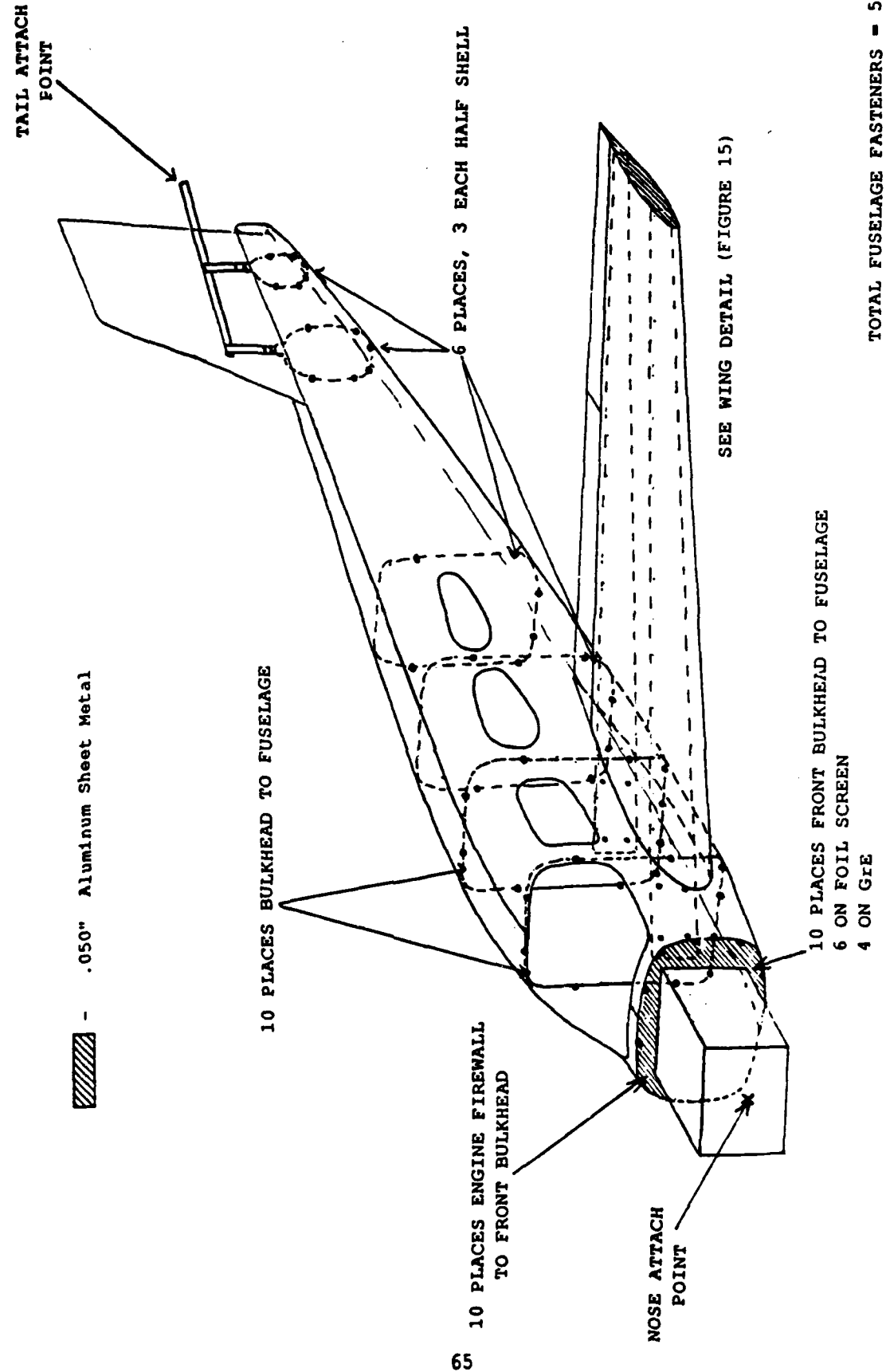


FIGURE 13 FUSELAGE FASTENER LOCATIONS

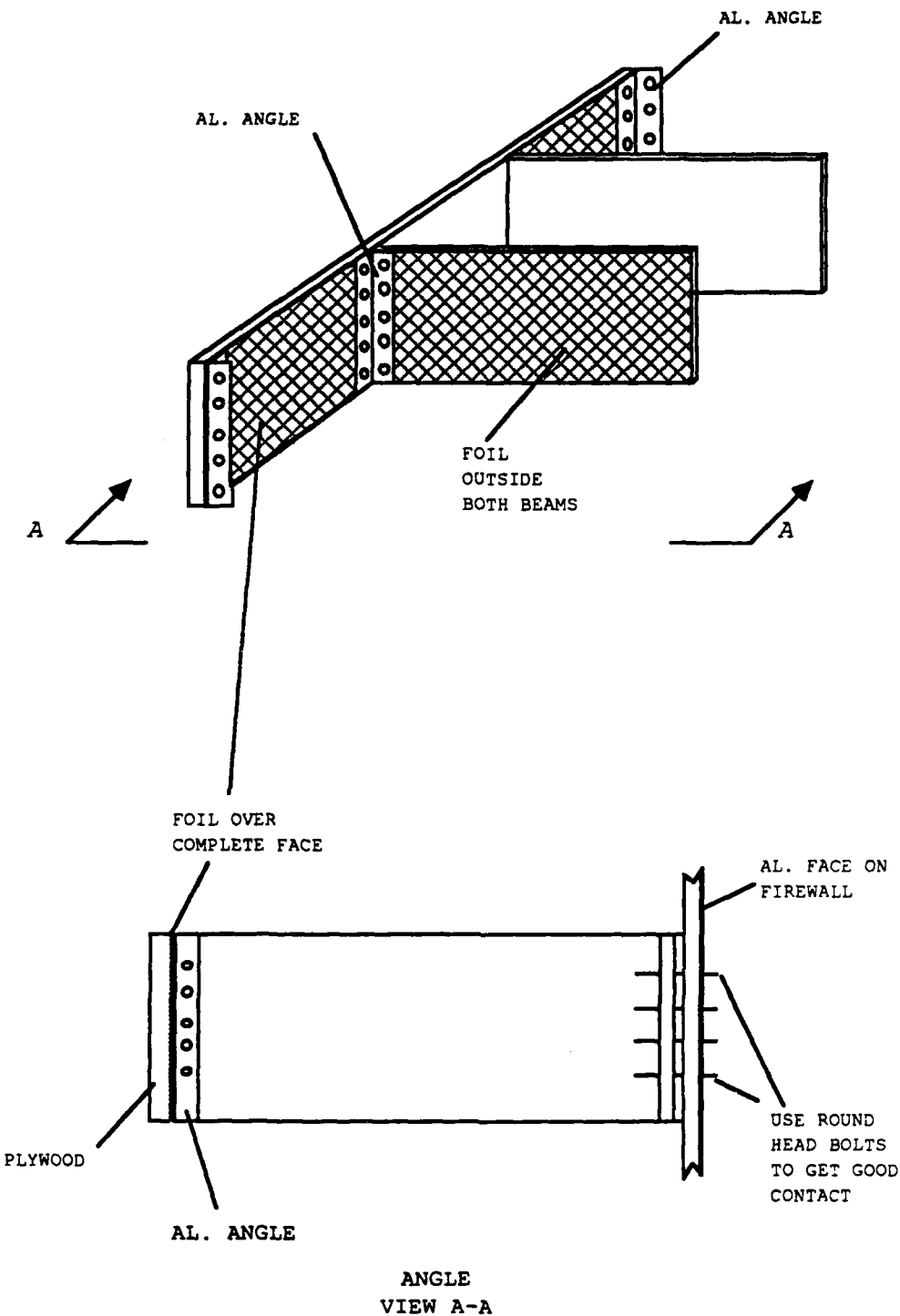


FIGURE 14 INSTRUMENT PANEL ASSEMBLY

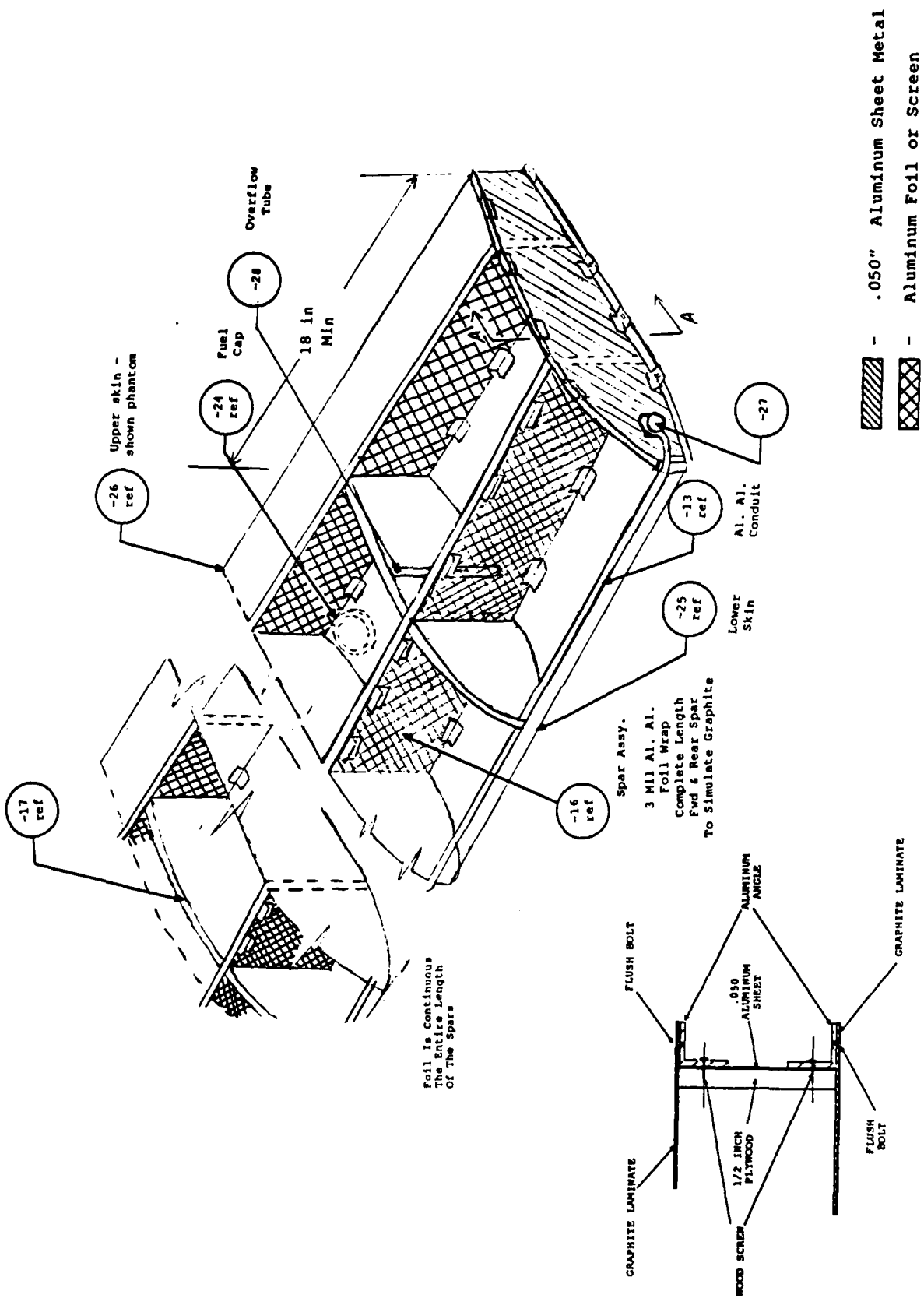


FIGURE 15 WING DETAIL

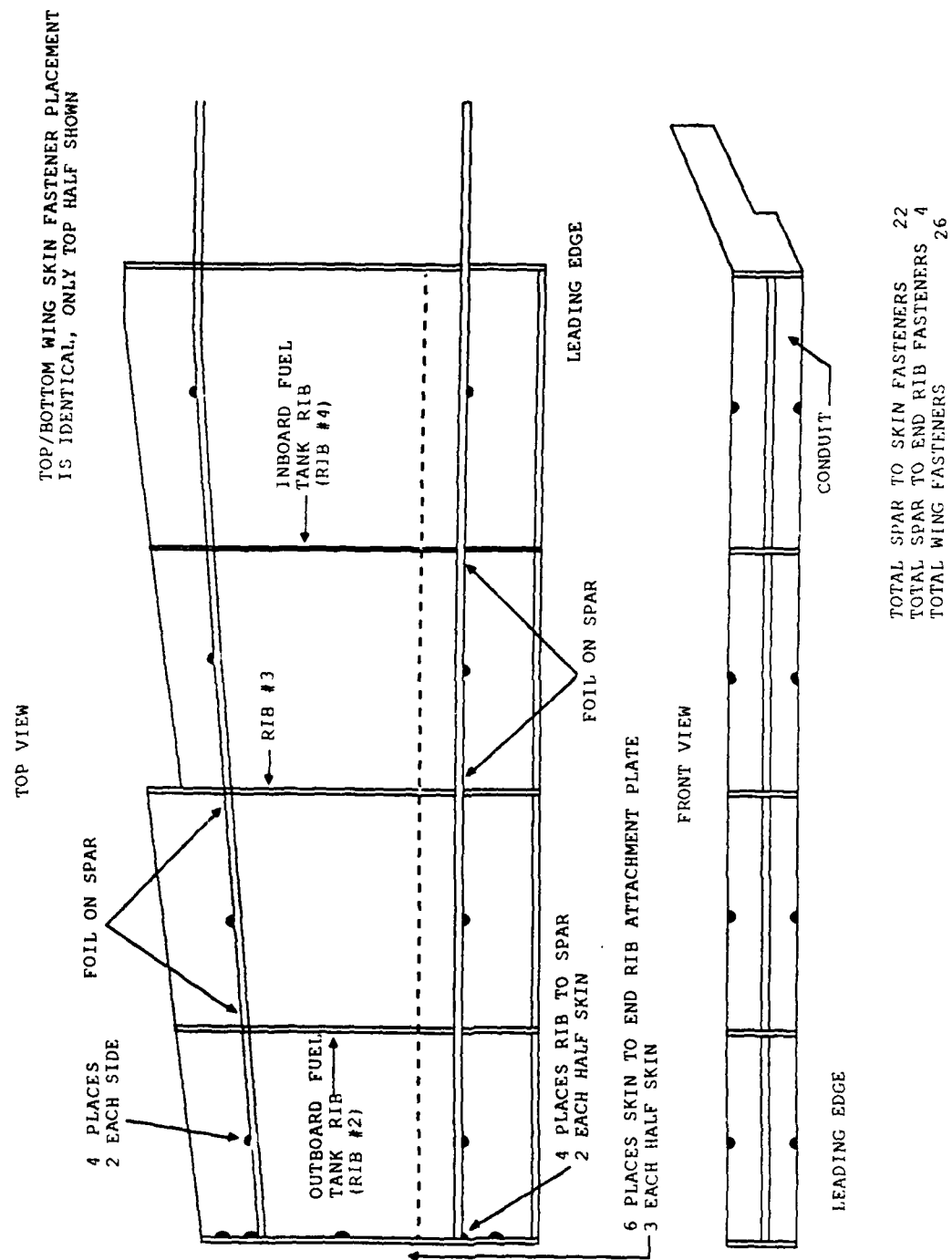
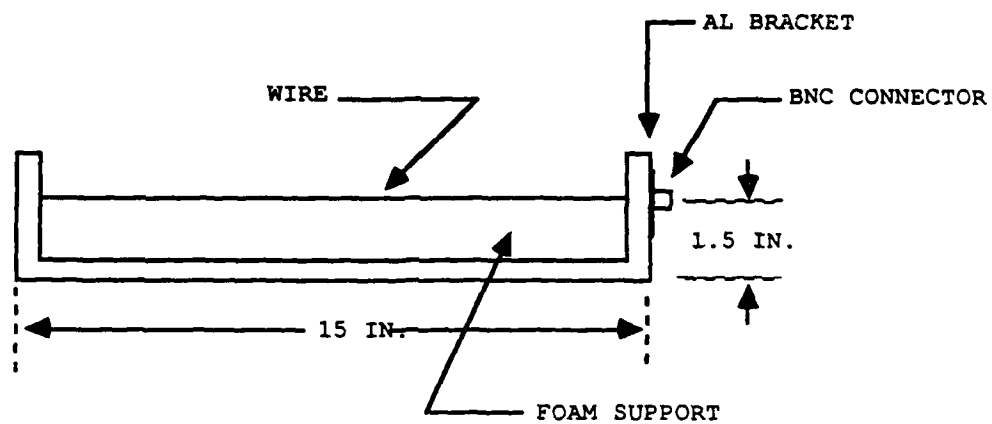
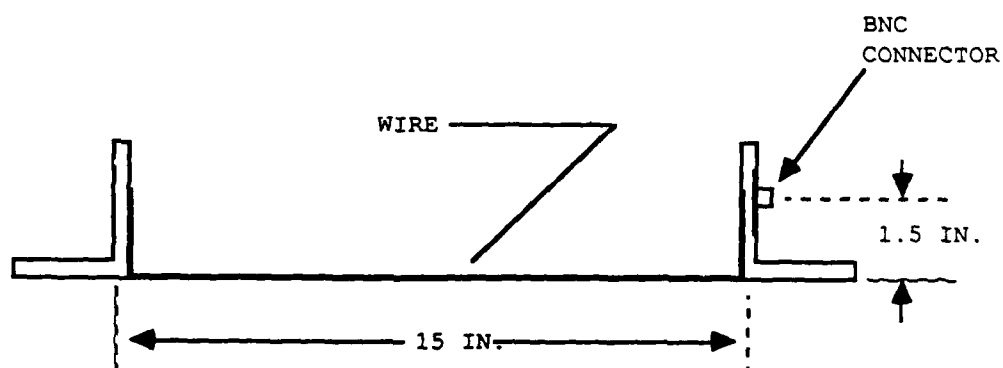


FIGURE 16 WING FASTENER LOCATIONS



a. MAGNETIC FIELD SENSOR



b. ELECTRIC FIELD SENSOR

FIGURE 17 EM SOURCE CHARACTERIZATION SENSORS

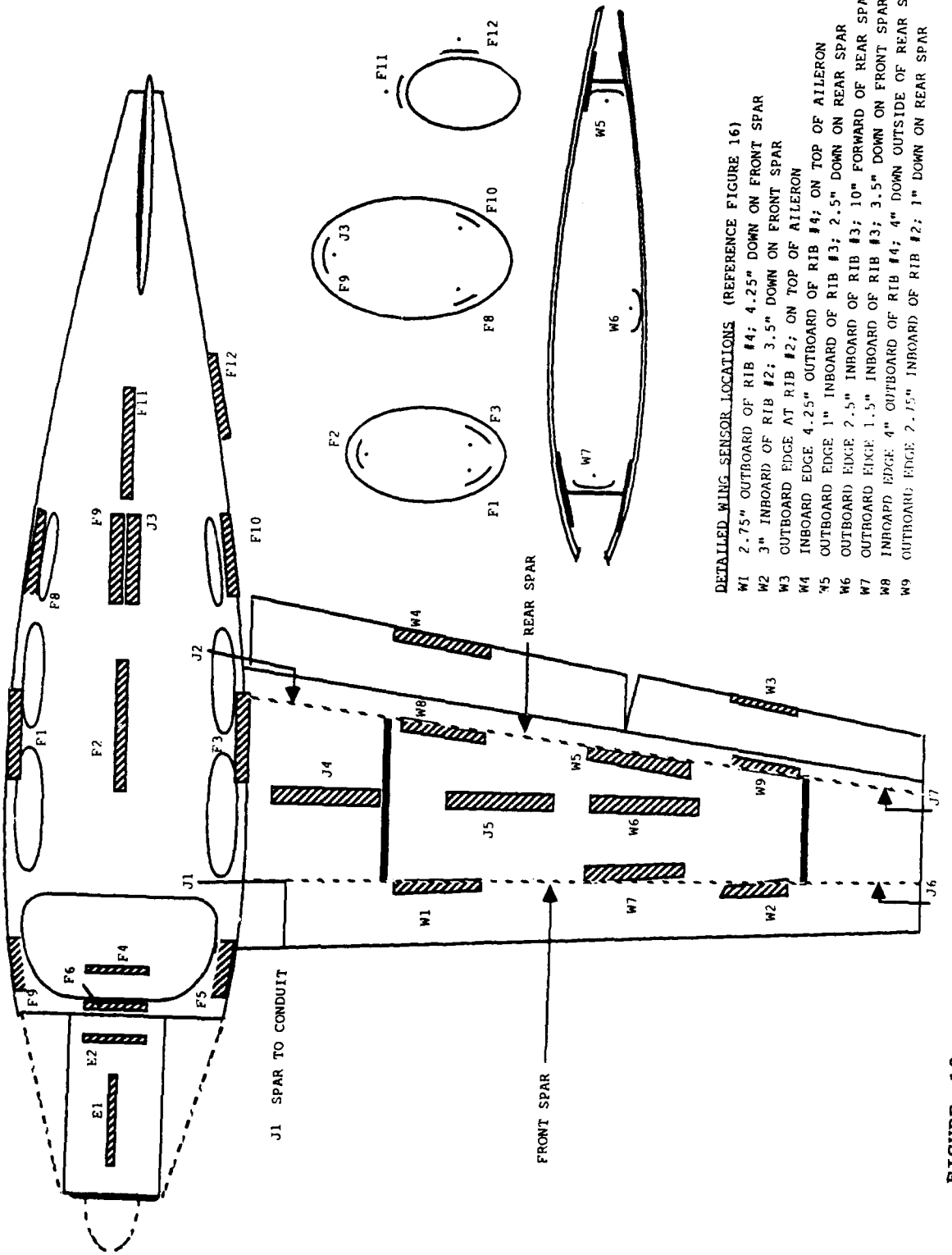


FIGURE 16 EM SOURCE CHARACTERIZATION SENSOR LOCATIONS (PLAN VIEW)

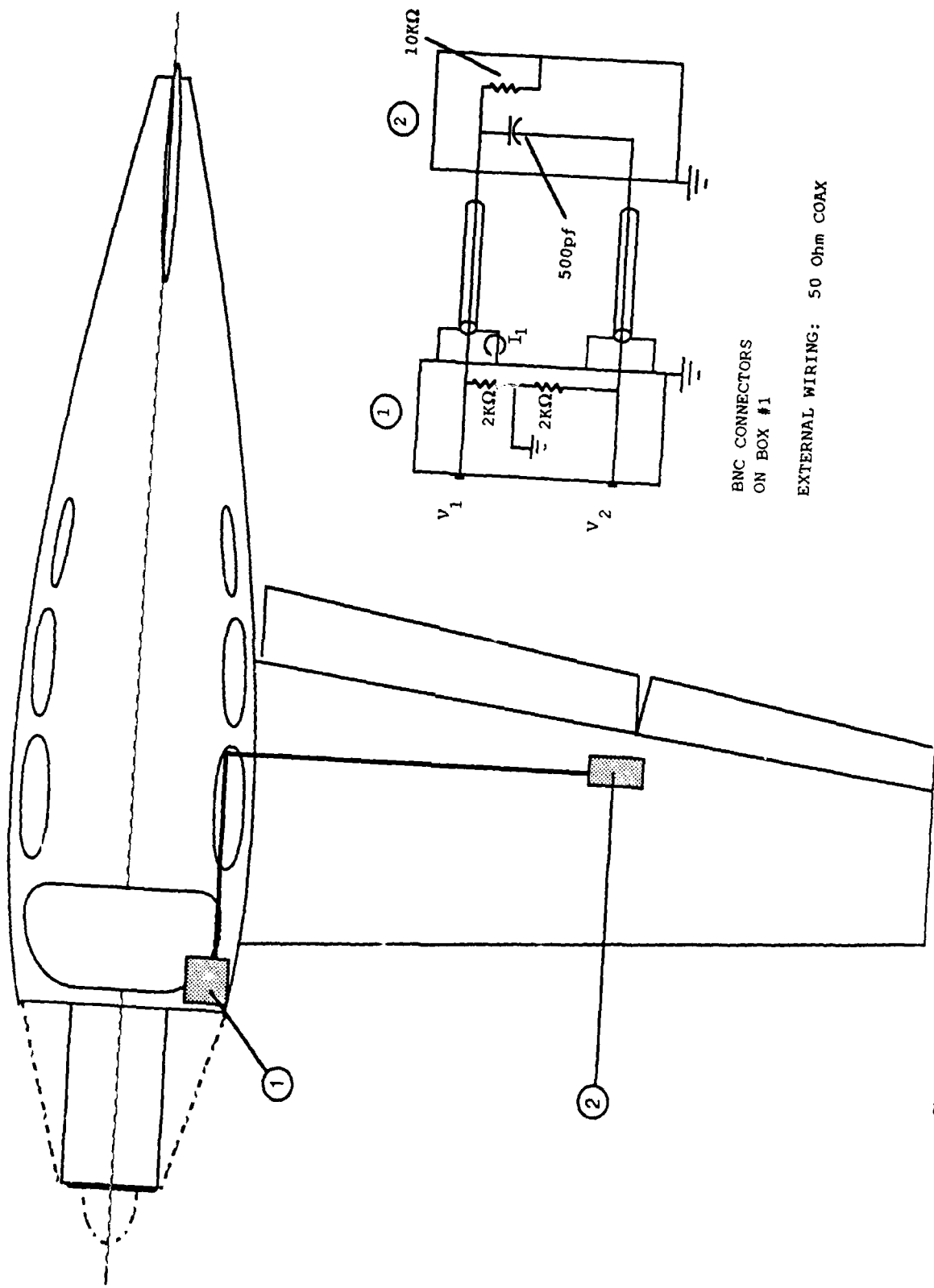


FIGURE 19 FUEL SYSTEM ELECTRICAL INSTALLATION AND CIRCUIT DETAIL

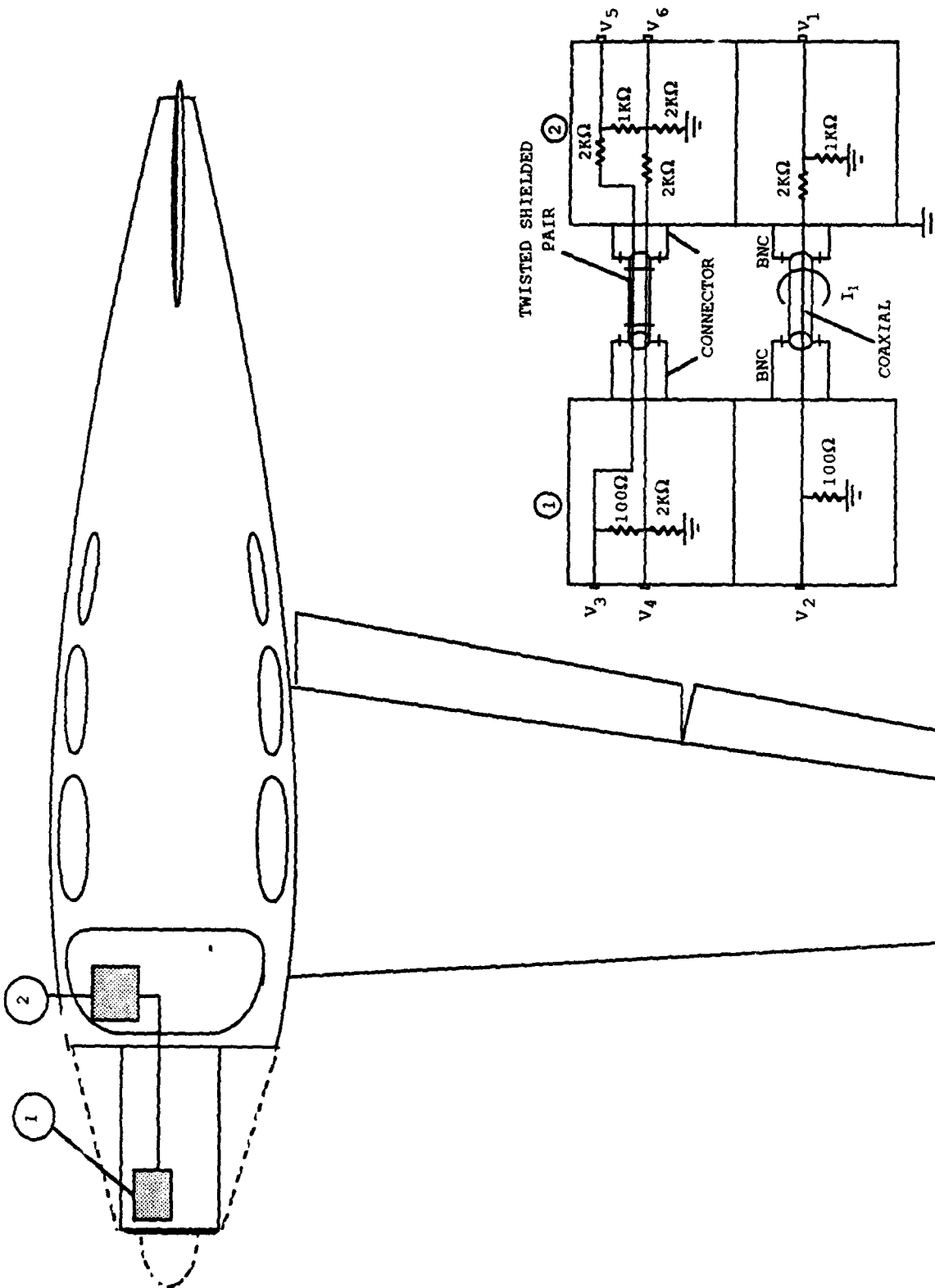


FIGURE 20 ENGINE CONTROL INSTALLATION AND CIRCUIT DETAIL

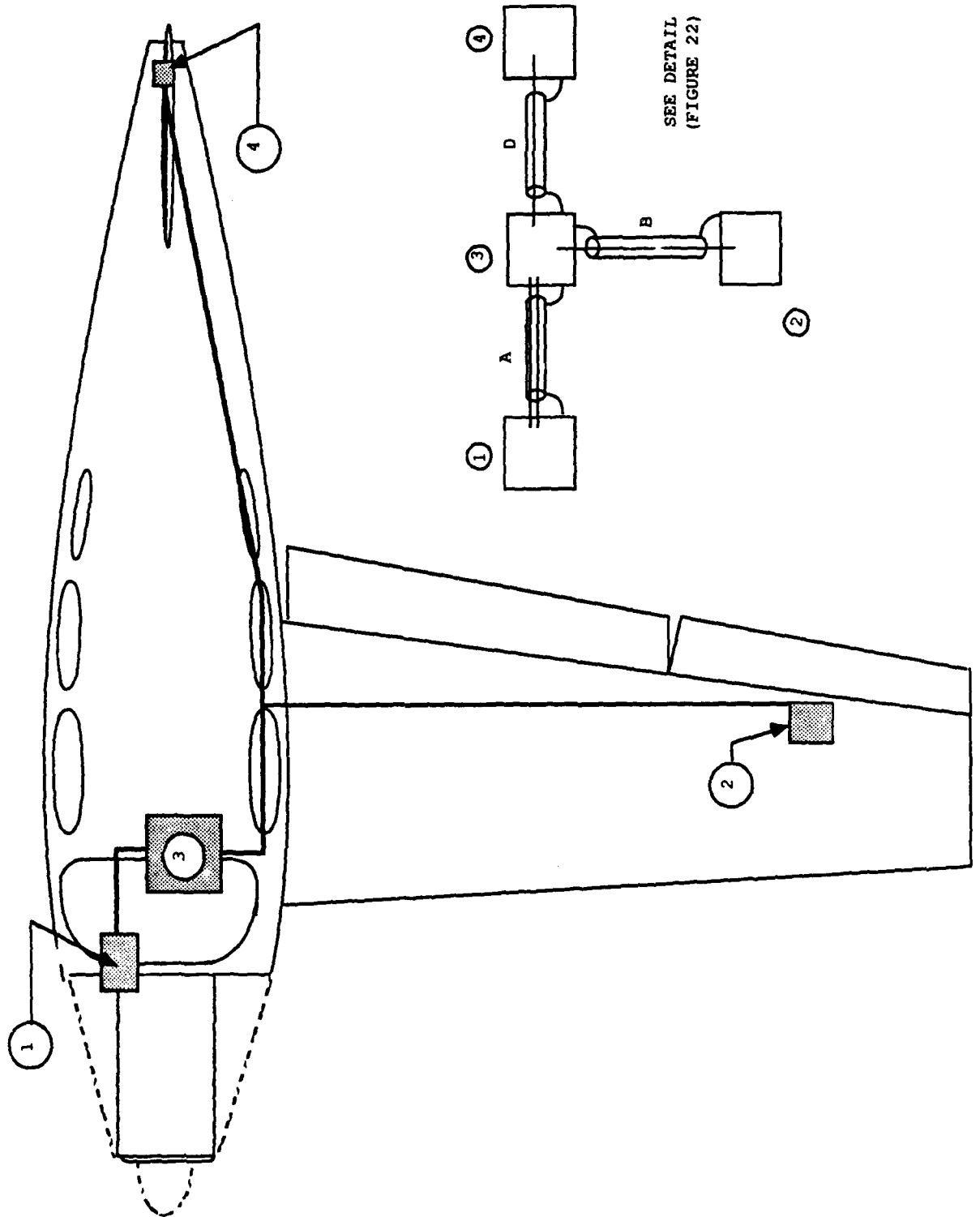


FIGURE 21 AUTOPILOT INSTALLATION

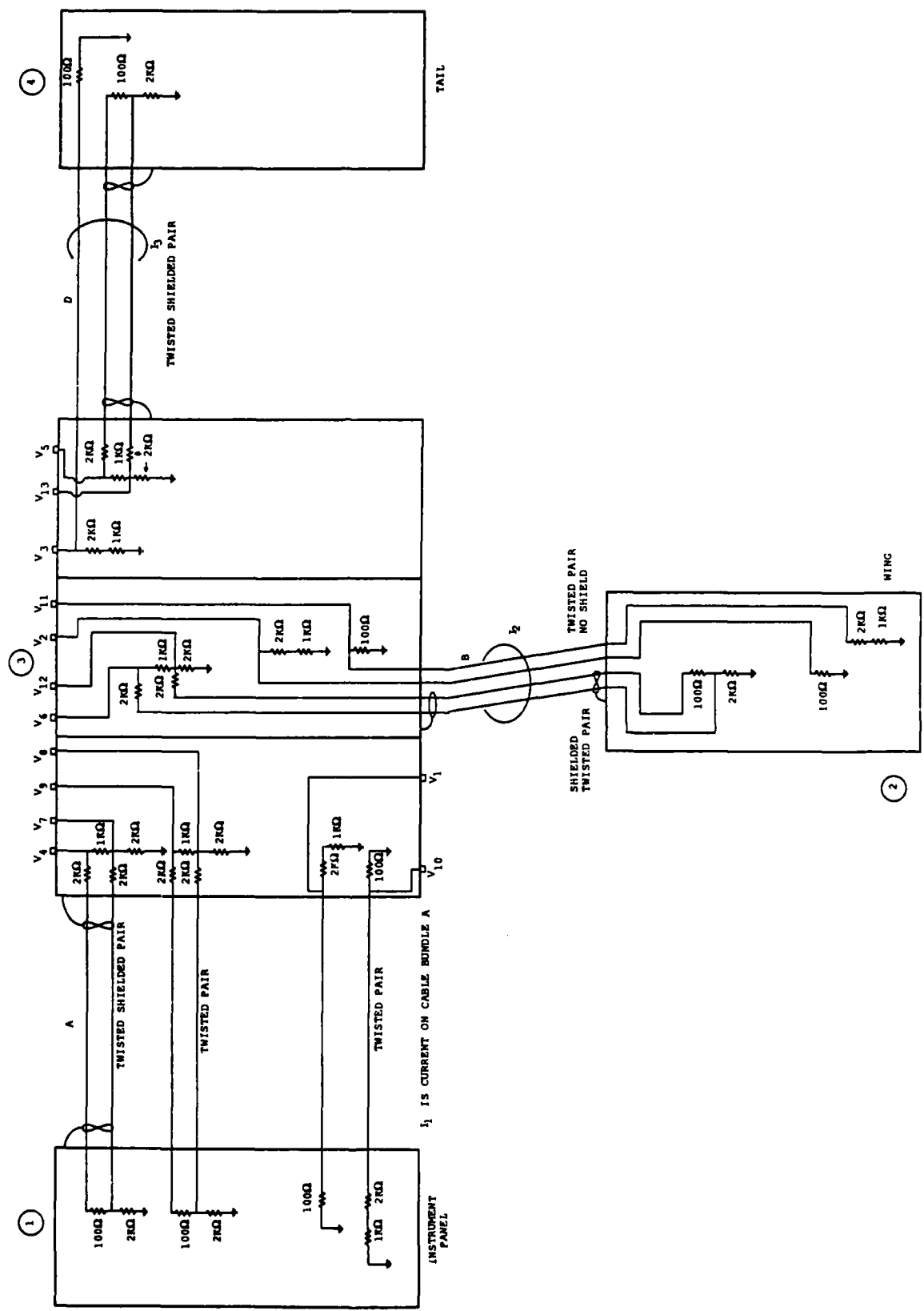


FIGURE 22 AUTO PILOT CIRCUIT DETAIL

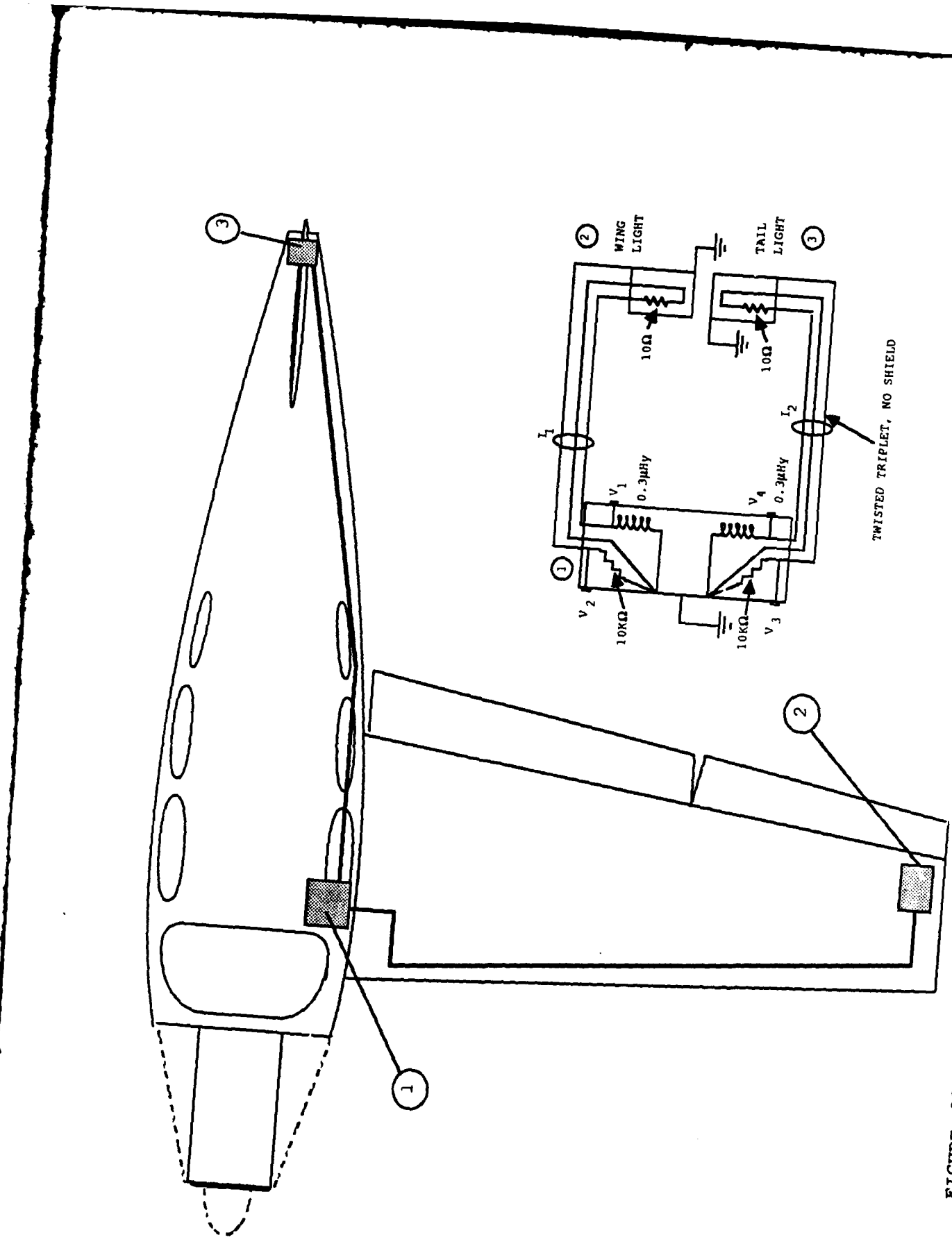


FIGURE 23 ELECTRIC POWER TO LIGHTS - INSTALLATION AND CIRCUIT DETAIL

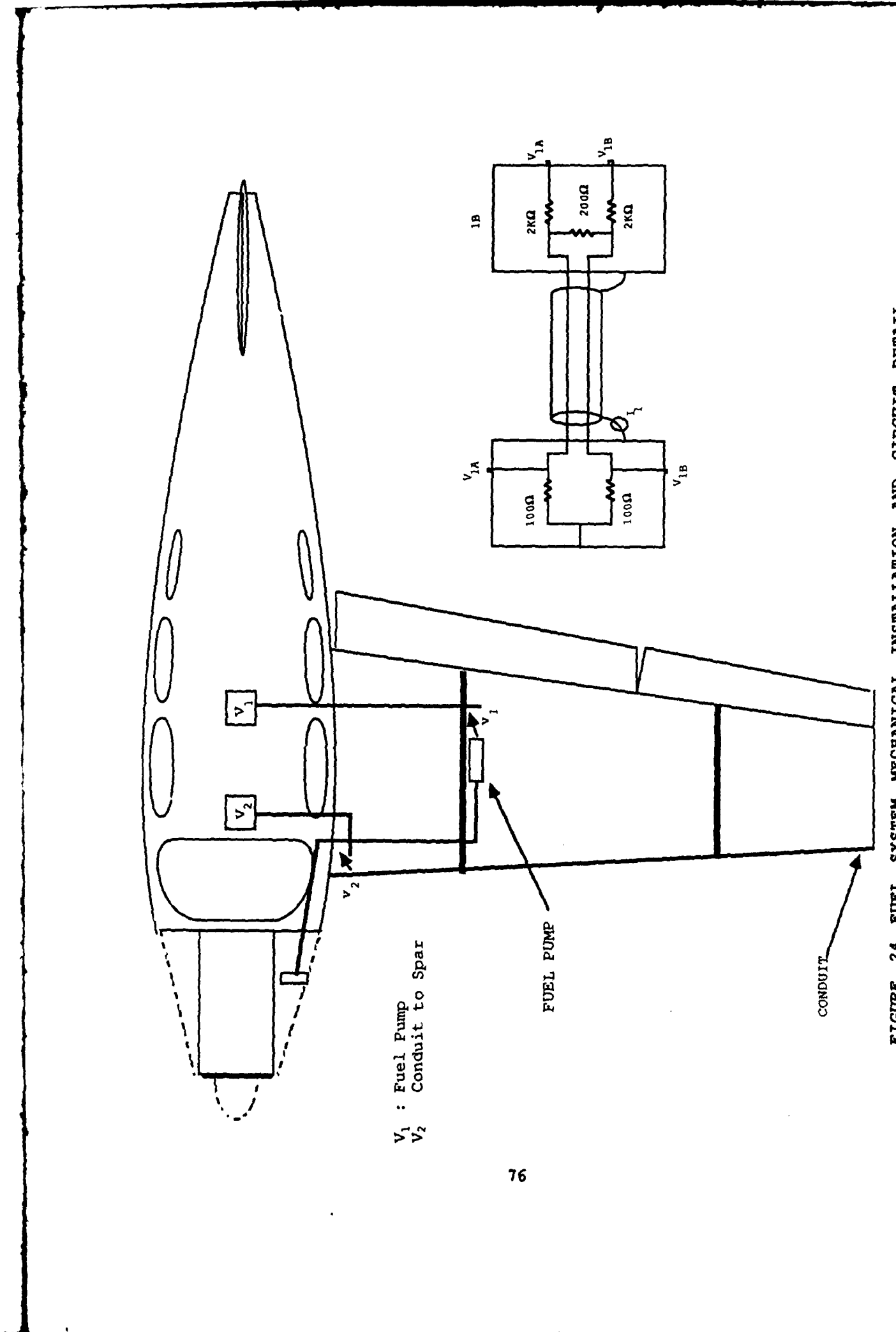


FIGURE 24 FUEL SYSTEM MECHANICAL INSTALLATION AND CIRCUIT DETAIL

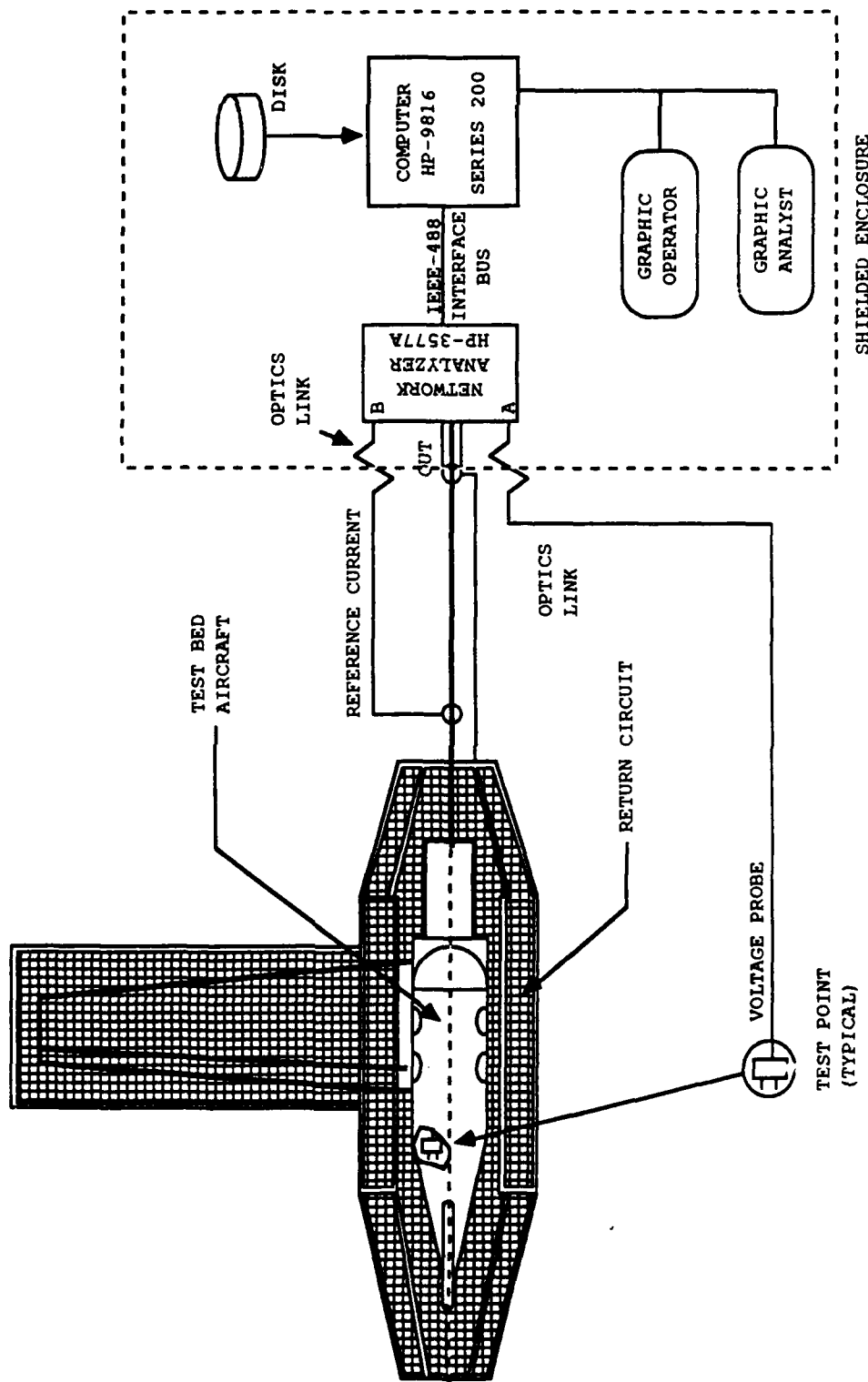


FIGURE 25 LOW-LEVEL SWEPT CONTINUOUS WAVE DATA ACQUISITION SYSTEM

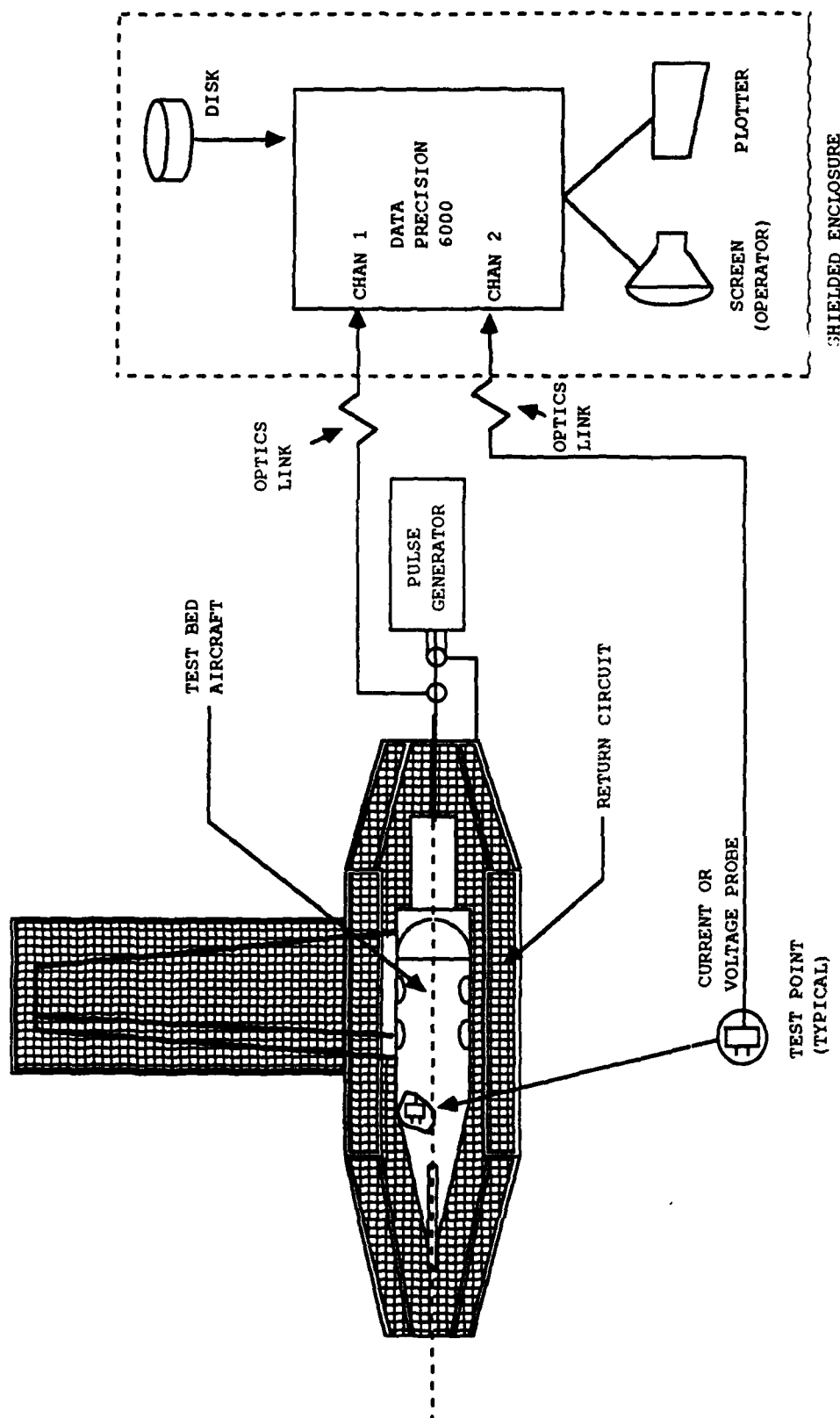


FIGURE 26 PULSE DATA ACQUISITION SYSTEM

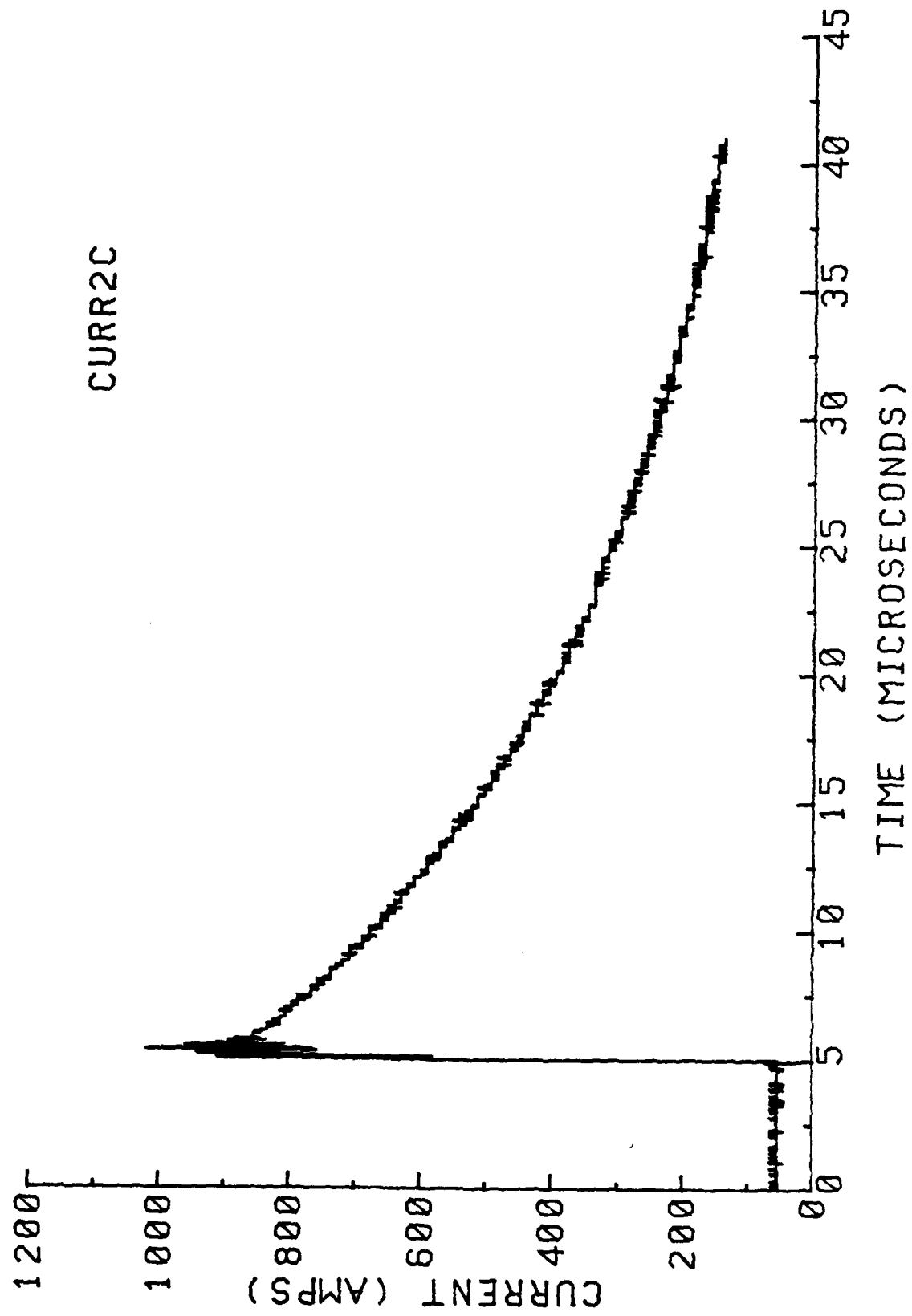


FIGURE 27 EXAMPLE LOW-LEVEL PULSE CURRENT WAVEFORM

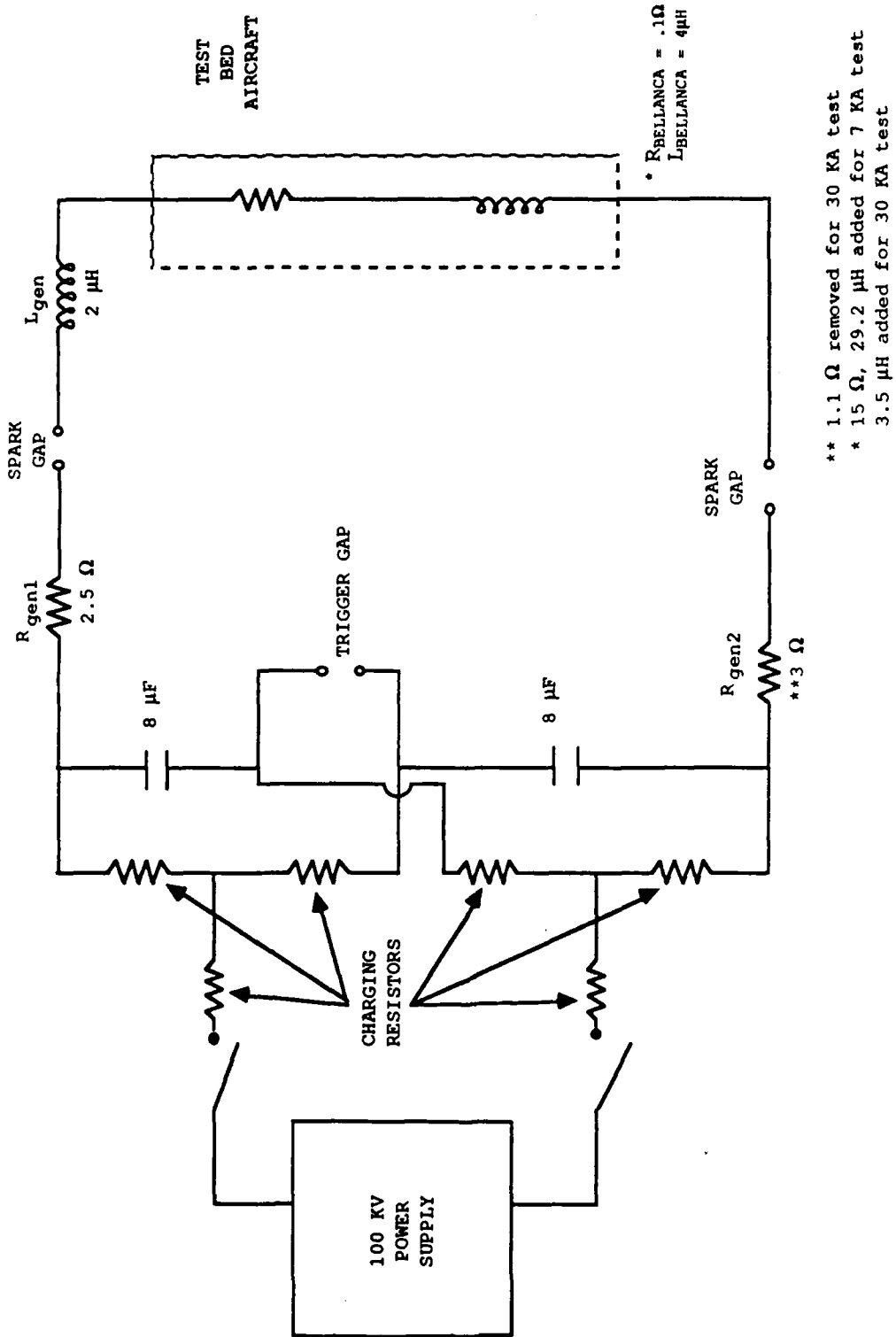


FIGURE 28 MODERATE-LEVEL PULSE GENERATOR CONFIGURATION

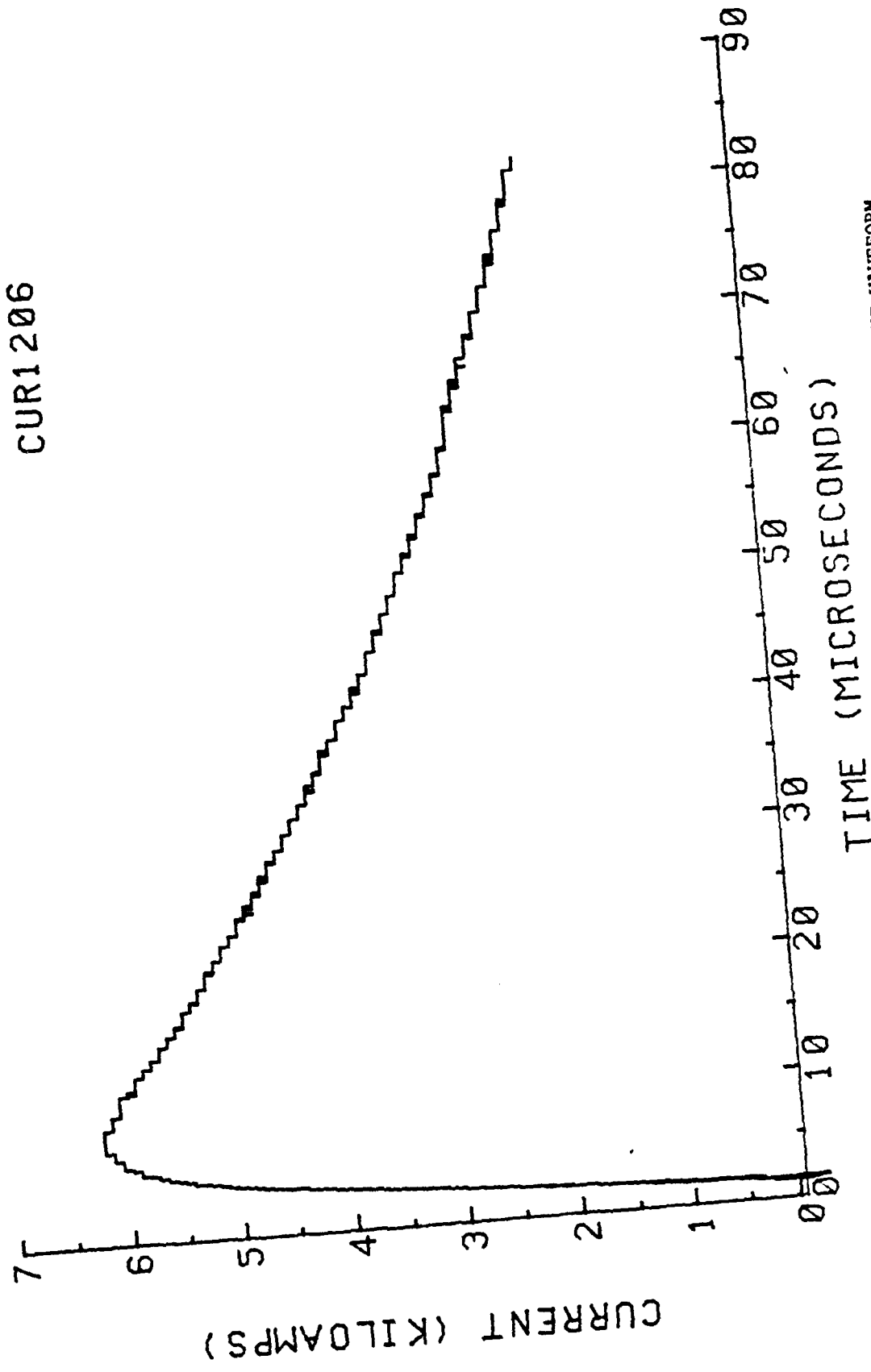


FIGURE 29 EXAMPLE 7 KA MODERATE-LEVEL PULSE CURRENT WAVEFORM

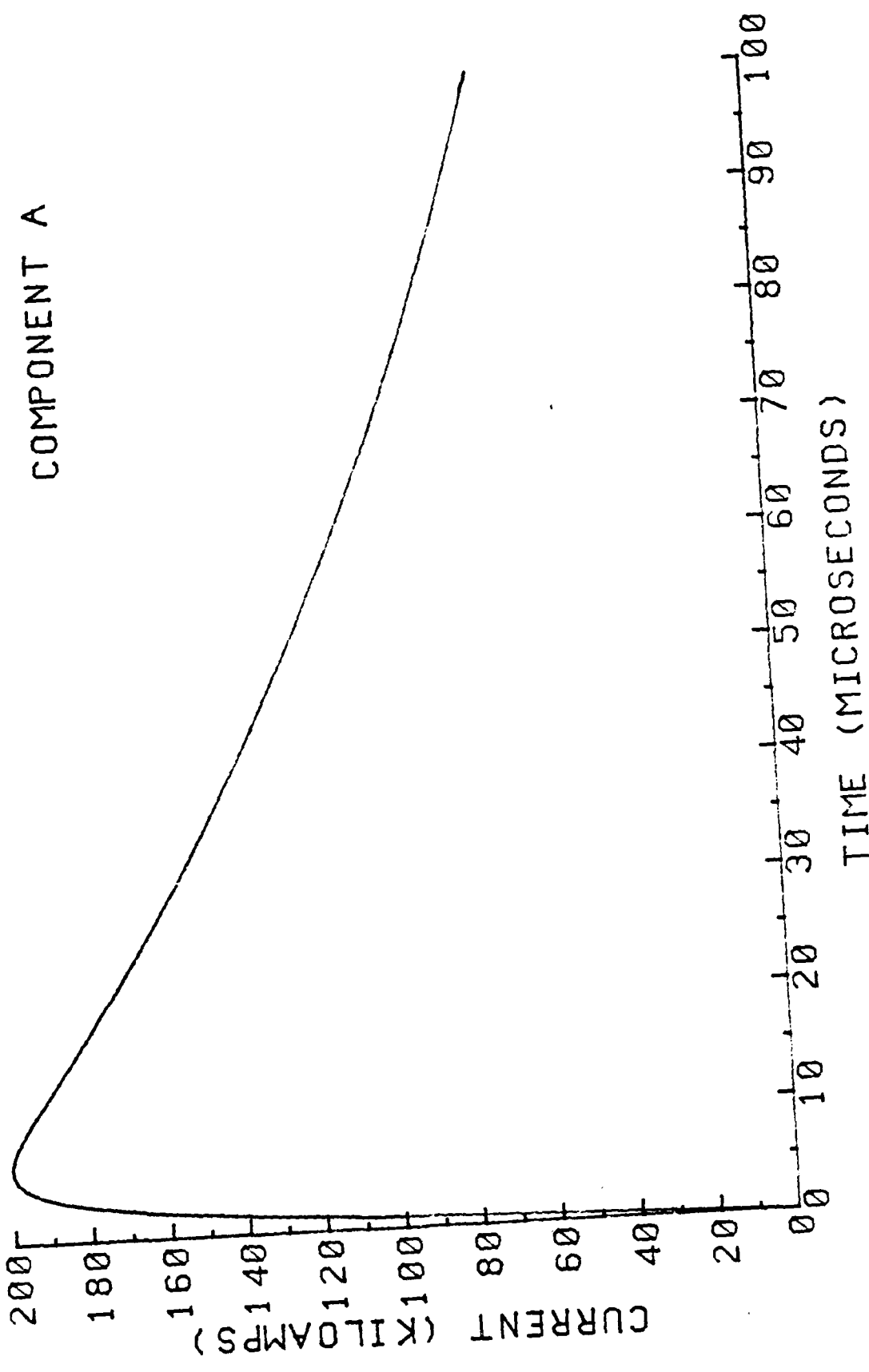


FIGURE 30 COMPONENT A SEVERE LIGHTNING THREAT CURRENT WAVEFORM

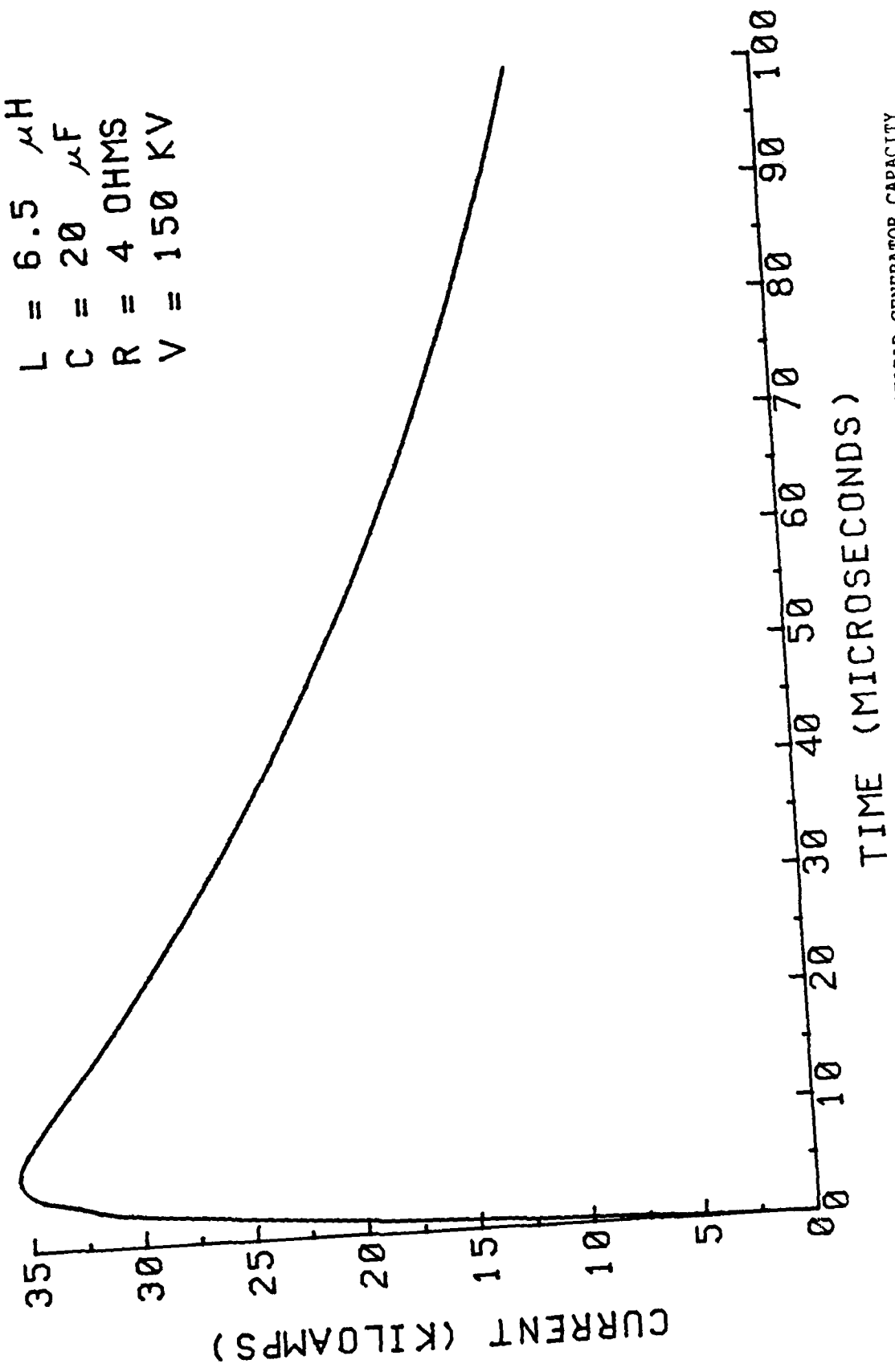


FIGURE 31 MODERATE-LEVEL PULSE CURRENT WAVEFORM WITH 20 MICROFARAD GENERATOR CAPACITY

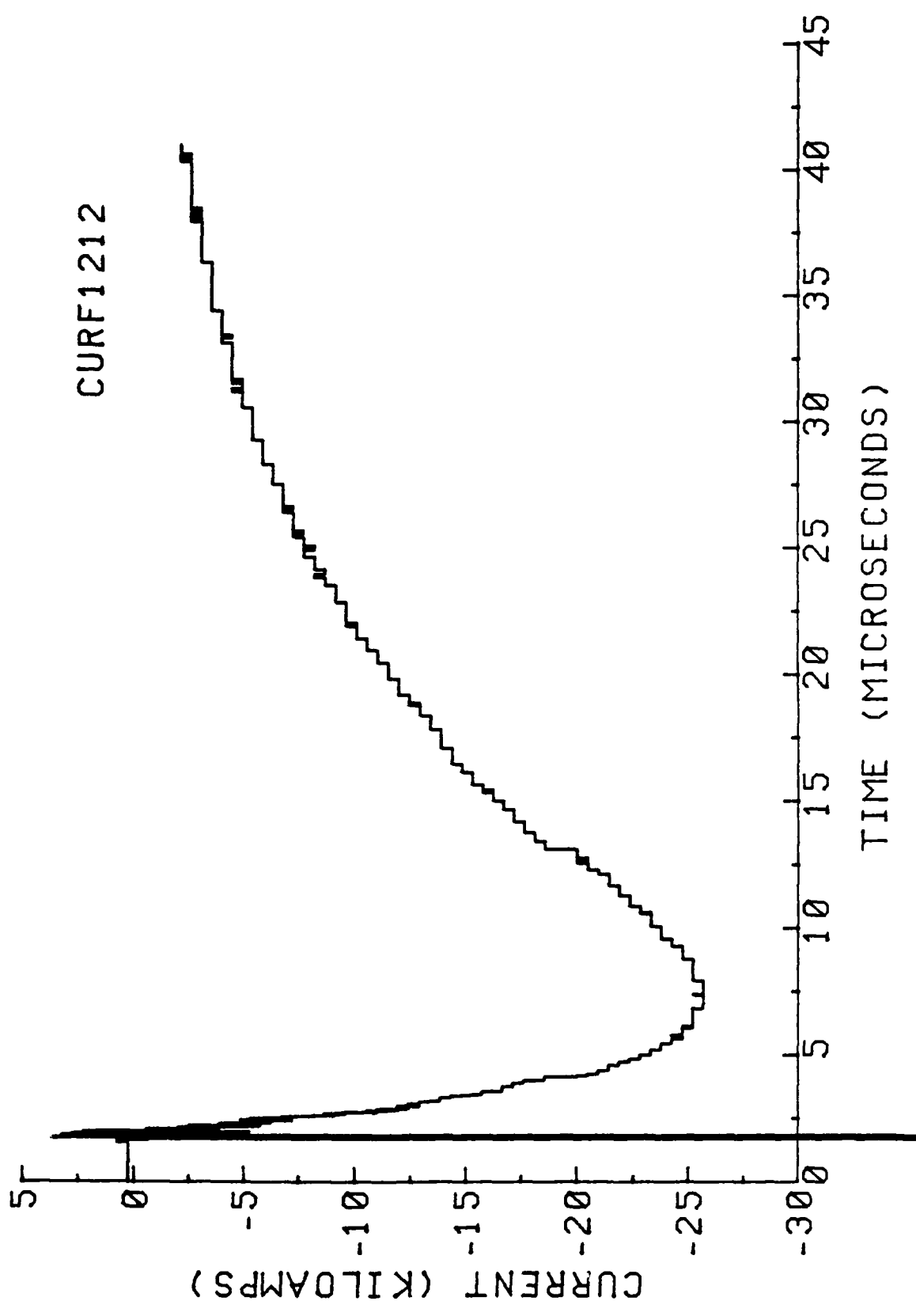


FIGURE 32 EXAMPLE 30 KA MODERATE-LEVEL PULSE CURRENT WAVEFORM

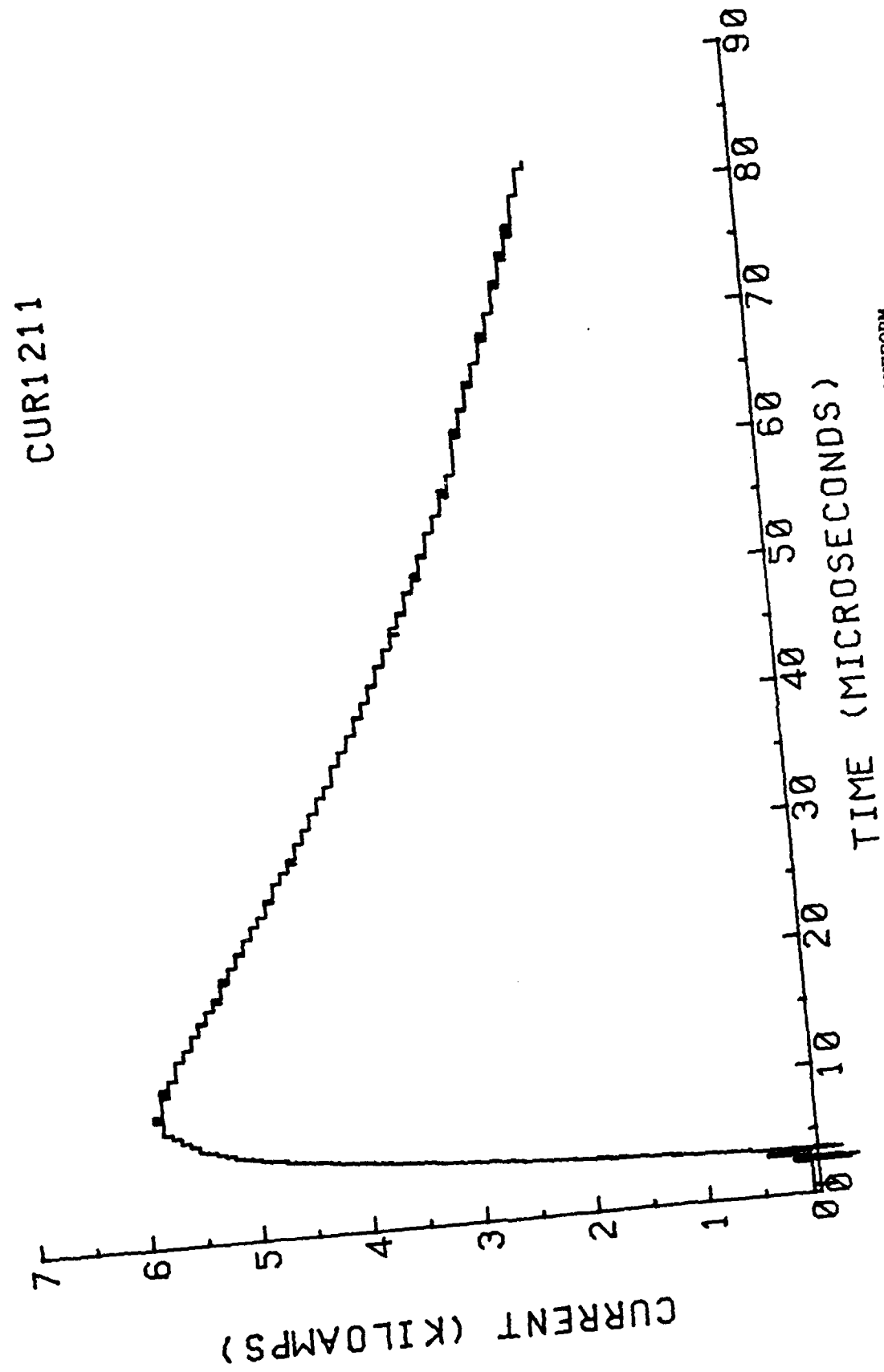


FIGURE 33 EXAMPLE SHOCK-EXCITATION CURRENT WAVEFORM

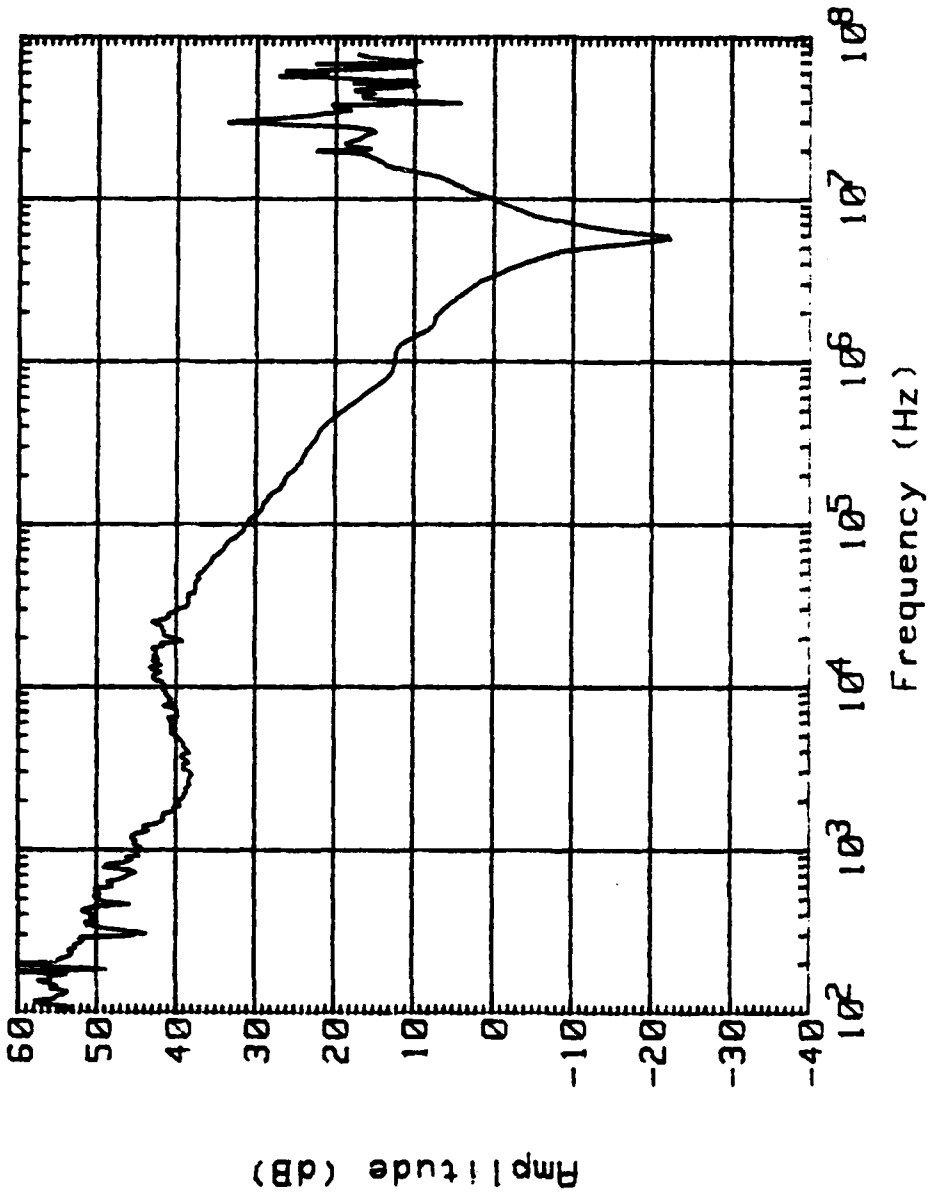


FIGURE 34 TEST BED INPUT IMPEDANCE INTO AN OPEN CIRCUIT - NOSE DRIVE

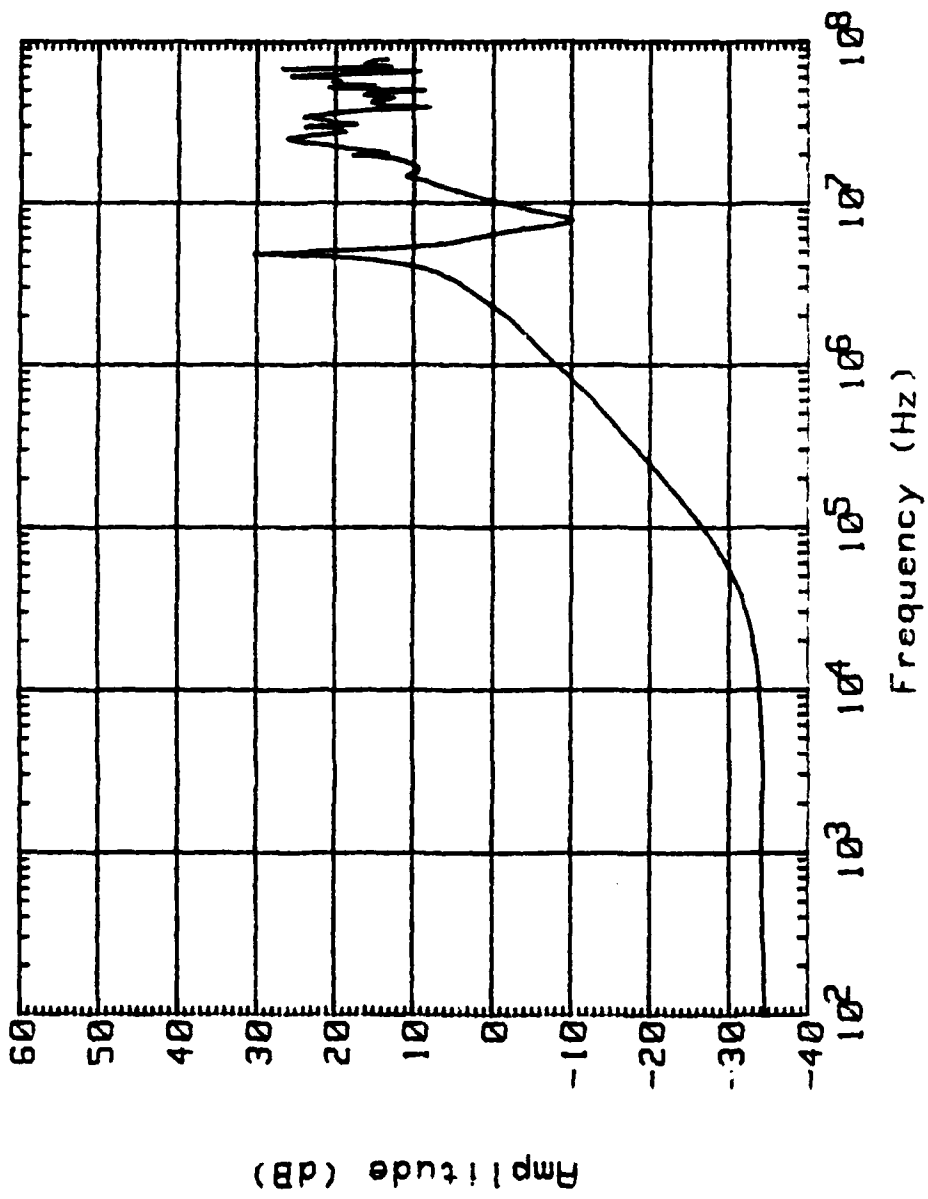
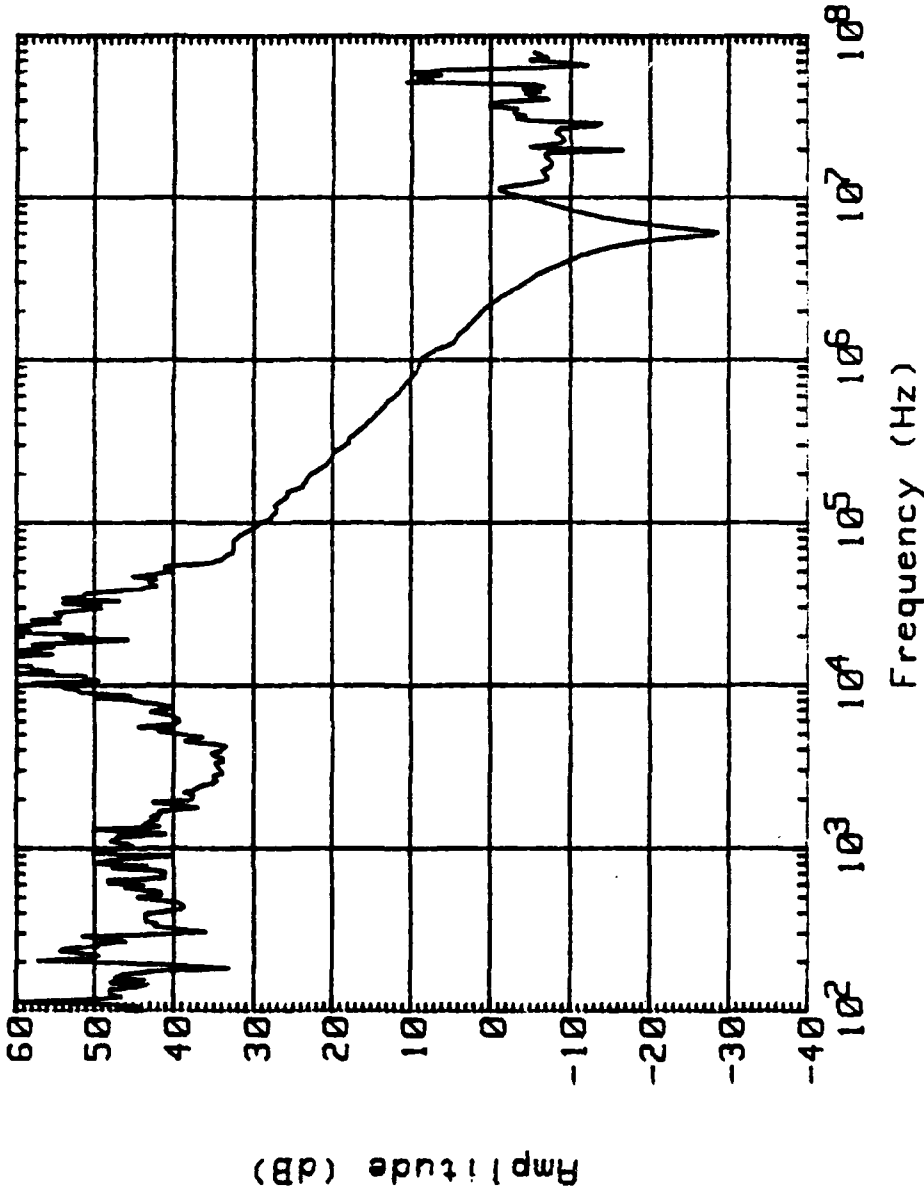
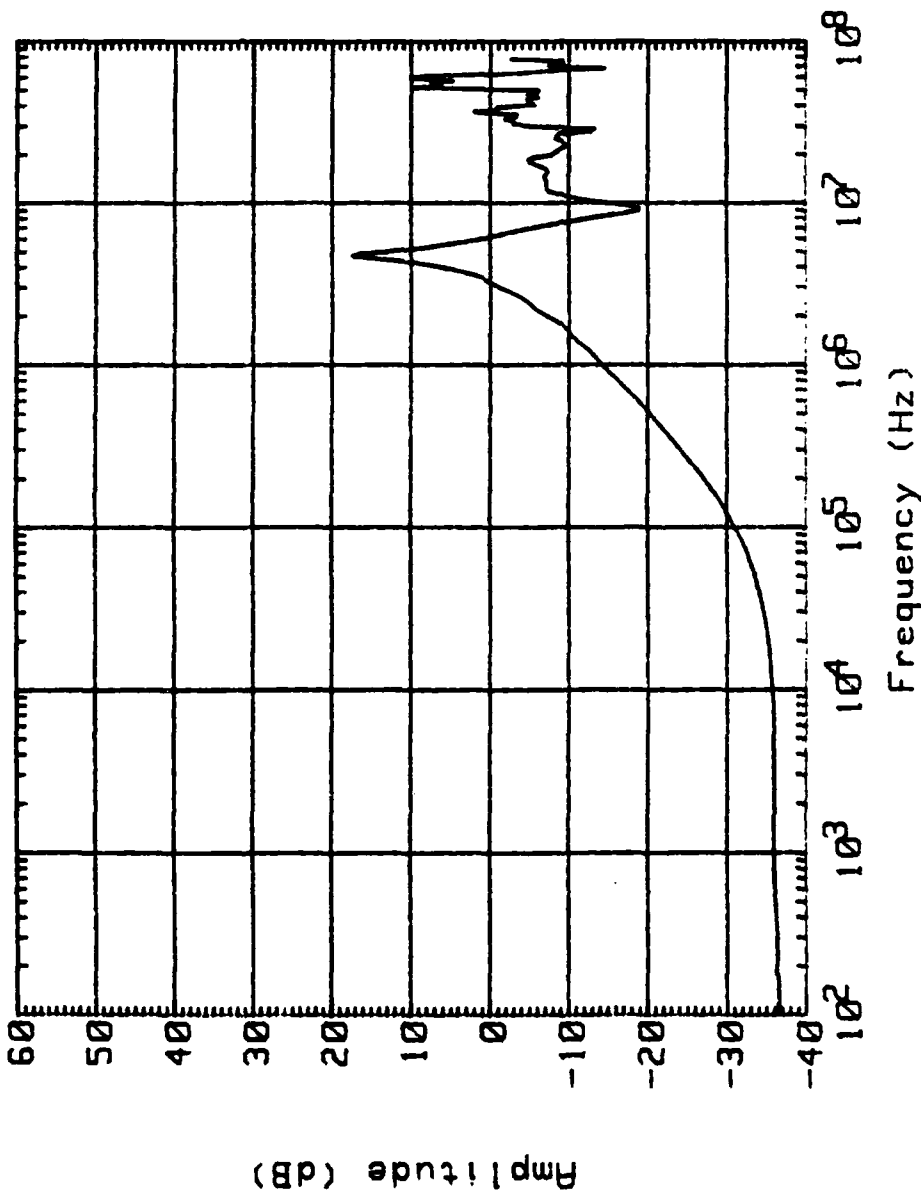


FIGURE 35 TEST BED INPUT IMPEDANCE INTO A SHORT CIRCUIT - NOSE DRIVE



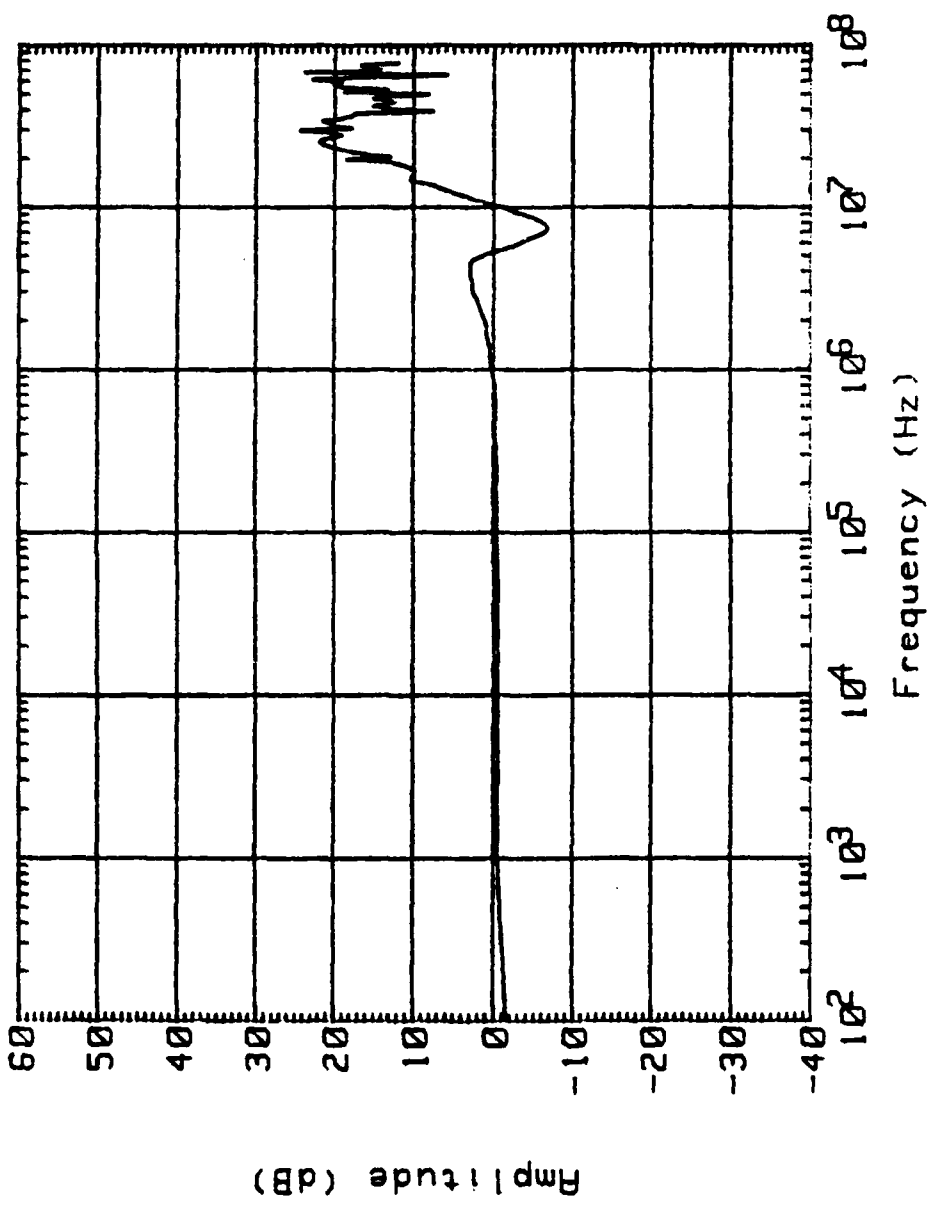
TEST ID. No.: ZINOCW
(8-12-85): INPUT IMPEDANCE INTO OPEN CIRCUIT;

FIGURE 36 TEST BED INPUT IMPEDANCE INTO AN OPEN CIRCUIT - WING DRIVE



TEST ID. No.: Z_{INSC}
(8-12-85): INPUT IMPEDANCE INTO SHORT CIRCUIT;

FIGURE 37 TEST BED INPUT IMPEDANCE INTO A SHORT CIRCUIT - WING DRIVE



TEST ID. No.: ZIN809
(8-9-85): INPUT IMPEDANCE INTO 50 OHMS; NOSE DRIVE

FIGURE 38 TEST BED INPUT IMPEDANCE INTO 50 OHMS - NOSE DRIVE

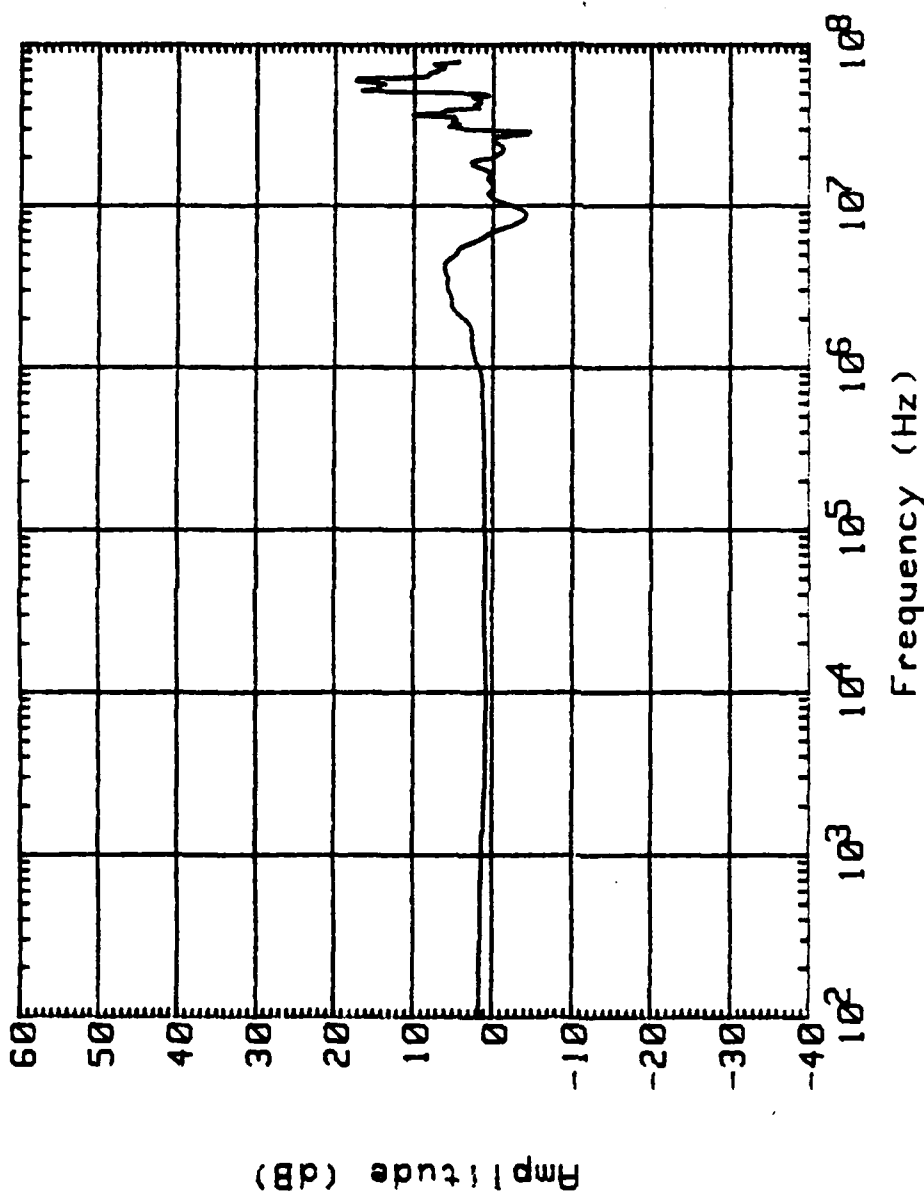


FIGURE 39 TEST BED INPUT IMPEDANCE INTO 50 OHMS - WING DRIVE

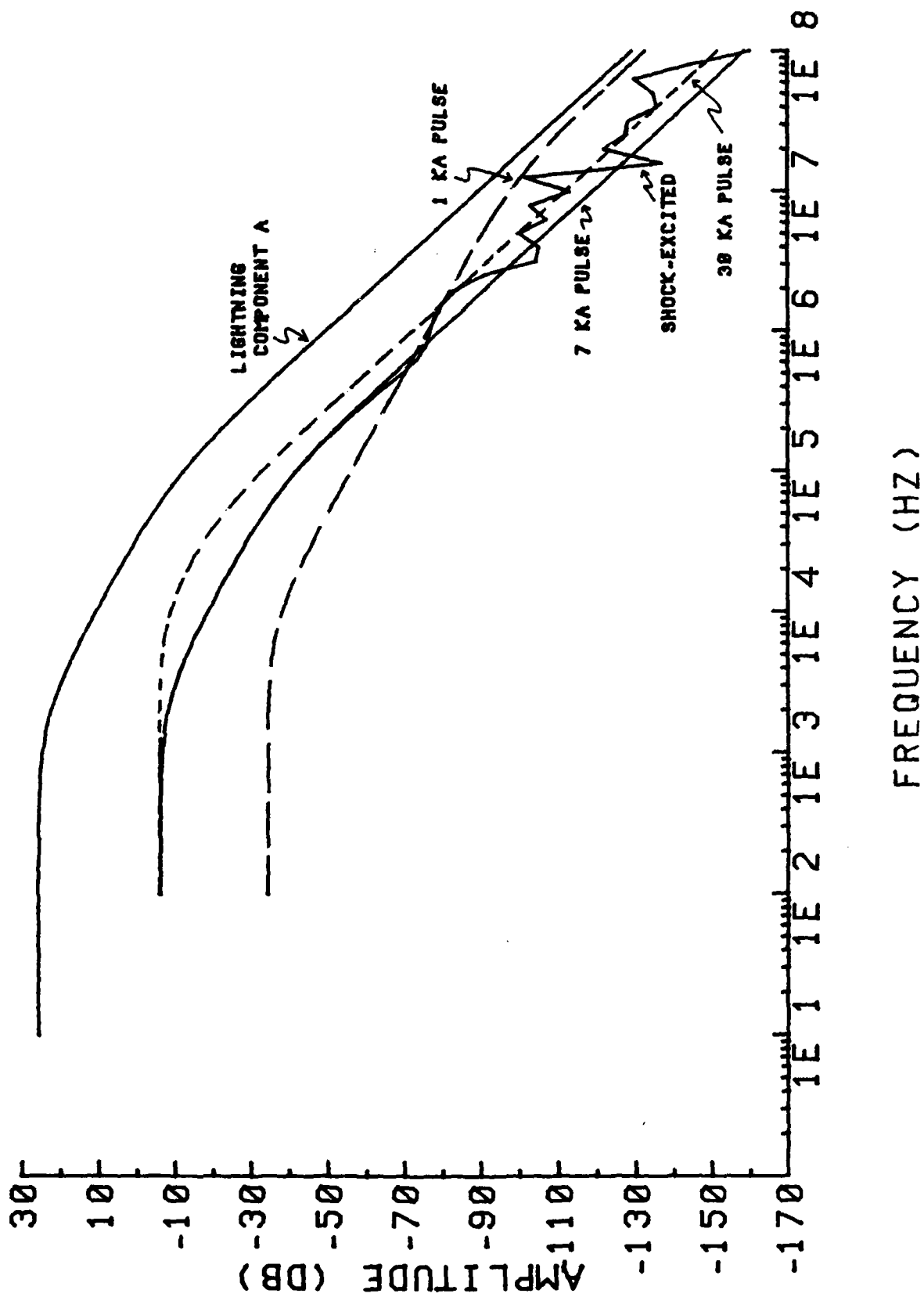


FIGURE 40 COMPARISON OF PULSE CURRENT SPECTRA WITH SEVERE LIGHTNING SPECTRUM

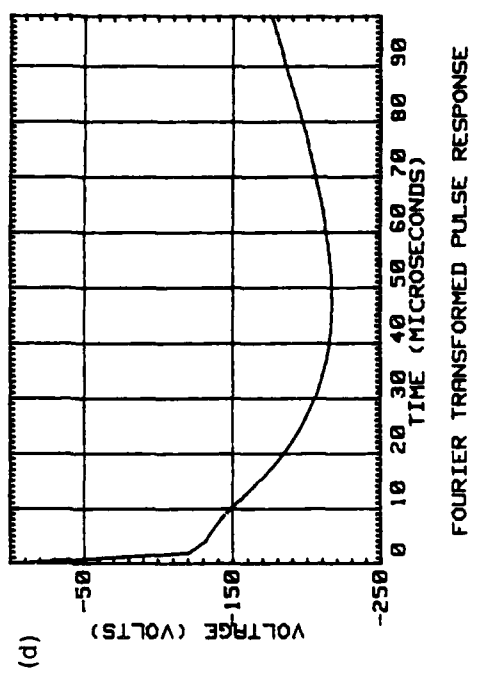
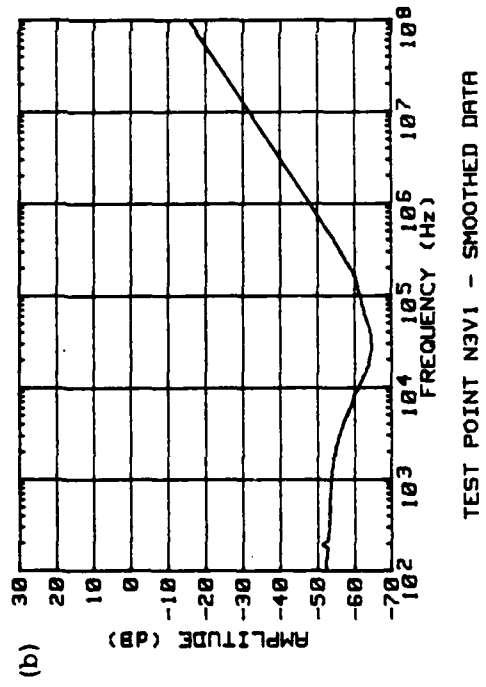
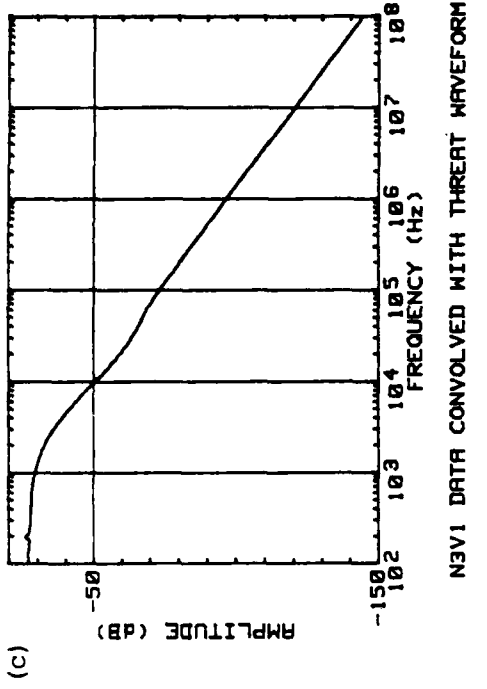
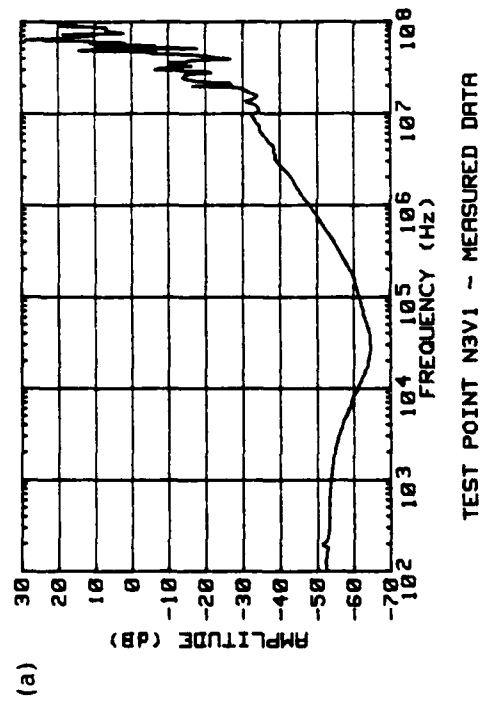


FIGURE 41 EXAMPLE TRANSFER FUNCTION MEASUREMENT

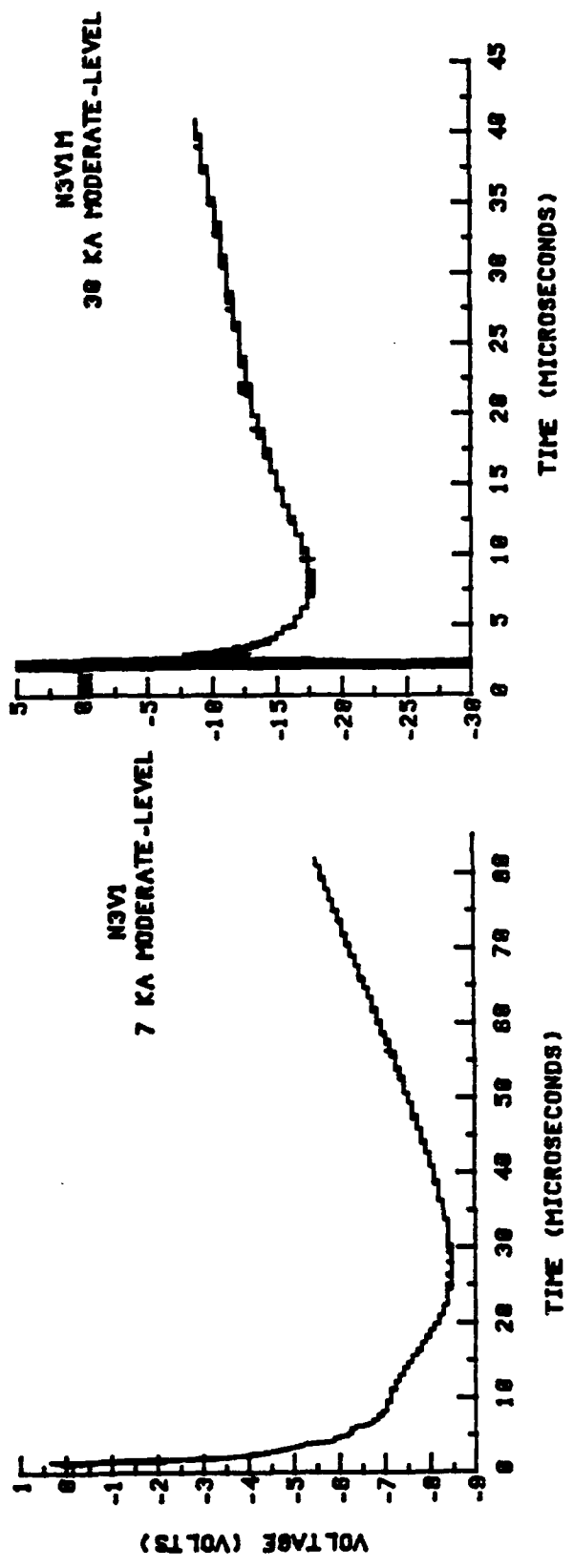
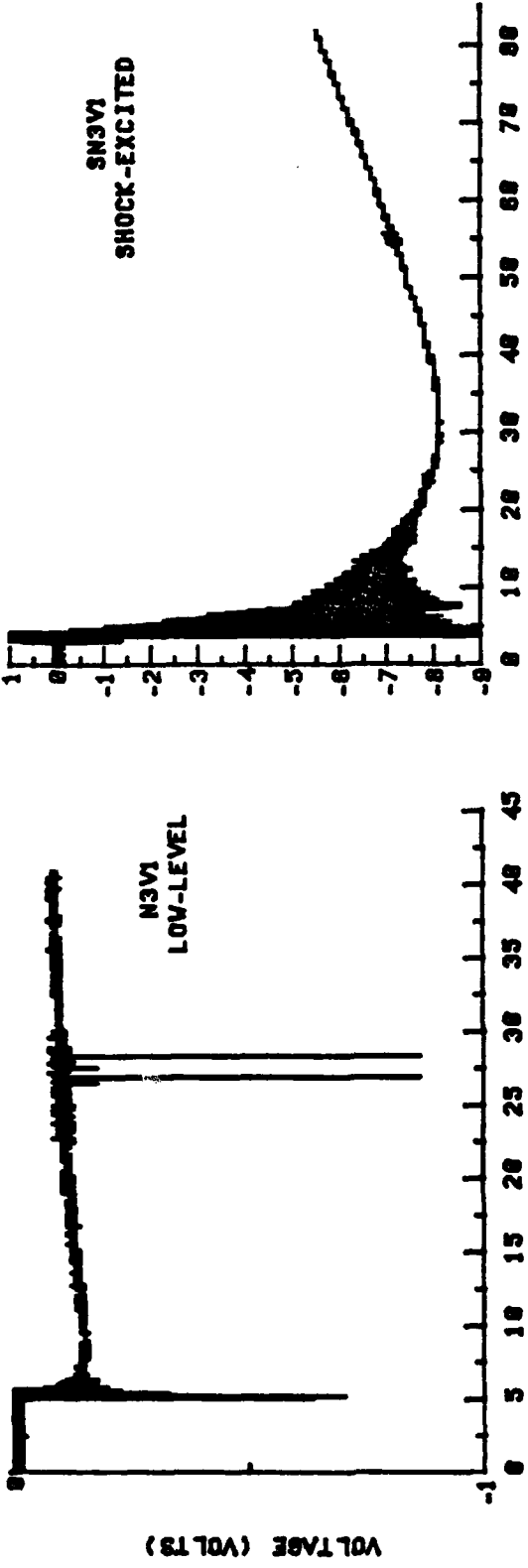


FIGURE 42 EXAMPLE RESISTIVE RESPONSE MEASUREMENT

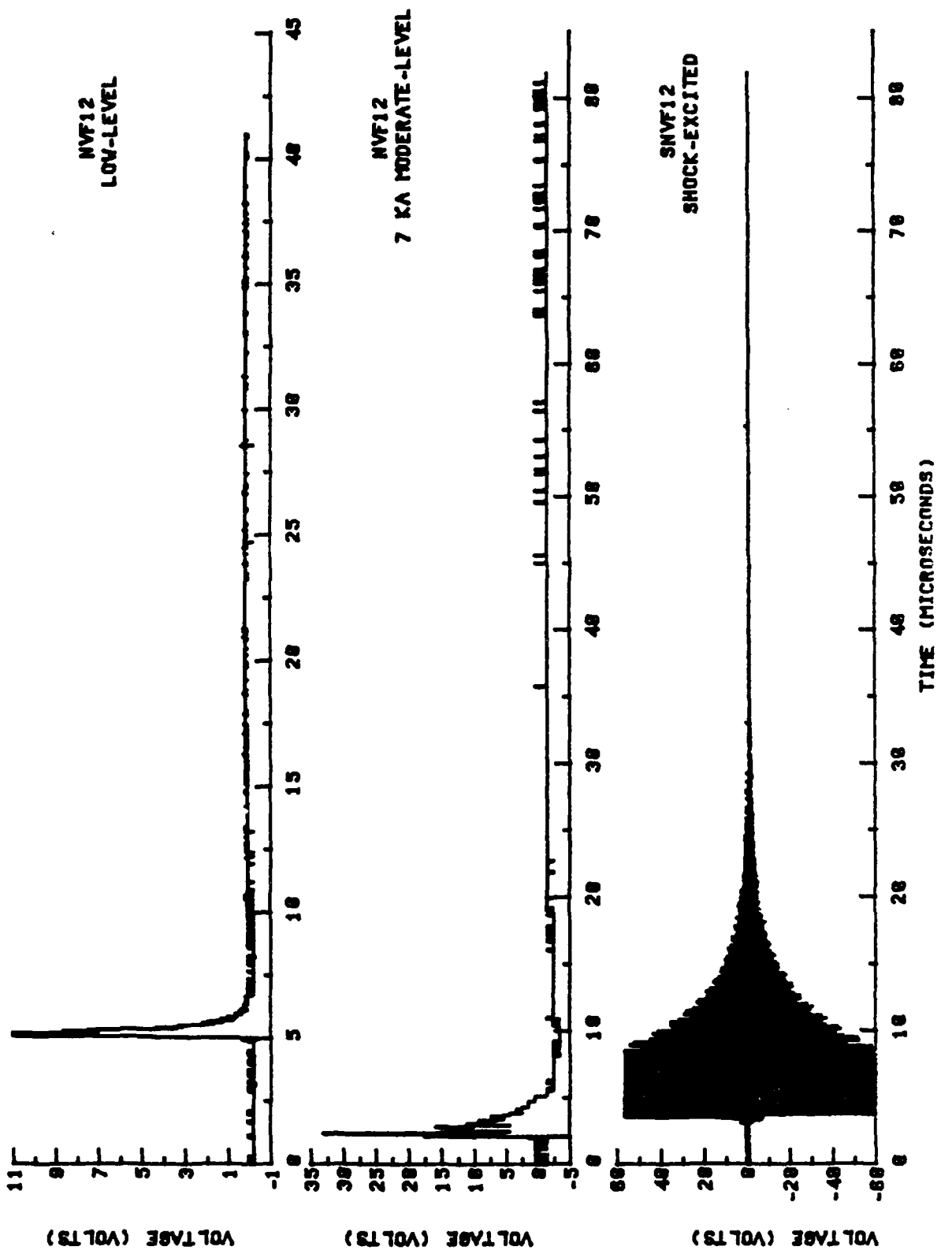


FIGURE 43 EXAMPLE I-DOT RESPONSE MEASUREMENT

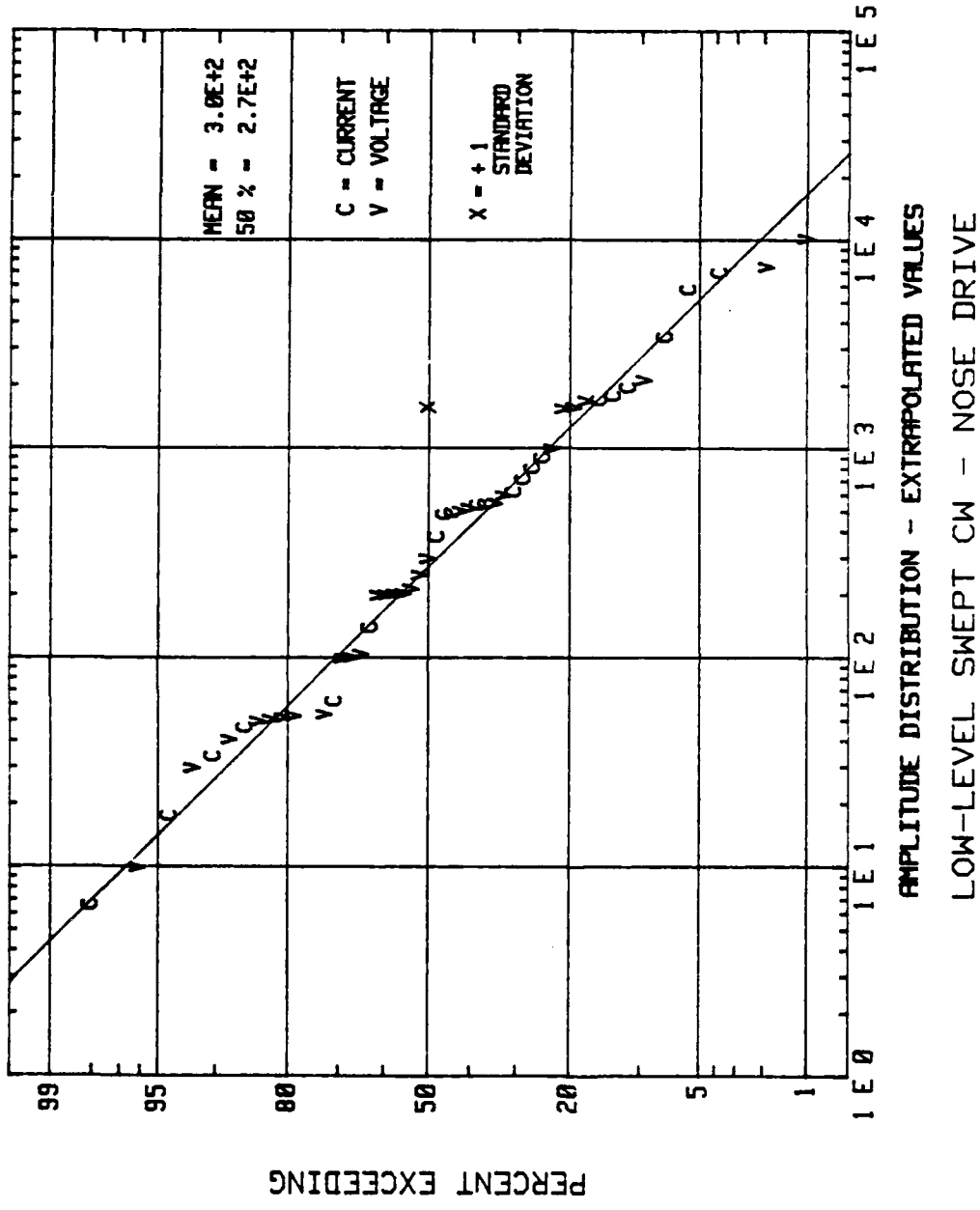


FIGURE 44 STATISTICAL DISTRIBUTION OF SWEPT CW EXTRAPOLATED VALUES - NOSE DRIVE

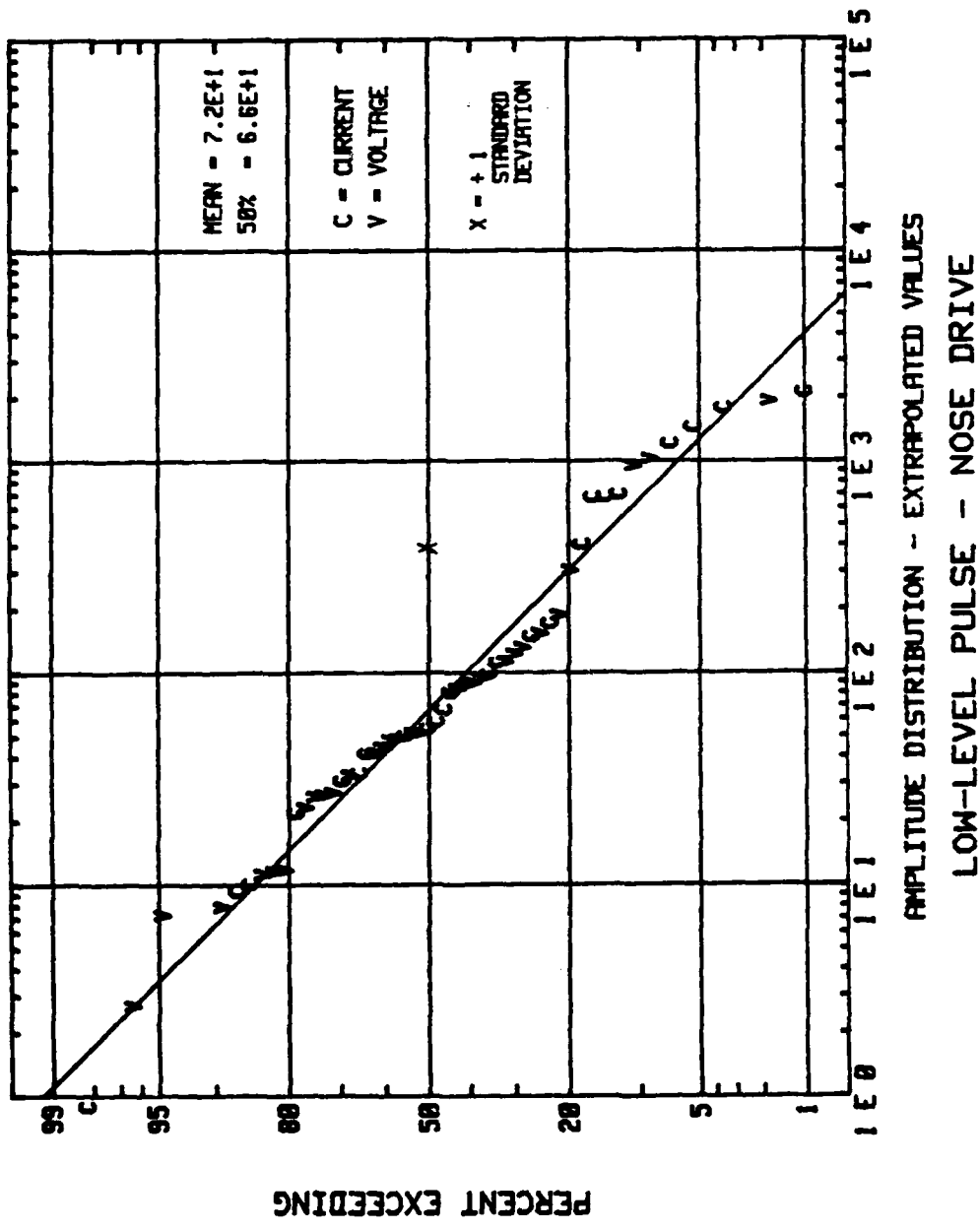


FIGURE 45 STATISTICAL DISTRIBUTION OF LOW-LEVEL PULSE EXTRAPOLATED VALUES
NOSE DRIVE

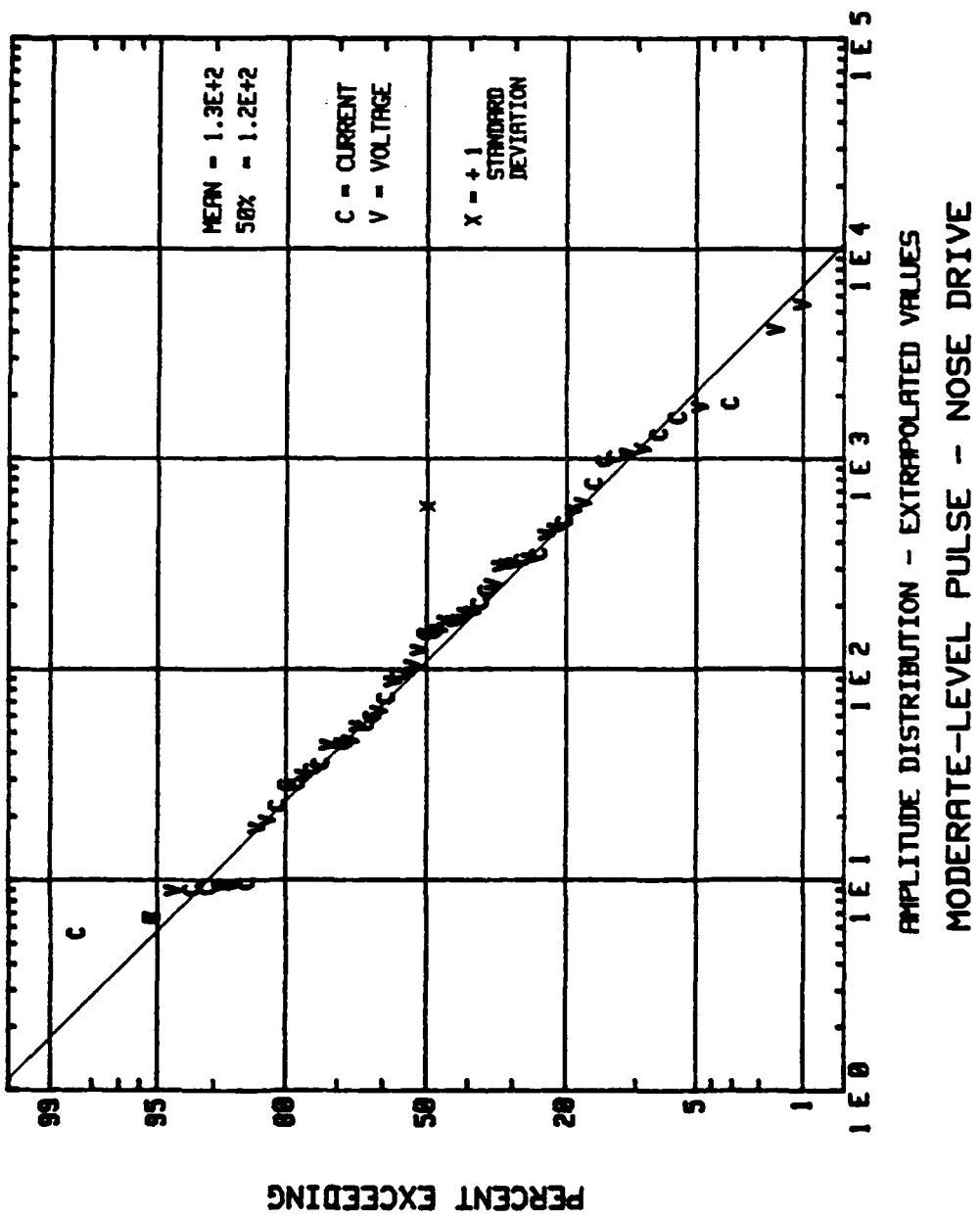


FIGURE 46 STATISTICAL DISTRIBUTION OF MODERATE-LEVEL PULSE EXTRAPOLATED VALUES
NOSE DRIVE

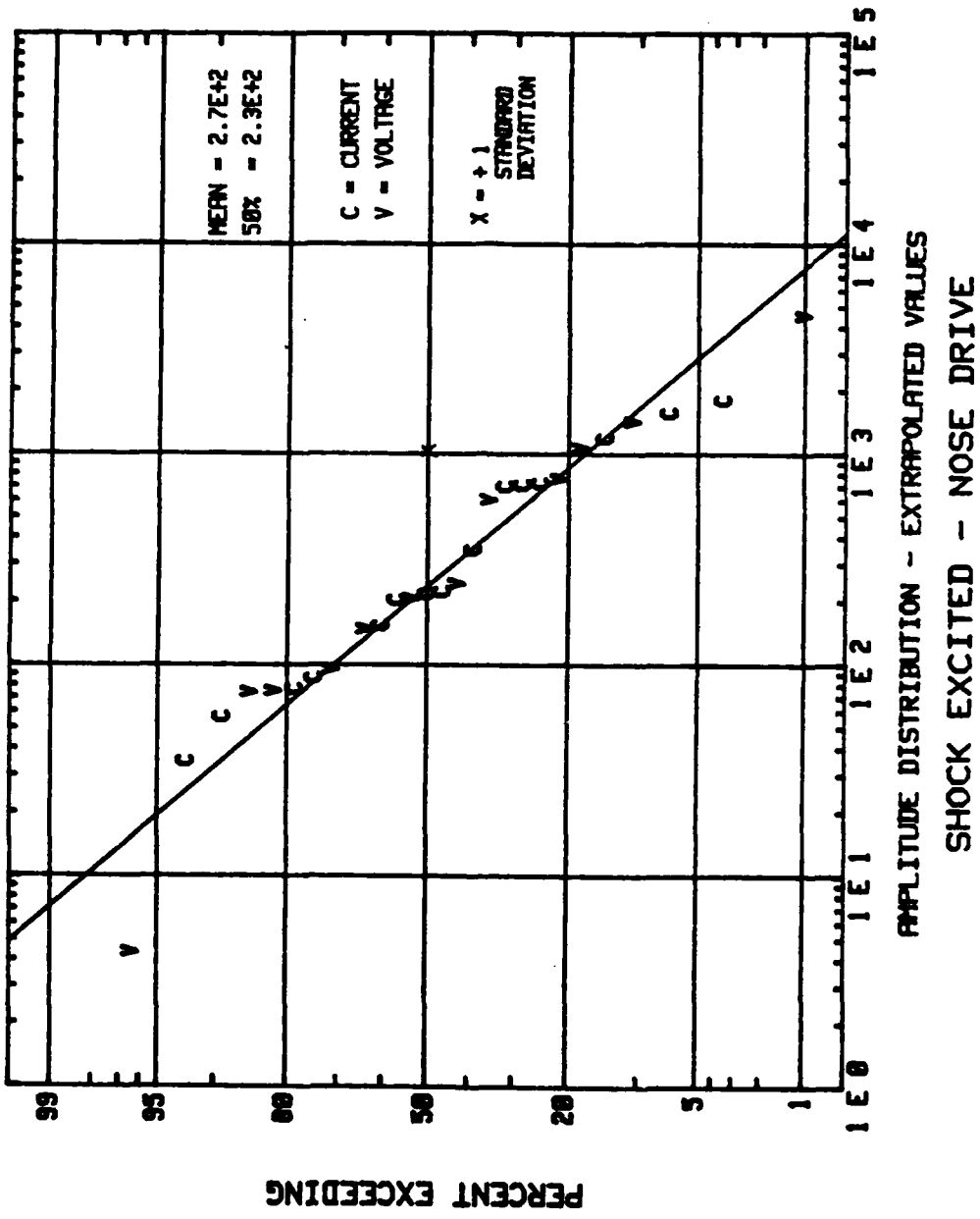


FIGURE 47 STATISTICAL DISTRIBUTION OF SHOCK-EXCITATION EXTRAPOLATED VALUES
NOSE DRIVE

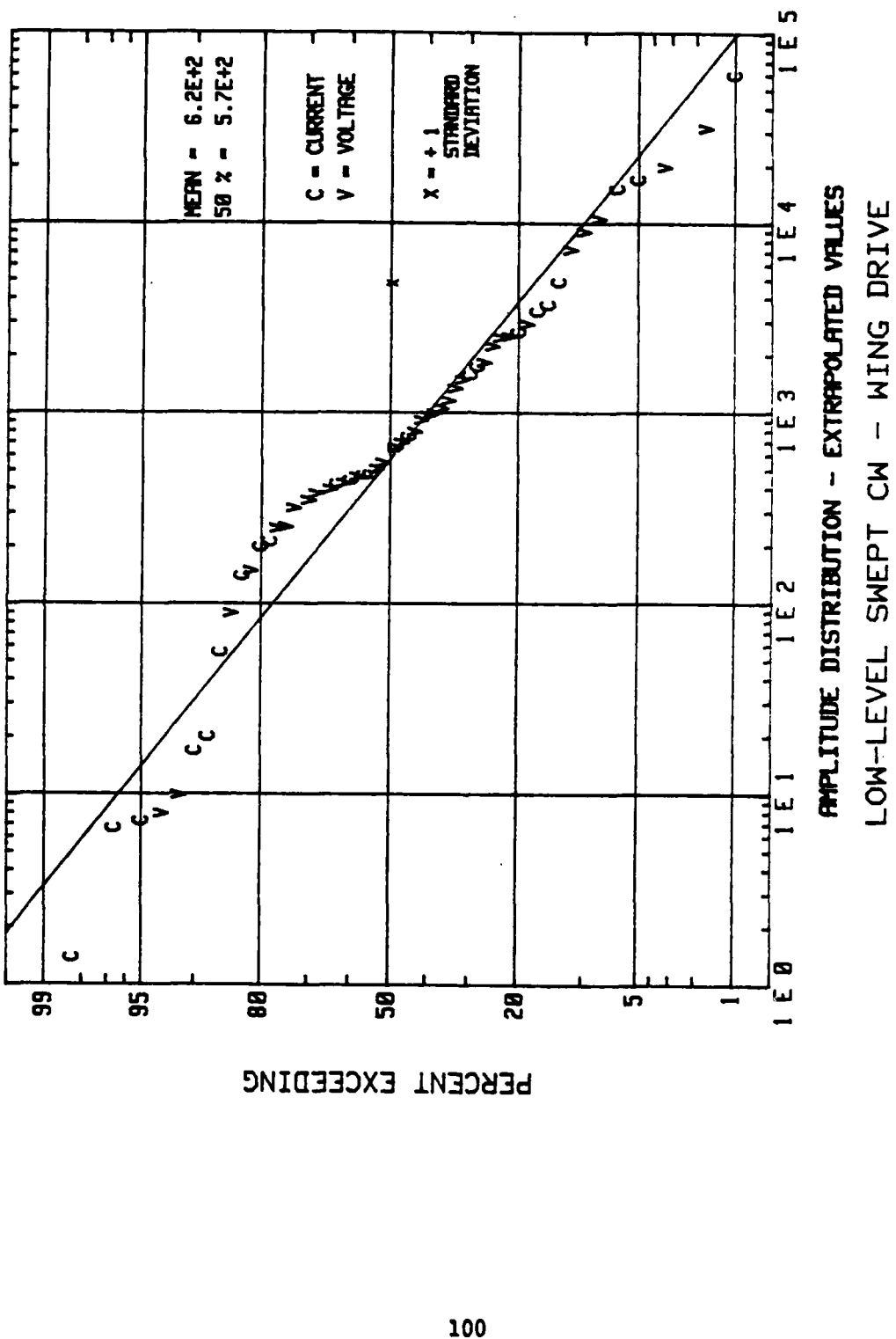


FIGURE 48 STATISTICAL DISTRIBUTION OF SWEPT CW EXTRAPOLATED VALUES - WING DRIVE

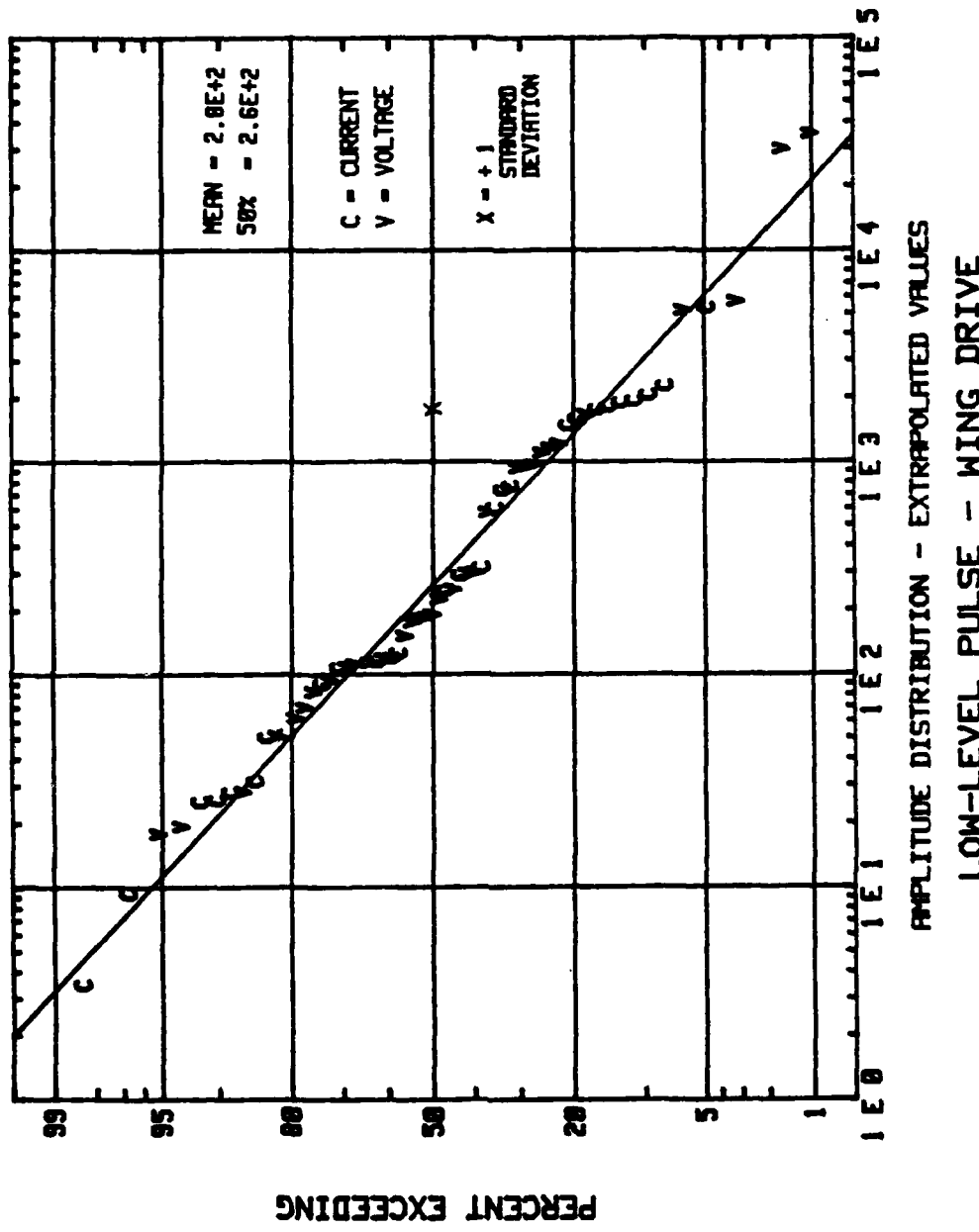


FIGURE 49 STATISTICAL DISTRIBUTION OF LOW-LEVEL PULSE EXTRAPOLATED VALUES
WING DRIVE

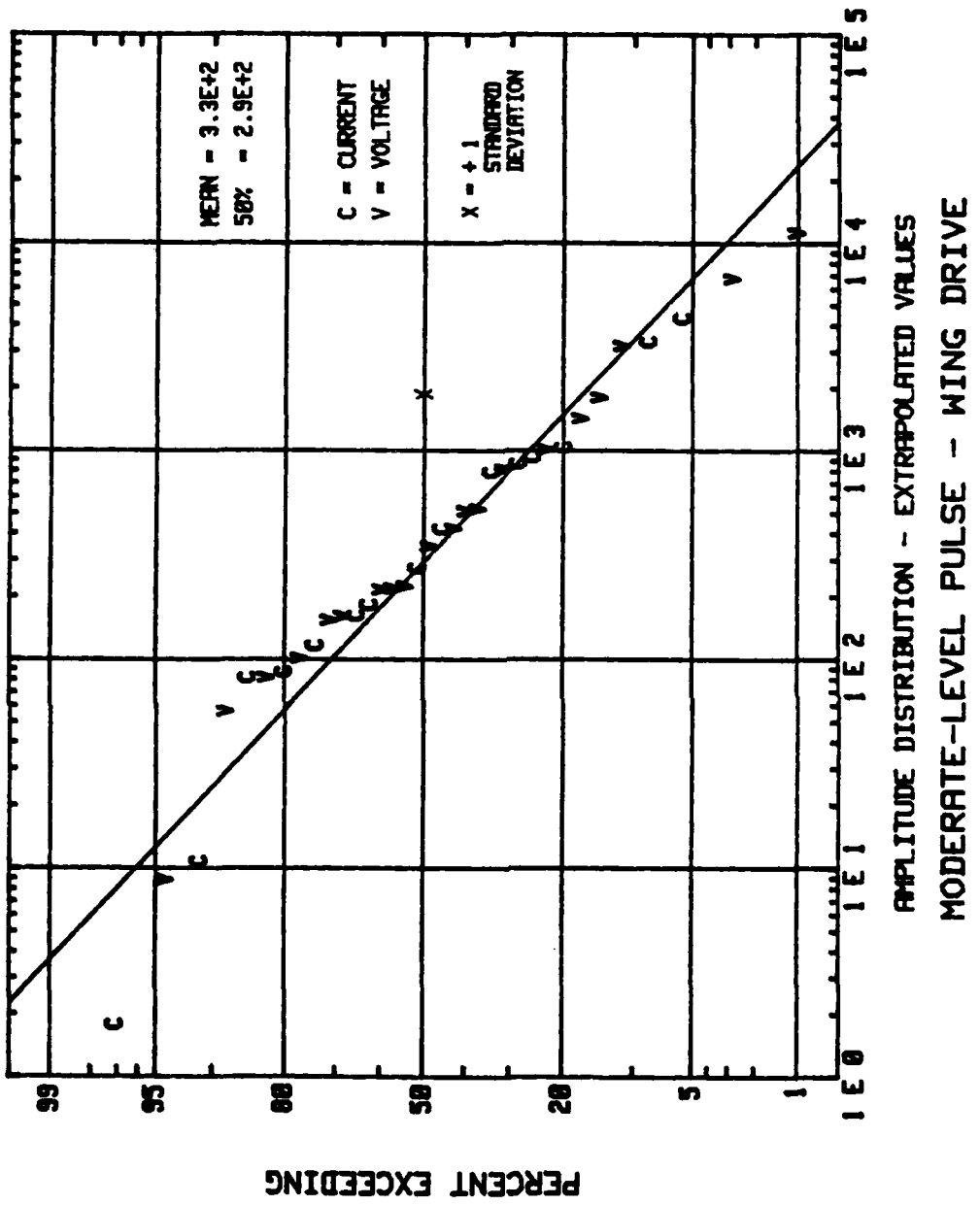


FIGURE 50 STATISTICAL DISTRIBUTION OF MODERATE-LEVEL PULSE EXTRAPOLATED VALUES
WING DRIVE

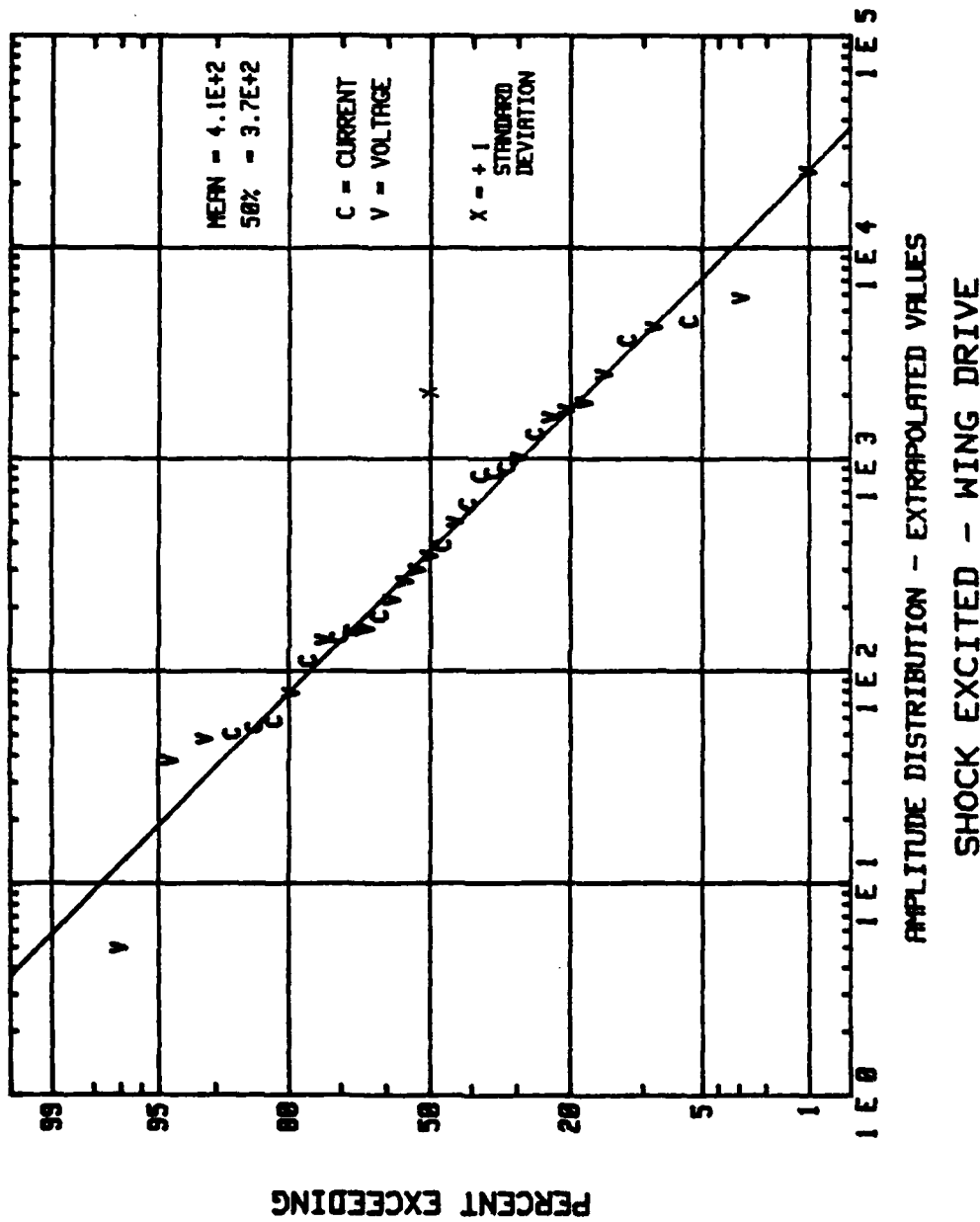


FIGURE 51 STATISTICAL DISTRIBUTION OF SHOCK-EXCITATION EXTRAPOLATED VALUES
WING DRIVE

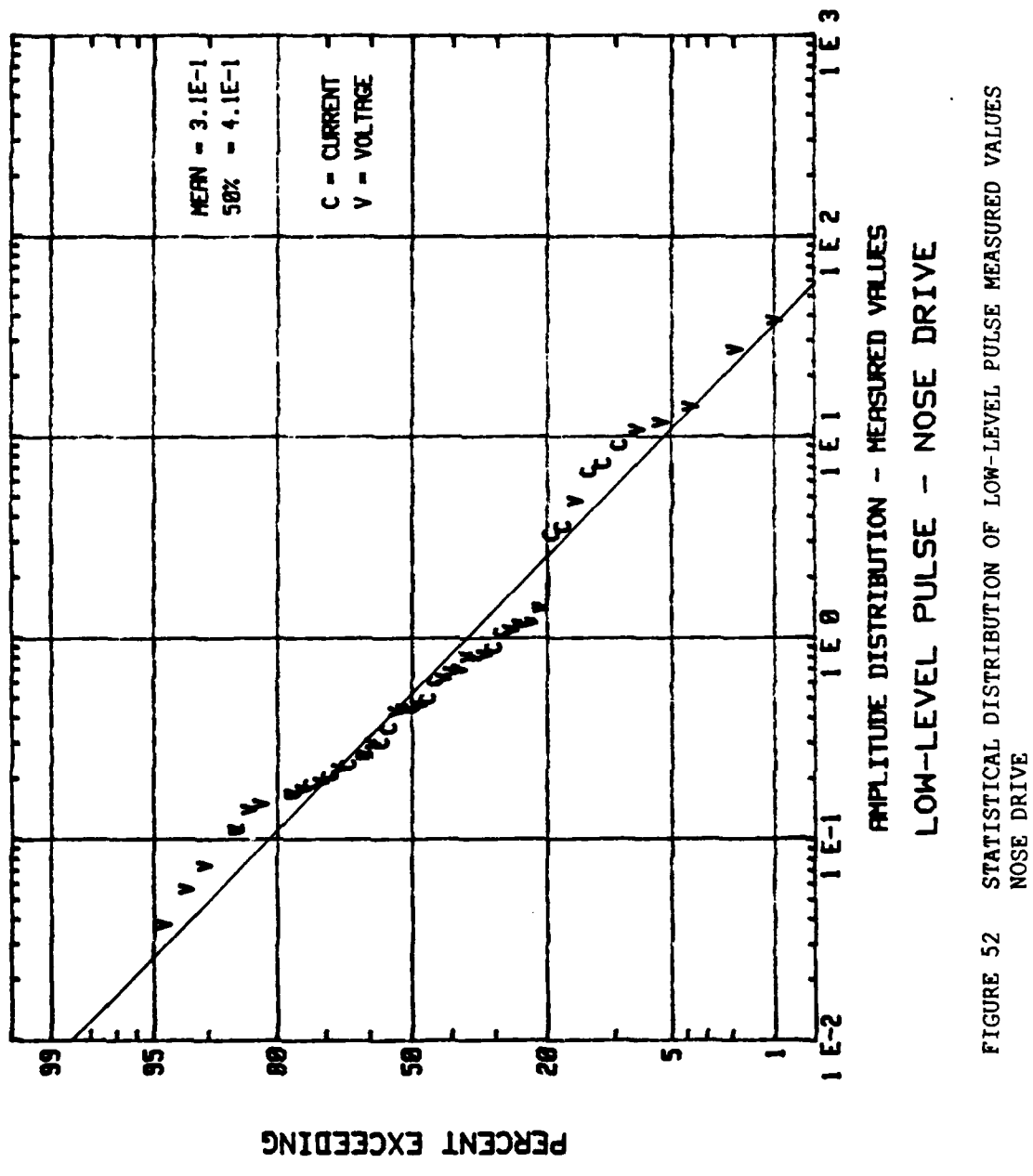


FIGURE 52 STATISTICAL DISTRIBUTION OF LOW-LEVEL PULSE MEASURED VALUES
NOSE DRIVE

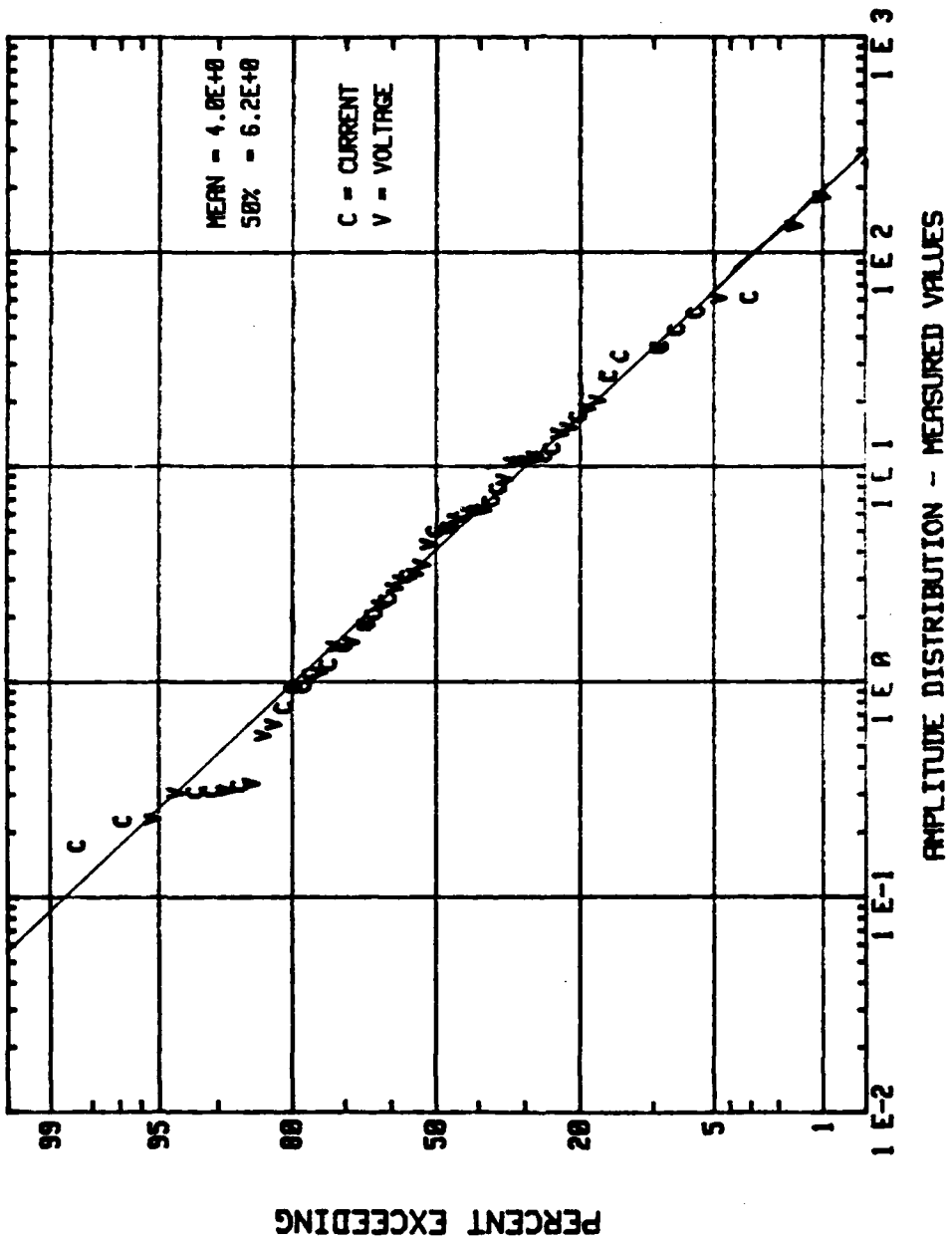


FIGURE 53 STATISTICAL DISTRIBUTION OF MODERATE-LEVEL PULSE MEASURED VALUES
MODERATE-LEVEL PULSE MEASURED VALUES - NOSE DRIVE

FIGURE 53 STATISTICAL DISTRIBUTION OF MODERATE-LEVEL PULSE MEASURED VALUES
NOSE DRIVE

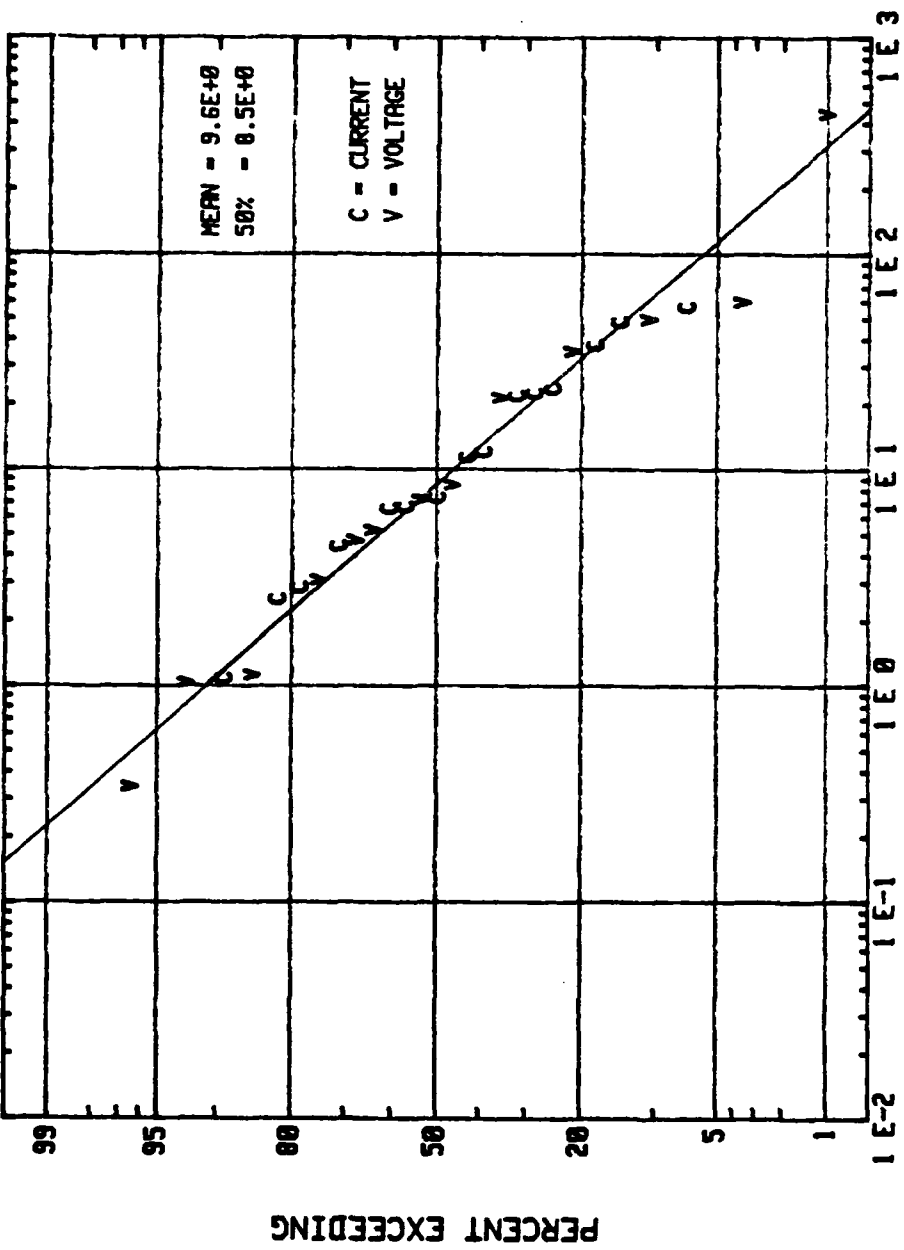


FIGURE 54 STATISTICAL DISTRIBUTION OF SHOCK-EXCITATION MEASURED VALUES
NOSE DRIVE

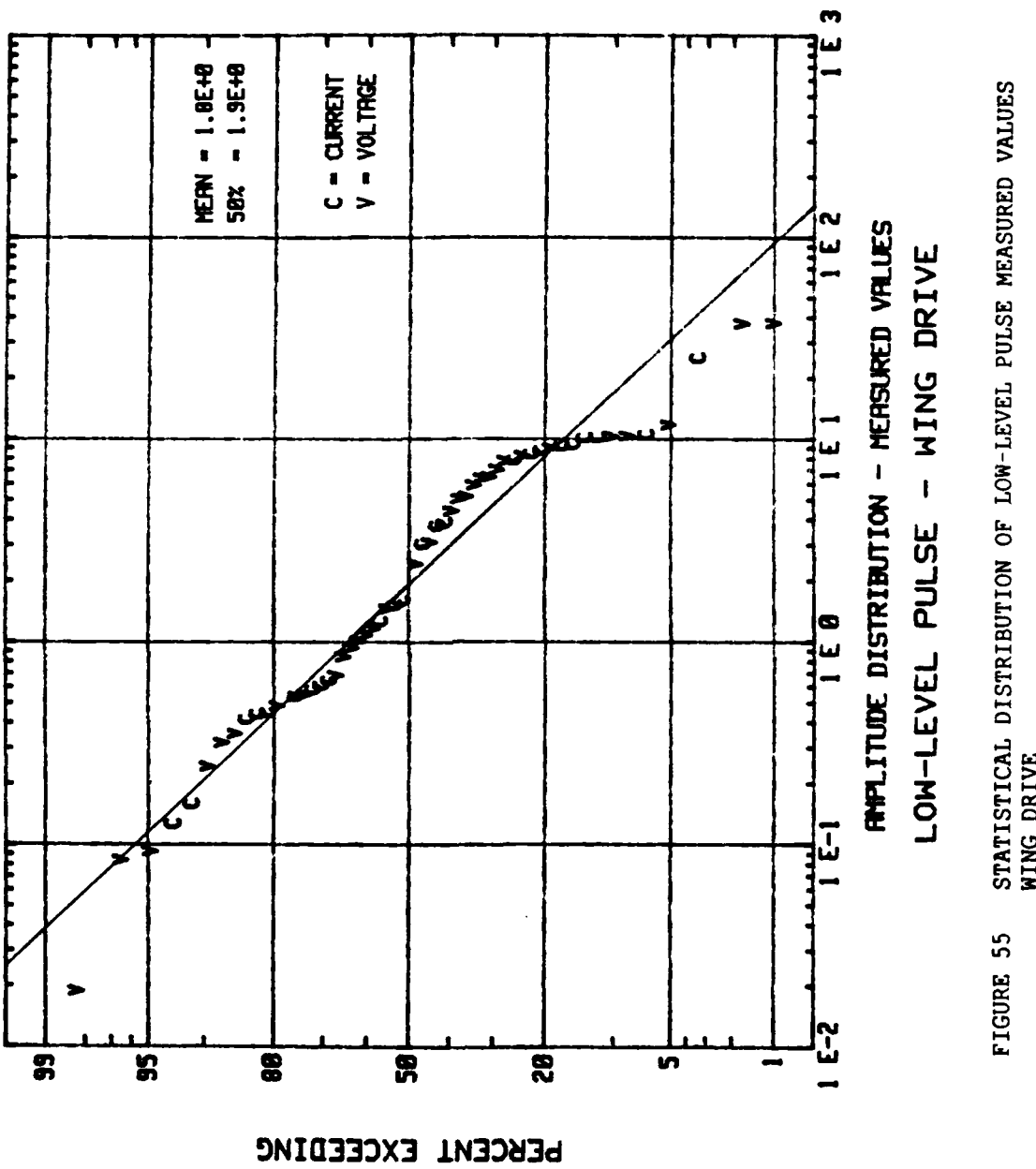


FIGURE 55 STATISTICAL DISTRIBUTION OF LOW-LEVEL PULSE MEASURED VALUES
WING DRIVE

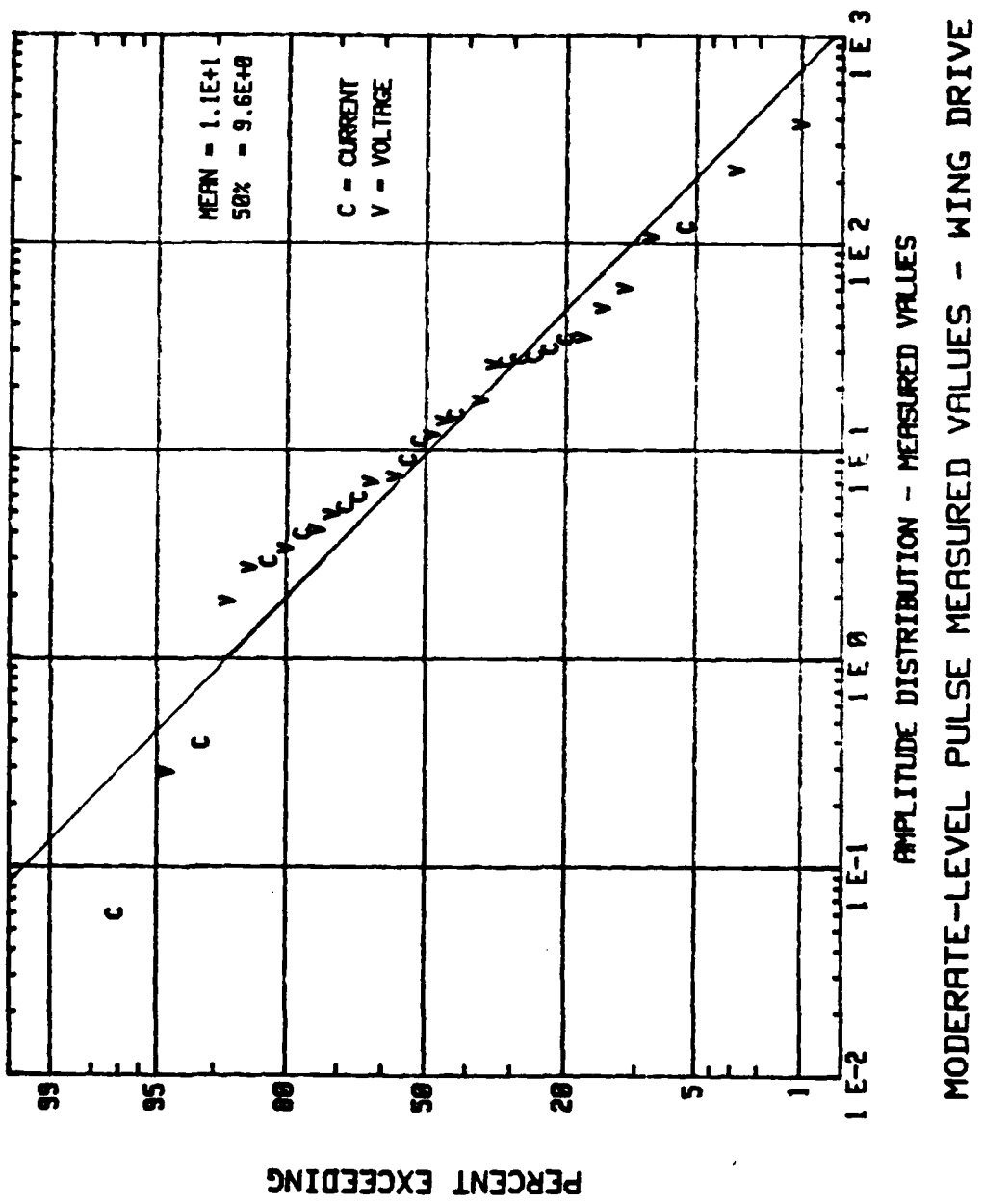


FIGURE 56 STATISTICAL DISTRIBUTION OF MODERATE-LEVEL PULSE MEASURED VALUES
WING DRIVE

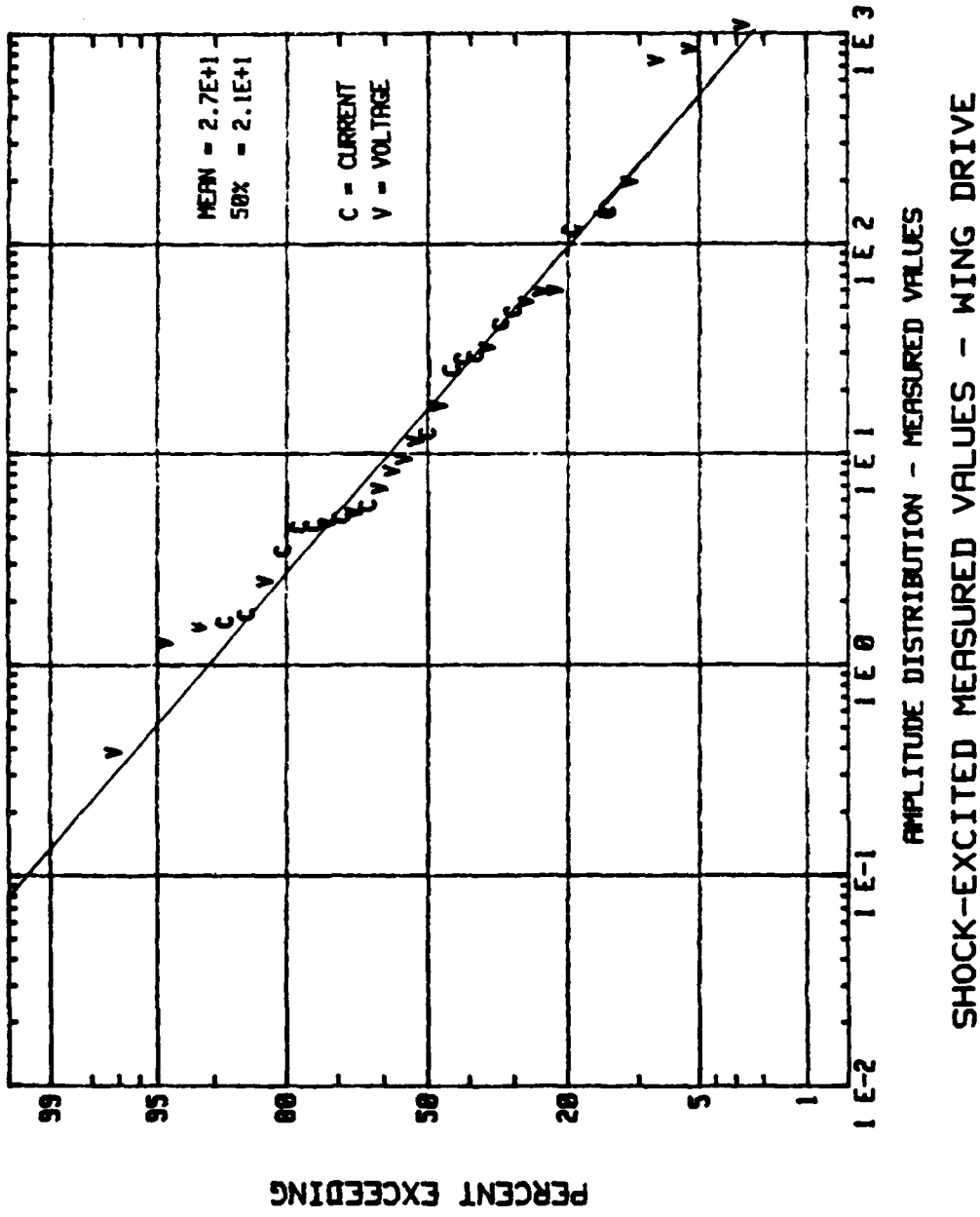


FIGURE 57 STATISTICAL DISTRIBUTION OF SHOCK-EXCITATION MEASURED VALUES
WING DRIVE

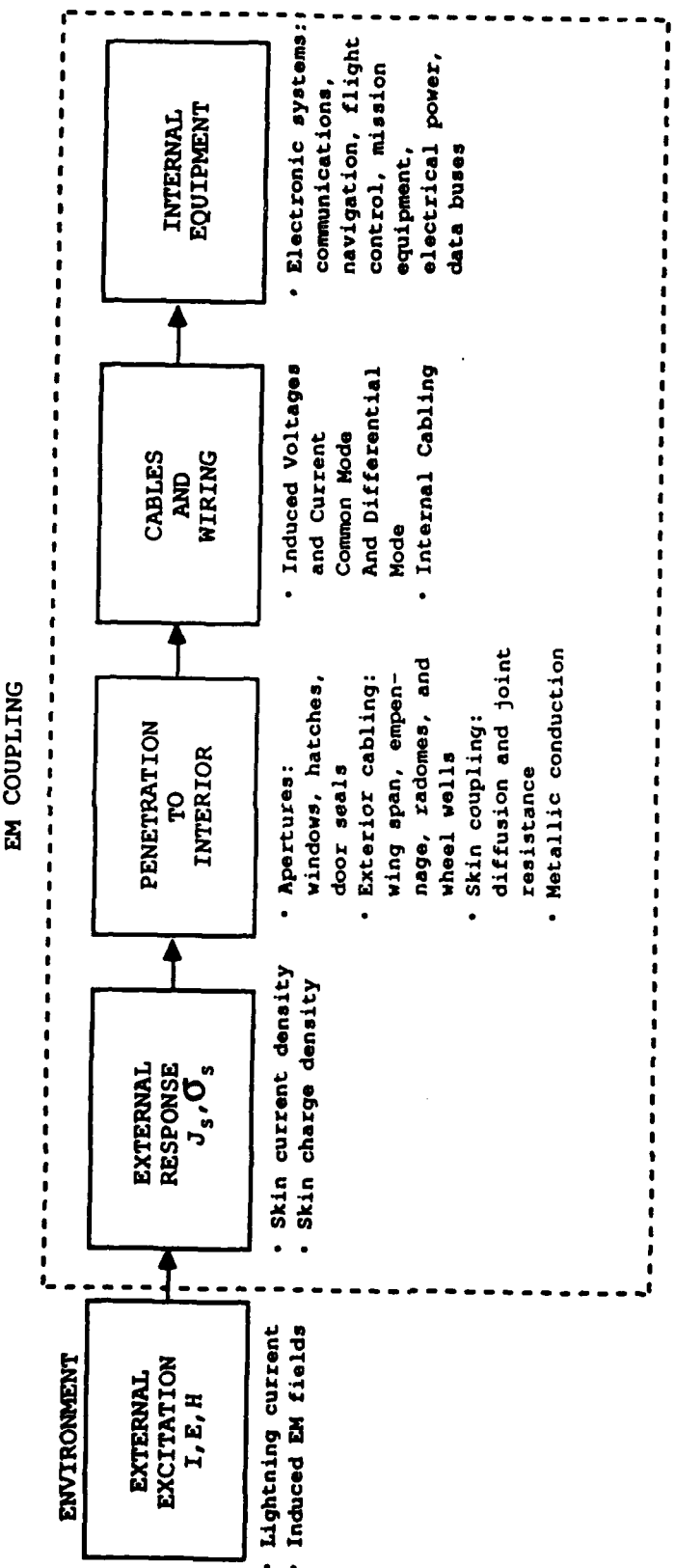
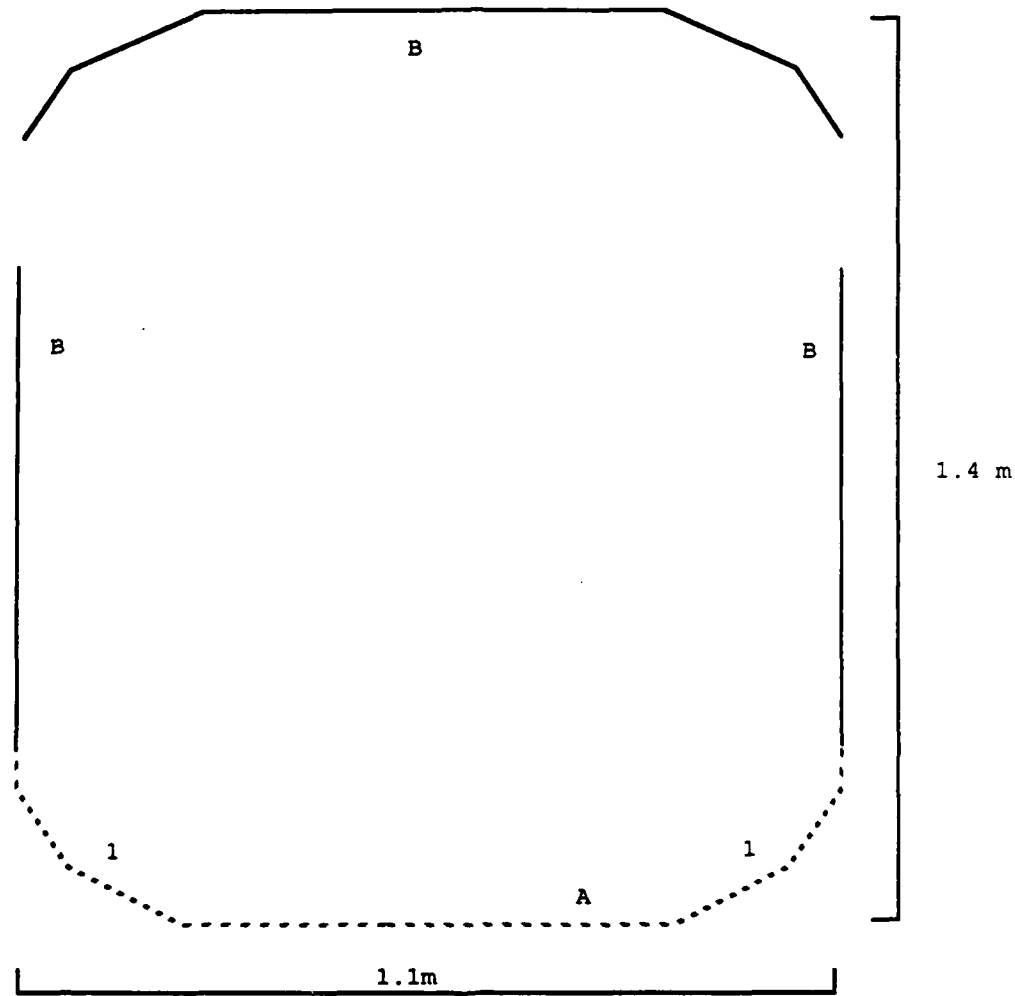
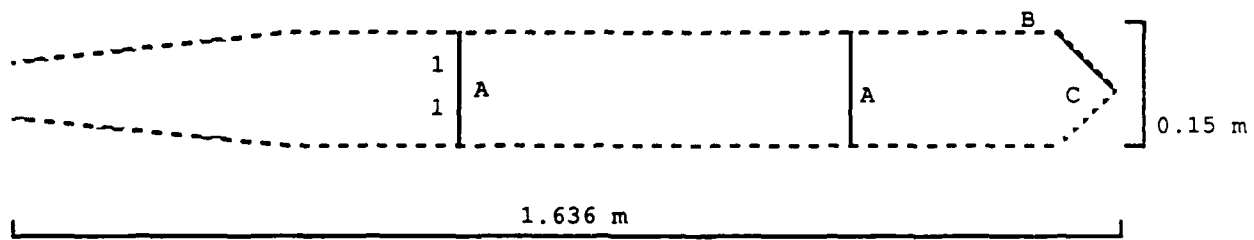


FIGURE 58 ELEMENTS OF EM MODELING AND ANALYSIS FOR INDIRECT EFFECTS



<u>WALL</u>	<u>THICKNESS (m)</u>	<u>CONDUCTIVITY (MHOS/m)</u>
A	2.29 E-5	3.7 E7
B	1.47 E-3	1.5 E4

FIGURE 59 REDIST FUSELAGE MODEL



C INDICATES POSITION OF CONDUIT

<u>WALL</u>	<u>THICKNESS (m)</u>	<u>CONDUCTIVITY (MHOS/m)</u>
A	1.27 E-4	3.5 E7
B	1.47 E-3	1.5 E4
C	1.02 E-3	3.5 E7

FIGURE 60 REDIST WING MODEL

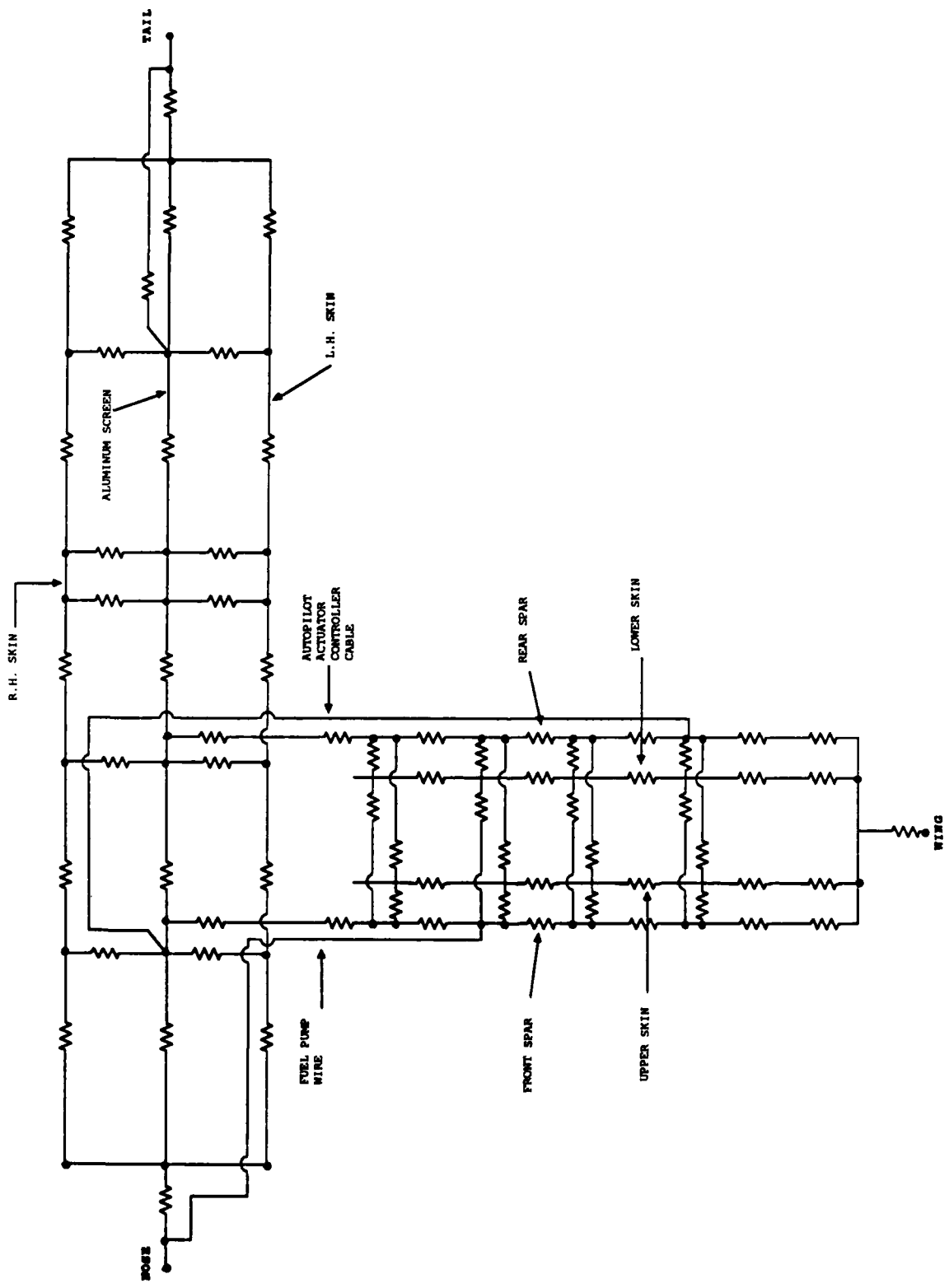


FIGURE 61 TEST BED RESISTOR MODEL

REFERENCES

1. Sommer, D.L.; "Protection of Electrical Systems from EM Hazards - Design Guide"; Boeing Military Airplane Co.; AFWAL-TR-81-2118; September 1981.
2. Military Standard MIL-STD-1757; "Lightning Qualification Test Techniques for Aerospace Vehicles and Hardware"; June 17, 1980.
3. "Lightning Test Waveforms and Techniques for Aerospace Vehicles and Hardware"; Report of SAE Committee AE4L; January 1978.
4. "International Aerospace and Ground Conference on Lightning and Static Electricity"; (8); Orlando, FL, June 21-23, 1984.
5. "International Aerospace and Ground Conference on Lightning and Static Electricity" (8); Fort Worth, Texas; AD-A135 100; June 21-23, 1983.
6. Melander, B.G., Cooley, W.W.; "Threat Environment Definition"; D180-27423-1; The Boeing Company; February, 1984.
7. "International Aerospace and Ground Conference on Lightning and Static Electricity"; (8); Oxford, Florida; 1982.
8. IEEE Electromagnetic Compatibility Society; Special Issue on Lightning and Its Interaction With Aircraft; "IEEE Transactions on EMC"; Volume 24, No. 2; May 1982.
9. Plumer, J.A. and Robb, J.D.; "The Direct Effects of Lightning on Aircraft"; IEEE Transaction on EMC, Vol. 24, No. 2; May 1982.
10. Corbin, J.C. and Cooley, W.W.; "Assessment of Aircraft Susceptibility/Vulnerability to Lightning and Development of Lightning - Protection Design Criteria"; IEEE Transactions on Electromagnetic Compatibility; May, 1982.
11. Fisher, F.A. and Plumer, J.A.; "Lightning Protection of Aircraft"; NASA RP-1008, 1977.
12. Blake, L. and Corbin, Jr., C.; "Electrical/Electromagnetic Concerns Associated with Advanced Composite Materials in Aerospace Systems"; AGARD Paper No. 283; 1979.
13. Military Specification MIL-B-5087B(ASG); "Bonding, Electrical, and Lightning Protection, for Aerospace Systems"; Amendment 2; August 31, 1970.
14. Federal Aviation Administration - Florida Institute of Technology; "Workshop on Grounding and Lightning Technology"; March 1979.
15. Federal Aviation Administration - Georgia Institute of Technology; "Workshop on Grounding and Lightning Protection"; FAA-RD-78-83; May 1978.
16. Radgowski, E. and Albrecht, R.; "Investigation of Electrostatic Discharge in Aircraft Fuel Tanks During Refueling"; Paper 78-1501 at the AIAA Aircraft Systems and Technology Conference, Los Angeles, California; August 21-23, 1978.

17. Riley, L.H., Perala, R.A., Robb, J.D., et al; "Lightning Tests of Pershing II"; paper 50; IAGC on Lightning and Static Electricity; June 1984.
18. Walko, L.C.; "A Test Technique for Measuring Lightning-Induced Voltages on Aircraft Electrical Circuits"; NASA CR-2348; NASA Lewis Research Center; February 1974
19. Butters, W.G., Clifford, D.W., Murphy, K.P., Zeisel, K.S., and Zuhlman, B.P.; "Assessment of Lightning Simulation Test Techniques"; Proceedings of IAGC on Lightning and Static Electricity; March 1982
20. Clifford, D.W., Crouch, K.E., and Schulte, E.H.; "Lightning Simulation Testing"; IEEE Transactions; EMC-24, v2, May 1982
21. Cooley, W.W. and Cooley, J.W.; "Low-level Swept Continuous Wave Test Report"; Science and Engineering Associates, Inc.; December 1985.
22. Cooley, W.W. and Hall, D.L.; "Low-level Pulse Test Report"; Science and Engineering Associates, Inc.; 1 July 1986.
23. Cooley, W.W. and Shortess, D.L.; "Moderate-level Pulse Test Report"; Science and Engineering Associates, Inc.; 12 January 1987.
24. Cooley, W.W. and Shortess, D.L.; "Shock-excited Test Report"; Science and Engineering Associates, Inc.; 9 February 1987.
25. Geren, W.P., Melander, B.G., and Hall, D.L.; "Lightning Current Redistribution"; paper 43-1; IAGC on Lightning and Static Electricity; June 1986.
26. Cooley, W.W.; "Determination of Electrical Properties of Grounding, Bonding, and Fastening Techniques for Composite Materials"; DOT/FAA/CT-86/8; December 1985.

BIBLIOGRAPHY

General Test Methodology

Baum, C. E.; "Direct Strike Lightning Environment on Aircraft Exterior and Their Simulation"; IAGC on Lightning and Static Electricity; Oxford, England; March 1982.

Beavin, R. C., Lippert, J. R., and LaVoie, J. E.; "Progress on the Atmospheric Electricity Hazards Protection Program"; IAGC on Lightning and Static Electricity; June 1984.

The Boeing Company; "Unified Transient Protection Requirements for Aircraft Line Replaceable Units"; Report number D180-27423-39; April 1985.

Burrows, B. J. C.; "Nanosecond Resolution of E, H, and I in Aircraft Lightning Test Rigs"; IAGC on Lightning and Static Electricity; Fort Worth, Texas; June 1983.

Burrows, W. C.; "Parallel Plate Transmission Tester Notes and Design Data"; IAGC on Lightning and Static Electricity; Oxford, England; March 1982.

Corbin, J. C.; "Vulnerability Assessment of Aircraft Systems to Indirect Lightning Effects"; Proceedings; AGARD Conference on Certification of Aircraft for Lightning and Atmospheric Electricity Hazards"; AFOSR-78-3653; September 1978.

Defense Nuclear Agency; "Technical Director's Report of the Project APACHE NAVCAMS EASTPAC Test"; Report number DNA 4284-HAS-1; December 1979.

Mississippi State University; "A Study of the Limitations and Applicability of Direct Drive Techniques for Nuclear EMP Tests"; Report number DNA-TR-82-185-V1; September 30, 1983.

Rabke, W. and Gage, B. P.; "A Comparison of the DNA CW System With the AESOP EMP Simulator"; Science and Engineering Associates Report for DNA; November 1982.

Robb, J. D.; "Atmospheric Electricity Hazards Analytical Model Development and Application Volume II, Simulation of the Lightning Interaction Event"; Electro Magnetic Applications, Inc.; Denver, Colorado; June 1981.

Swept Continuous Wave (CW) Tests

Burrows, B. J. C., et al; "A Comparison of Low-Level Swept CW and High-Level Transient Current Injection Testing on Full-Size Aircraft with Graphite Epoxy Panels"; IEEE International Symposium on Electromagnetic Compatibility; 1981.

East, D. A. and Geren, W. P.; "Application of the Swept CW Measurement Method to the Prediction of Transients Induced in Aircraft Wiring by Lightning"; IEEE International Symposium on Electromagnetic Compatibility; 1981.

East, D. A.; "Lightning Induced Transient Protection for Commercial Airplanes Using Frequency-Domain Analysis and Low-Level Test Methods"; IAGC on Lightning and Static Electricity; June 1984.

Robb, J. R., Loncrini, D., Ogasian, H., and Geren, P.; "Lightning Tests of an Electronic Engine Control With Associated Wiring"; IAGC on Lightning and Static Electricity; June 1983.

Walen, D. and Cooley, W.; "Atmospheric Electricity Hazards Vulnerability Test and Assessment"; AEHP Program; The Boeing Company; June 1984.

Fast Rise-Time Low-Level Pulse Tests

AEHP Program Draft Document - Assessment of Advanced Aircraft Vulnerability to Lightning and Static Electrification; April 1984.

Alliot, J. C. and Levesque, P.; "Laboratory Evaluation of Lightning Induced Transients in Aircraft Wiring"; paper 16; IAGC on Lightning and Static Electricity; June 1984.

Burrows, B. J. C., Luther, C. A., and Pownall, P.; "Induced Voltages in a Full-Sized Aircraft at $1E+11$ A/sec"; Proceedings of the IEEE 1977 International Conference on EMC; August 1977.

Crouch, K. E.; "Recent Lightning Induced Voltage Test Technique Investigations"; IAGC on Lightning and Static Electricity; June 1983.

Wallace, B. J., et al; "Composite Forward Fuselage Systems Integration"; Volume II, Technical Report AFFDL-TR-78-110; September 1978.

Full Threat Fast Rise-Time Tests

Evans, R. H. and Bishop, J.; "Induced Transients in a Simulated Lightning Test of the Fly-by-Wire Jaguar Aircraft"; IAGC on Lightning and Static Electricity; June 1983.

FLLASH (Full-Level Lightning Aircraft System Hardening) tests performed on the F-14A and F-18F/A aircraft at Albuquerque, NM; Spring-Summer 1982; under the direction of J. Birkin, NASC.

Naval Air Development Center; "Results of Low-Level and Full Threat Lightning Testing of the F/A-18A Aircraft"; Report NADC-84137-20; October 1984.

Perala, R. A., Rudolph, T. H., McKenna, P. M., and Robb, J. D.; "The Use of a Distributed Peaking Capacitor and Marx Generator for Increasing Current Rise Rates and the Electric Field for Lightning Simulation"; IAGC on Lightning and Static Electricity; June 1984.

Robb, J. D. and Perala, R. A.; "Measurements with Theoretical Analysis of a Full Scale NEMP Type Lightning Simulator"; IAGC on Lightning and Static Electricity; June 1984.

Walen, D. B.; "High Level Lightning Simulation Tests on The AGM 86 ALCM"; IAGC on Lightning and Static Electricity; June 1984.

Shock Excitation Tests

Heady, B. D. and Zeisel, K. S.; "NASA F-106 Lightning Ground Tests"; IAGC on Lightning and Static Electricity; June 1983.

Analytical Models

The Boeing Company; "AEH Protection Evaluation Test Predictions - F-14A"; Report number D180-27423-41; April 1985.

Cooley, W. W., Mahaffey, D.W., and Rudzitis, A.; "DNA Preempt Program C3 Facility EMP Response - Prediction Techniques"; IEEE International Symposium on EMC; August 1977.

Cooley, W. W.; "EMP Facility Response Predictions-AECO AUTOVON Results"; DCA/DNA/ USAF Working Group for HEMP testing of C3 Facilities; August 1976.

Cooley, W. W.; "EMP Response Prediction Techniques"; Inter-System Communications/ Electronics for Contributing Scientists and Engineers; July 1974.

Cooley, W. W.; "Shielding Effectiveness of Non-Uniform Enclosures"; GEC Transactions, Vol. EMC-10, No. 1; March 1968.

Eriksen, F. J., Rudolph, T. H., Perala, R. A.; "Atmospheric Electricity Hazards Analytical Model Development and Application"; Report AFWAL-TR-81-3084, Vol. III; August 1981.

General Dynamics; Fort Worth, Texas; "F-16 Lightning Analysis Report"; Report number 16PR757A; June 1978.

Hahn, G. J. and Shapiro, S. S.; "Statistical Models in Engineering"; John Wiley and Sons; 1968.

Hewitt, R. P., Koo, F. H., and Keys, D.; "Test and Evaluation of Graphite/ Epoxy Composite Structure"; Martin Marietta Aerospace; Orlando, FL; U.S. Army Materials and Mechanics Research Center; Report AMMRC-TR-79-39; July 1979.

Naval Air System Command, U.S. Department of the Navy; "Electromagnetic Coupling Calculations on an Advance Composite and Metal F-14 Fighter Aircraft"; Report number AIR-518-12; January 1982.

Williams, J. W. and Simpson, L. T.; "Preliminary Report of Finite-Difference Calculations of Simulated Lightning Response for the ALCM and F-16 Mockup"; MRC Report AMRC-R-434; December 1982.

Zeitler, R. T. and Droste, C. S.; "Flight Control System Lightning Susceptibility Test Report"; General Dynamics Report TIS GA4013; No. 16PR623; Revision A; March 1979.

Design Guides/Specifications

Chamis, C. C.; "Design Concepts for Low-Cost Composite Engine Frame"; NASA Report NASA-TM-83544; 1983.

Dunbar, W. G.; "High Voltage Design Guide"; Vol. V. Spacecraft; Boeing Aerospace Co.; Report AFWAL-TR-82-2057 Vol-5; January 1983.

Naval Air Systems Command; "Airframe Electrical Grounding Requirements Program"; Final Report-AD-A115-06418; Vol. 1; February 1981.